

Flow Design for Migrating Fish

Elianne M. Lindmark

Luleå University of Technology
Department of Applied Physics and Mechanical Engineering
Division of Fluid Mechanics

2008:55 | ISSN: 1402-1544 | ISBN: LTU-DT-- 08/55 -- SE



Flow Design for Migrating Fish

Elianne M. Lindmark

Luleå University of Technology
Department of Applied Physics and Mechanical Engineering,
Division of Fluid Mechanics

Cover figure: Salmon by Mats Nordström.

FLOW DESIGN FOR MIGRATING FISH

Copyright © Elianne M. Lindmark (2008). This document is freely available at

<http://epubl.ltu.se/1402-1544/2008/55>

or by contacting Elianne Lindmark,

`elianne.lindmark@ltu.se`

The document may be freely distributed in its original form including the current author's name. None of the content may be changed or excluded without permissions from the author.

ISSN: 1402-1544

ISRN: LTU-DT--08/55--SE

This document was typeset in L^AT_EX 2_ε

PREFACE

The research in this thesis has been carried out at the Division of Fluid Mechanics at Luleå University of Technology in Luleå Sweden. The work with the attraction channel was performed within the Swedish R&D programme "Hydropower - Environmental impact, remedial measures and costs in existing regulated waters", which is financed by Elforsk, the Swedish Energy Agency, the National Board of Fisheries and the Swedish Environmental Protection Agency. The work with the smolt guidance device was financed by Skellefteå Kraft AB.

There are many people I would like to thank, who made this work possible: first of all, my supervisor Prof. Håkan Gustavsson, for your great interest and knowledge of fluid mechanics in nature and your enthusiastic involvement in the project, and my co-supervisors Fredrik Engström and Daniel Marjavaara for your expertise and for contributing to this work.

I am also grateful to: Allan Holmgren, who built all the models, and followed me on endless excursions; Jan-Erik Almqvist, who initiated the project with the attraction channel and helped with building the field test site; Torbjörn Green for your excellent work with the PIV measurements and Markus Larsson and Claes Oderstad, who helped me monitor the field experiments and scan all the fish recordings manually.

Obviously the work at the Division would not be half as fun without all the people working there. Thank you all for all the coffee breaks and lunches we shared. And a big thank you to Gunnar; what would I do

without you. You are my computer and CFD guru and I could not have anyone better to share the office with.

Thanks to: everyone in the research trainee group of 2003/04 for a great start to my years as PhD student, fellow researchers involved in the research program "Hydropower - Environmental impact, remedial measures and costs in existing regulated waters" for a great cooperation and friendship, all the people involved in the NOWPAS network for the interesting meetings and a lot of fun and to all of you at the Department of Wildlife, Fish, and Environmental Studies at SLU for our collaboration and for taking care of me during conferences.

Thank you Skellefteå Kraft for letting me perform the field experiments at Sikfors hydropower plant and a special thanks to all of you working there, who always helped when I needed it.

But none of this would be possible without my family and friends who supported me and cheered me on. Most of all, thank you Jonas for always being there for me and for putting up with me. And Elvira you are everything to me, thank you for teaching me what is important in life.

A handwritten signature in black ink, reading "Thane Lindmann". The script is cursive and fluid, with the first name "Thane" written in a larger, more prominent style than the last name "Lindmann".

October 2008

ABSTRACT

The utilization of rivers for hydropower production leads to problems for migrating fish, such as Atlantic salmon (*Salmo salar*) and sea trout (*Salmo trutta*). Both salmon and trout reproduce in fresh water, but spend their adult years at sea. To overcome man-made obstructions to and from the spawning grounds the fish needs help. Fishways for upstream migrating fish is an old technique; however the efficiency is often low due to inefficient attraction water. The upstream migrating fish are attracted to high water velocities and often approach the dominating flow from the turbine outlet instead of entering the fishway. For the downstream migrating smolt (young fish) the only way to pass a power plant is often via the turbines, with a high mortality as a result. The smolt follow the main flow in the river on the way downstream avoiding high accelerations or retardations.

This thesis covers investigations on both an attraction channel to increase the water velocity at the inlet of a fishway for upstream migraters and a smolt guidance device to guide the smolt away from the turbine inlet to a safer passage route.

To investigate the properties of the attraction channel both model and field experiments have been carried out, as well as numerical studies. The velocity in the channel has been examined with Laser-Doppler-Velocimetry and the flow field in the channel was studied using Particle-Imaging-Velovimetry. The results show that the water can be accelerated 38 % compared with the surrounding velocity. How far the increase in velocity is present depends on the depth of the attraction channel.

The field tests carried out at Sikfors hydropower plant in Piteå River (Sweden) show that the fish do swim through the channel, providing that the channel is black.

The flow around a smolt guidance device has been studied using numerical simulations. The aim of the device is to redirect the surface flow from the turbines to the spillway. By doing this, the shallow swimming smolt will also be guided towards the spillway and a much safer route. The results show that the guidance device successfully redirects the surface flow without creating any strong acceleration that may scare the fish.

This thesis is based on the following papers, in August 2007 the author changed name from Wassvik to Lindmark:

Paper A: Wassvik E.M. and Engström T.F. 2004. Model test of an efficient fish lock as an entrance to fish ladders at hydropower plants. *In the Proceedings of the Fifth International Symposium on Ecohydraulics, September 12-17, Madrid, Spain.*

Paper B: Wassvik E. 2006. Attraction channel as an entrance to fishways - model assessment using LDV. *Manuscript.*

Paper C: Lindmark E.M., Green T.M., Lundström T.S. and Gustavsson L.H. 2008. Flow measurements in an attraction channel as entrance to fishways. *Submitted to River research and applications*

Paper D: Lindmark E. and Gustavsson L.H. 2008. Field study of an attraction channel as entrance to fishways. *River research and applications.* 24: 564-570

Paper E: Lindmark E.M. 2008. Numerical solution of the flow field in an attraction channel for migrating fish. *Manuscript.*

Paper F: Lundström T.S., Hellström J.G.I. and Lindmark E.M. 2008. Flow design of guiding device for down-stream fish migration. *Submitted to River research and applications*

Additional publication of interest

Lindmark E.M., Green T.M., Gustavsson L.H. and Lundström T.S.
2008. Increasing the attraction water velocity at fishway entrances;
model and field experiments. *In the Proceedings of The 19th In-
ternational Symposium on Transport Phenomena, 17-20 August,
2008, Reykjavik, Iceland*

CONTENTS

I	Summary	1
1	Introduction	3
1.1	Attraction channel	5
1.2	Smolt guidance device	6
1.3	The aim of the thesis	8
2	Laboratory Experiments	9
2.1	Laser Doppler Velocimetry	12
2.2	Particle Imaging Velocimetry	13
2.3	Errors	15
2.4	The flow in the attraction channel	17
2.5	The flow downstream the attraction channel	20
3	Field Experiments	25
3.1	Study area	25
3.2	Attraction channel	27
3.3	Measuring procedure and data processing	29
3.4	Results and observations	31
4	Simulations	35
4.1	Computational fluid dynamics	35
4.2	The attraction channel	38
4.3	The attraction channel performance in a free stream	40
4.4	Guiding downstream migrating smolt	40

4.5	The flow around the guidance device	45
5	Summary	47
6	Division of Work	51
II	Papers	57
A	Model Test of an Efficient Fish Lock as an Entrance to Fish Ladders at Hydropower Plants	
B	Attraction Channel as an Entrance to Fishways - Model Assessment Using LDV	
C	Flow Measurements in an Attraction Channel as Entrance to Fishways	
D	Field Study of an Attraction Channel as Entrance to Fishways	
E	Numerical Solution of the Flow Field in an Attraction Channel for Migrating Fish	
F	Flow Design of Guiding Device for Downstream Fish Migration	

Part I

Summary

CHAPTER 1

INTRODUCTION

Hydropower is a renewable way of producing electricity where the head difference between reservoir and outlet is converted into electricity via turbine and generator. The hydropower in Sweden stands for approximately half the production of electricity and in the world that number is 16 % (Energy in Sweden). The first hydropower plant in Sweden was built in 1882 (Montén, 1988), and today the number of hydropower plants in Sweden are about 1900, of which 1200 are small (under 1.5 MW). Even though hydropower is a "green" energy there are severe environmental consequences such as fish migration barriers, damming of the river, flow alterations, loss of habitat etc. (Banks, 1969; Rivinoja, 2005). Sweden has four rivers ("nationalälvar") and 38 parts of drainage basins protected from hydropower development (Lundin and Carles, 2006).

Atlantic salmon (*Salmo salar*) and sea trout (*Salmo trutta*) spend their adult life in sea, but reproduce and spend their early years in rivers. They hatch in gravel river beds and stay in the river for one to four years (sometimes longer) before migrating out to sea during April-May. When migrating out the young fish is called smolt. After one to four years at sea the fish return to the river to spawn. The size of the fish returning to the river depend on how many years they have spent at sea; a one-sea-winter salmon weighs 1.5 - 3 kg and a three-sea-winter salmon weighs approximately 15 kg (Erlandson, 1988). The adult fish migrate upstream during April-November (Ferguson, 2005) and spawn

in the main river and tributaries during the fall (Heggberget, 1988). When migrating upstream the adult fish are influenced by many factors such as water turbidity, cloud cover, wind direction etc. (Banks, 1969). But most importantly are the fish attracted to high water velocities (Weaver, 1963; Williams, 1998). After spawning the fish either die or migrate back to sea. The out migrating adult fish are called kelt.

In regulated rivers the migrating fish encounter man-made obstructions, such as hydropower plants and regulation dams, on their way to or from the spawning ground. This is a problem for the upstream migrating adult fish as well as for the downstream migrating smolt and kelt. The upstream migrating fish have problems passing the dams, and to help the fish fishways are often used. There is a great variety of fishways such as pool and weir, Denil fishways, fish locks and fish lifts, etc. (Clay, 1995). But a common problem with these fishways is that the fish have difficulties finding the entrance to the fishway and are instead attracted to the dominating flow from the turbine outlet (Arnekleiv and Kraabøl, 1996; Rivinoja et al., 2001). It is not only important that the fish finds the entrance, it is important for the fish to find it quick in order to reduce stress on the fish (Clay, 1995).

For the smolt and kelt the problem with hydropower plants is that often the only way downstream is via the turbines. The mortality from a turbine passage depends on the water temperature, the type of turbine and the size of the fish etc. (Schilt, 2007; Montén, 1985). To help the downstream migrating fish, different types of guidance can be used, such as to guide the fish through a safer passage route, like a fishway or spillway. Also, reduction of mortality in the turbines can be achieved by fish friendly turbines (Čada, 2001). The smolt follow the mainstream in the river on their way to the sea but when encountering obstacles the fish reacts and can spend days upstream a power plant searching for a safe route down (Schilt, 2007).

The swimming speed of fish can be categorized in three levels: cruising, sustained and burst speed. It is important that the velocity at fishway entrances do not exceed burst speed; 1.2 - 2.4 m/s is recommended for Pacific salmon (Clay, 1995). The swimming speed varies with the length of the fish, the water temperature and with different species (Clay, 1995).

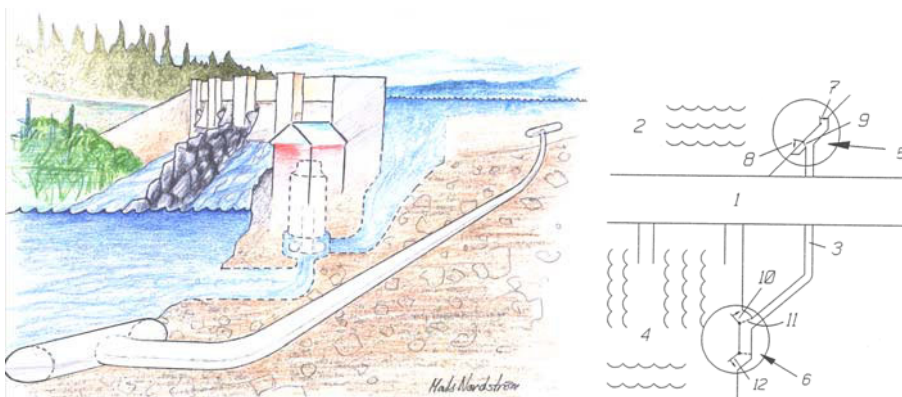


Figure 1.1: *Drawing of the original idea of the attraction channel by inventor Jan-Erik Almqvist. The fish swim into the lower channel (6) which is then closed and the fish is guided upstream via the pipe (3) to the upper channel (5) where the fish is released. Courtesy of Jan-Erik Almqvist.*

1.1 Attraction channel

The water flow out of a fishway is called attraction water since it is used to help the fish find the entrance. As the migrating fish is triggered to swim in high velocities (Weaver, 1963; Williams, 1998) the goal with the attraction water is to have higher velocities out of the fishway than the surrounding water velocity. In order to get an efficient water flow at the fish entrance it is often necessary to lead extra water from the reservoir to the inlet of the fishway, (Clay, 1995). Fish are otherwise attracted to the dominating flow from the turbine outlets (Arnekleiv and Kraabøl, 1996), causing a delay in the migration, stressing the fish and thus reducing their odds to reach the spawning grounds (Clay, 1995).

To guide adult migrating fish without using any extra water from the reservoir the inventor Jan-Erik Almqvist in Boden, Sweden, came up with an idea of using the water in the river and accelerate it to attract the fish; see Figure 1.1. The original idea was then further developed at Luleå University of Technology to be an open U-shaped channel that is partly submerged at the entrance of a fishway or any free stream, like the turbine outlet. The channel was first called fish lock (**Paper A**), but after 2004 the name was changed to attraction channel. At the

flow outlet of the channel an underwater constriction in the form of a bump is placed to accelerate the flow; see Figure 1.2. The design goal is to generate a considerably higher velocity out of the channel than the surrounding water velocity, and thereby attract fish to swim into the channel.

Flow patterns downstream fishway entrances have been studied by Kamula (2001), who describes the flow pattern for three common fishways. The result show that the flow from a pool-and-weir fishway dives while the flow from Denil and vertical slot fishways are more surface oriented.

With the pressure uniform over the free surface, the only way to change the velocity is by varying the surface level. A first analysis of the flow in the attraction channel assumes 2-d flow and uses the Bernoulli equation:

$$\frac{V_1^2}{2g} + d_1 = \frac{V^2}{2g} + (h + d) \quad (1.1)$$

and continuity

$$V_1 d_1 = V d \quad (1.2)$$

(Finnemore and Franzini, 2002). The variables are explained in Figure 1.2. The case where the flow over the bump is critical ($Fr = \frac{V}{\sqrt{gd}} = 1$) also creates the highest velocity over it. Steady 2-d flow over submerged bodies is a well known area of research as exemplified by numerical studies by for example Forbes and Schwartz (1982) and Vanden-Broeck (1987), who study the wave phenomena due to submerged semi circular cylinders. In the case with the attraction channel where the water not only takes the path through the attraction channel but also is allowed to pass on the outside of the channel is somewhat more complicated than the 2-d theory. The flow inside the channel is subcritical and therefore the bump will cause a blockage in the channel and parts of the water aimed for the channel will be forced to the outside of the channel.

In this thesis the flow in the attraction channel is studied using a model setup in laboratory, a full-scale setup in field and numerically using computational fluid dynamics.

1.2 Smolt guidance device

Guiding upstream migrating adult fish has been done for about 300 years (Clay, 1995), but the problem of guiding smolt downstream has just

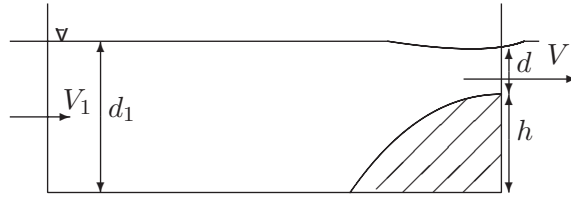


Figure 1.2: *Sketch of the attraction channel.*

recently been addressed. The smolt swim downstream in the main flow of the river, which means that many of them pass through the turbines. The mortality of smolt passing through the turbines depends on many factors such as the size of the fish, the water temperature and the type of turbine. The potential mechanisms for fish mortality in the power plant are: mechanical (hitting for example turbine blades), hydraulic (shearing forces), pressure (injuries to organs and swim bladder) and noise (Ferguson, 2008). The mortality of smolt passing through the turbines in Sikfors hydropower plant is about 20 % (Rivinoja, 2005). When the smolt migrate downstream they swim close to the surface in the main flow of the river and try to avoid strong accelerations and retardations (Taft, 2000; Moore et al., 1998; Johnson et al., 2000).

To safely guide the smolt (and kelt) past a power plant their route must be directed away from the turbine inlet, towards a safe route such as a fishway or the spillway. One way to direct the smolts are by louvers, which are plates placed broad-side perpendicular to the flow. In one design the size of the plates is 8×64 mm (Ruggles and Ryan, 1964). The depth of the plates needs to be as deep as the swimming depth of the smolts. Ducharme (1972) reports that 80 % of Atlantic salmon smolt swim between the surface and a depth of 1.3 m. The guiding efficiency of louver systems is high if operated correctly; Ruggles and Ryan (1964) report an efficiency of 85 - 95 % for Sockeye and Coho salmon smolts.

In this thesis the flow around an impermeable screen smolt guidance device is investigated using computational fluid dynamics.

1.3 The aim of the thesis

The aim of this thesis is to further develop the methods to help migratory fish species to safely pass man-made structures in rivers, such as hydropower plants. This is done by investigating (**Paper A - E**) an attraction channel as entrance to fishways and constructing a guiding device for downstream migrating smolt and kelt (**Paper F**).

CHAPTER 2

LABORATORY EXPERIMENTS

A model of the attraction channel has been tested in laboratory to investigate the flow in and around the channel. Two techniques have been used to investigate the flow. To start with, Laser Doppler Velocimetry (LDV) was used to measure the water velocity in and around the channel with the purpose to capture the expected increase in water velocity out of the channel, compared with the surrounding velocity (**Paper A**) and to determine how far downstream the increase in water velocity lasts (**Paper B**). In a subsequent study, Particle Imaging Velocimetry (PIV) was used to further investigate the flow field in and beyond the channel (**Paper C**).

The attraction channel model

The model is a 500 mm long glass channel with 1.7 mm thick glass walls and an inner cross section of 200 mm \times 96 mm, cf. Figure 2.1(a). The bump in the channel is made of Styrofoam with a plastic film cover to create a smooth surface. The shape of the bump is described with the following formula

$$h(x') = B - \frac{1}{36B}x'^2 (x' \geq 0, h \geq 0) \quad (2.1)$$

where B denotes the maximum height of the bump and x' originates at the highest part of the bump and runs in the negative x direction;

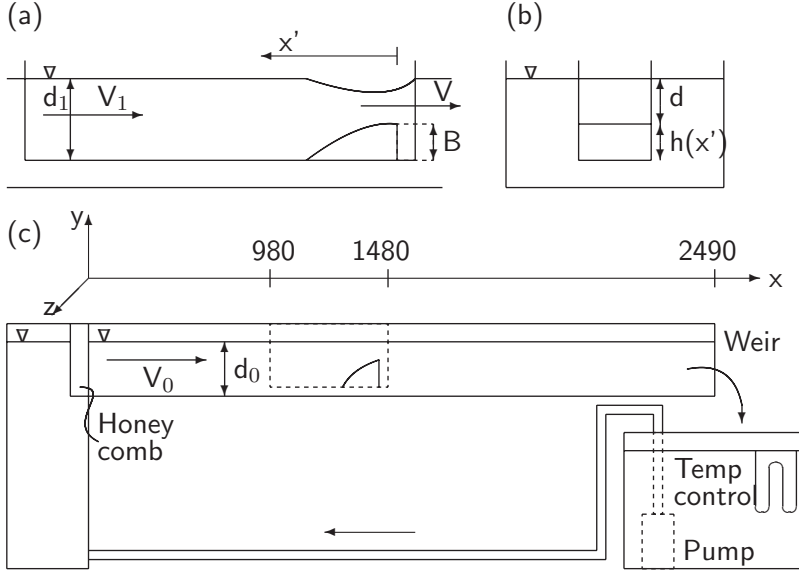


Figure 2.1: (a) *Attraction channel with bump.* (b) *Cross section of flume and attraction channel.* (c) *Experimental setup of water flume with attraction channel and defining coordinate system.* All dimensions in mm.

see Figure 2.1(c). The bump was placed 40 mm from the outlet of the channel to be able to measure the velocities close to the bump with LDV. When using PIV the bump and parts of the channel were painted black to prevent light to reflect from the surface. In **Paper A** a series of different bumps was used to measure the effect of the bump on the attraction water velocity; the bump heights (B) were 22, 34, 47, 70 and 80 mm. In the following experiments (**Paper B and C**) only the 80 mm bump was used, which was the bump that gave the highest water velocity in the first experiment.

The water flume

Two different water flumes have been used during the experiments. The flume used in **Paper A and B** is a 2.5 m long plexiglass channel with a cross section of 200 mm \times 300 mm (depth \times width); see Figure 2.1. In **Paper C** a new water flume with glass walls was obtained for flow

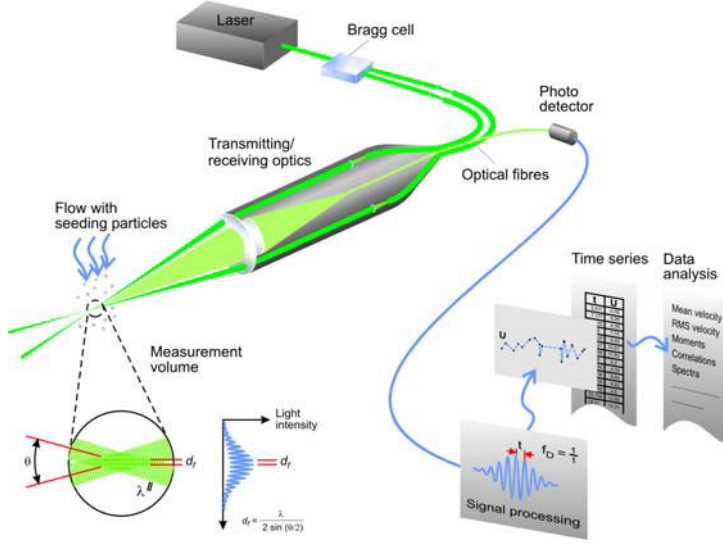


Figure 2.2: *Principle of the LDV setup. Courtesy of Dantec Dynamics A/S.*

experiments. The new flume is 7.5 m long and has a cross section of 310 mm \times 295 mm (depth \times width). The inlet is horizontal and converging compared with the smaller flume that has a straight vertical inlet. In both flume inlets a metal net and a honeycomb was placed to provide a more uniform velocity distribution. The honeycomb is 75 mm thick and the holes have a diameter of 7.6 mm. At the outlet of the small flume a V-notch weir was used to keep a constant water depth and in **Paper A** the weir was used to measure the flow rate. In **Paper B and C** a Danfoss MassFlo coriolis flow meter (error $< \pm 0.5\%$) was used to monitor the flow rate. In the long flume a straight weir keep the water depth. The flow rate in the flumes was controlled to $5.3 \times 10^{-3} \text{ m}^3/\text{s}$ for the short flume and $5.6 \times 10^{-3} \text{ m}^3/\text{s}$ for the long flume. The temperature in the flumes was held constant with a cooling system in the tank to within $21 \pm 1.6^\circ\text{C}$ and the water depth in the flumes was kept at $118 \pm 1 \text{ mm}$ ($117 \pm 1 \text{ mm}$ for **Paper B**).

2.1 Laser Doppler Velocimetry

The Laser Doppler Velocimetry (LDV) technique is based on the doppler shift in the reflecting light from moving particles in a fluid. It is a non-intrusive method (apart from tracer particles) that is indifferent to the temperature or compound of the fluid, as long as it is transparent. The fluid is seeded with small particles, small enough to follow the fluid. When introducing a powder (seeding particles) into water it is important to avoid agglomeration, which is done by first mixing the powder using lubricants and a small amount of water which is then poured in the water. When a moving particle is illuminated the reflected light contains information about the velocity of the particle (the Doppler effect) according to the formula

$$f_r = f_b + \frac{v_p(e_{pr} - e_b)}{\lambda_b} \quad (2.2)$$

where f_r is the reflected frequency from the particle, f_b the frequency of the original beam, v_p the velocity of the particle, $(e_{pr} - e_b)$ the difference between the direction of the reflected beam and the beam from the laser source and λ_b is the wave length of the original laser beam (Albrecht et al., 2003). As the doppler shift is of the order 1 - 100 MHz and the beam frequency is approximately 10^{14} Hz, the doppler shift is not possible to measure. But, if two beams is used (dual-beam configuration) the difference between the two beams can be measured since

$$f_D = f_2 - f_1 = \frac{v_p(e_1 - e_2)}{\lambda_b} \quad (2.3)$$

where f_D is the doppler frequency, f_1 and f_2 are the reflected frequencies from the two beams and $e_1 - e_2$ is the difference between the direction of the two incoming beams (Albrecht et al., 2003). This means that the measured frequency is directly proportional to the velocity of the particle, the angle between the beams and the wave length of the laser beam, i.e. no calibration is needed. The wave length of the light should be of the same order as the diameter of the particles in the fluid. The diameter of the particles is usually around $1 \mu\text{m}$, so visible light can be used ($0.45\text{-}0.7 \mu\text{m}$). Even ultraviolet light can be used, but setting up an optical system with non-visible light is much harder. In theory, LDV is able to measure velocities from 0.01 mm/s to 10^6 m/s .

From equation 2.3 the velocity of the particle can be determined but its direction is still unknown. This problem can be solved by shifting the

frequency of one of the beams, typically by 10-80 MHz. This is practically done by letting one of the beams pass an opto-acoustic modulator e.g. a Bragg-cell (see Figure 2.2). The direction can now be determined; if the resulting frequency is lower than the shifted frequency the particles are moving in one direction and if the resulting frequency is higher than the shifted frequency the particles are moving in the opposite direction. LDV measures the velocity pointwise in the flow and to measure the velocity in more than one point, which is typically done, a traverse system is used to navigate the measuring volume in the fluid.

In the present setup the equipment used was a two-component system from Dantec with an 85 mm fibre optics probe. The measuring volume was $0.076 \text{ mm} \times 0.838 \text{ mm}$ for the streamwise component (514.5 nm). The water was seeded with polyamide particles with a diameter of $5 \text{ }\mu\text{m}$ (Dantec's PSP-5). The sample time in each measuring point was determined by testing different sample times. The times tested were: 60, 90, 180, 360 and 450 s. Measurements were done at sixteen points in the channel, vertically from the bottom of the channel to the surface of the water, with different sample times. Each profile was measured five times with each sample time. The mean velocity for each measuring point at each sample time were calculated and the velocities were compared with the mean. The criterium for a good sample time was an error of $\pm 1 \%$ in the channel with no bump. The sample time was set to 90 s. The second criterium for the measurements was to have at least 10,000 samples in each measuring point. This resulted in sample times between 90 and 4500 s.

2.2 Particle Imaging Velocimetry

PIV is the other method used for visualizing and measure fluid flow. This technique enables instantaneous measurements of the fluid velocity in a two-dimensional plane (or in three dimensions).

The PIV setup consists of a pulsed laser source, a cylinder lens to create a (thin) light sheet and a camera to record the position of seeding particles visible in the light sheet, cf. Figure 2.3. A laser is used because of the high brightness and the shortness of the laser pulses. If the marker particles is small enough to follow the fluid and $\Delta \mathbf{x}$ is the distance the particle moves between the exposures then the velocity of the particle is

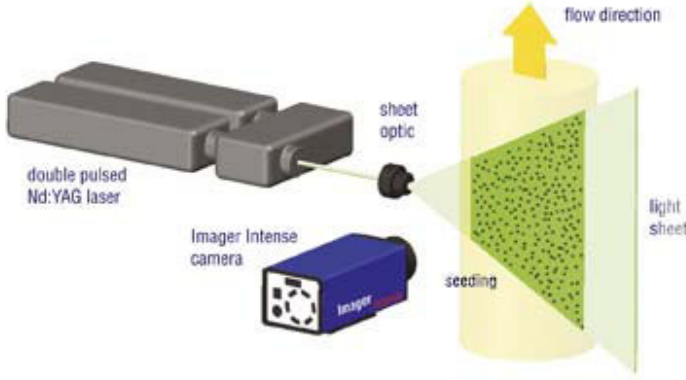


Figure 2.3: *Principle of the PIV setup. Courtesy of LaVision.*

by definition equal to

$$\mathbf{u}(\mathbf{x}, t) \doteq \frac{\Delta \mathbf{x}}{\Delta t} \quad (2.4)$$

where Δt is the time between the exposures (Adrian, 1996). Having a time differentiated double frame image, each frame is divided into small interrogation areas where it is assumed that the particles move homogeneously between the exposures. The duration of the illumination must be short enough so that the particles are frozen in time, to avoid blurring of the image. In each interrogation area cross-correlation, based on the Fast Fourier Transform, is performed. The result is a velocity vector field of the entire measured plane (Raffel et al., 1998). The time delay between the exposures must be long enough to be able to determine the distance, but short enough to avoid the out of plane velocity particles to leave the plane. Optimally the particles should not move more than $1/4$ the length of the interrogation area (Adrian, 1996).

The PIV-system used in this thesis is a commercially available system from LaVision GmbH. It consists of a Litron Nano L PIV laser, i.e. a double pulsed Nd:YAG with a maximum repetition rate of 100 Hz, and a LaVision FlowMaster Imager Pro CCD-camera with a spatial resolution of 1280×1024 pixels per frame. The tracer particles used were hollow glass spheres with a diameter of $6 \mu\text{m}$ also from LaVision GmbH.

The flow in the pure fume was measured and a repeatability test was performed. The velocity profiles are presented in Figure 2.4. At each

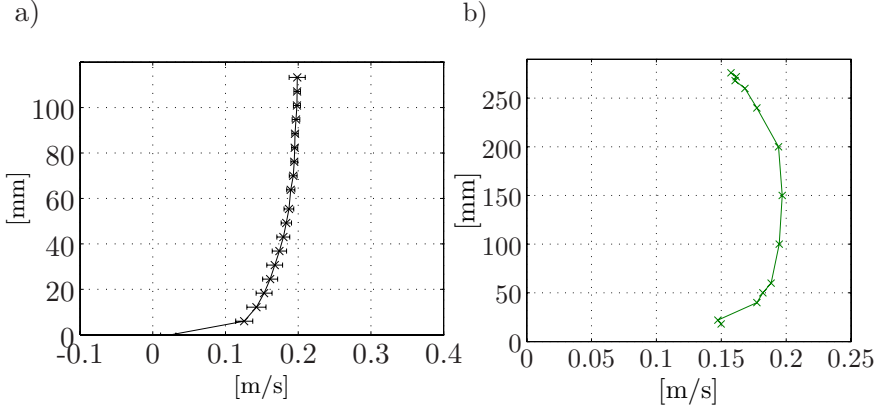


Figure 2.4: *Velocity profiles in the pure flume 4015 mm downstream the flume inlet. (a) Horizontal velocity profile vs. distance from bottom of the flume and (b) horizontal velocity profile vs. spanwise distance.*

measuring location a set of 250 double-frame images was taken at the speed of 50 Hz. The recorded sets were post processed with DaVis 7.1 using a multi-pass cross-correlation scheme with decreasing interrogation window size. For the first pass a 64×64 pixel interrogation window was used, for the second pass a 32×32 pixel interrogation window was applied with a 75 % overlap.

2.3 Errors

Uncertainty in the measurements originates from the experimental setup and the measurement system. The setups have been carefully designed to yield stable experimental conditions. The measurement uncertainty is composed of uncertainty due to bias errors and precision errors (or measurement errors).

A cornerstone in all experimental design is to randomize the experimental procedure. By proper randomization the effect of the uncertainties are averaged out (Montgomery, 2005). All measuring points presented in this thesis are retrieved in random order.

LDV

LDV measurements are associated with a variety of bias errors, such as error in the calibration factor, velocity bias, validation bias, angular bias and probe alignment/configuration bias. The system was set up to minimize the different bias errors.

The velocity bias is due to the fact that the particle rate through the measuring volume is related to the flow velocity, leading to a bias towards a higher velocity (Albrecht et al., 2003). The bias was compensated for by weighting each velocity sample with its residence time in the measuring volume.

The precision error was estimated by a repeatability test. Each profile was measured twice and the standard deviation of each pair of measurements was estimated to yield a 95% confidence interval. The overall accuracy of the velocity measurements was $\pm 5\%$, with locally larger errors close to the walls and the free surface.

PIV

Unless the velocity of the fluid is very large the uncertainty in time between two pulses can be neglected compared to the error caused by the uncertainty in measuring the displacement between two images (Adrian, 1996). The optimum diameter of an image particle is 2 pixels (Raffel et al., 1998). The uncertainty in measuring the displacement of particles in an interrogation window is nearly constant with respect to the displacement length (displacement up to 10 pixels), unless the displacement is less than 0.5 pixels where the uncertainty is much lower (Raffel et al., 1998). Adrian (1996) recommend displacements of 1/4 of the interrogation window. The displacement bias due to in-plane loss of particles can be completely removed with the right weighing function. If the out of plane motion is large this need to be cared for by reducing the time between illuminations, thickening the light sheet or by offsetting the light sheet between illuminations (Raffel et al., 1998). The probability of a valid displacement detection increases when more particle image pairs enter the correlation calculation, so the higher the density of particles is in the interrogation window the higher the accuracy. The background noise has an affect on the uncertainty of the measurements, but low noise levels (10 % white noise) have little effect on the measurements. A velocity gradient in the interrogation window will always result in a bias towards a lower velocity, but smaller interrogation windows can tolerate

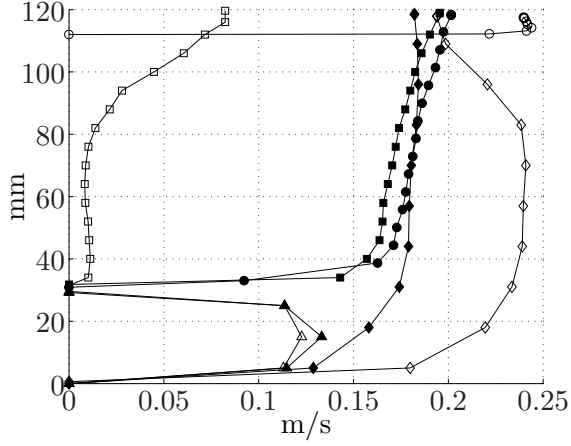


Figure 2.5: *Velocity in and around the attraction channel.* \square, \blacksquare = velocity at channel inlet; \circ, \bullet = velocity at the channel outlet (fish inlet); $\triangle, \blacktriangle$ = velocity under the channel; \diamond, \blacklozenge = velocity outside the channel. Open symbols represent setup with 80 mm bump and filled symbols represent reference setup with no bump.

a higher displacement gradient (Raffel et al., 1998).

2.4 The flow in the attraction channel

The purpose with the attraction channel is to increase the velocity of the water coming out of the channel (the fish inlet), so that the velocity out of the channel is larger than the surrounding velocity. To investigate the bump height effect of the velocity increase different bumps were tested in the attraction channel model at constant water depth of the channel. The velocities in the channel were measured with LDV. As LDV is a point-wise measuring system a number of profiles in and around the channel was measured for the different bump heights (22, 34, 47, 70 and 80 mm). Vertical velocity profiles in the channel were taken at the water inlet of the channel (48 mm from the inlet) and over the bump (in the middle of the channel). At the same x-position the profiles were measured outside the channel between the channel and flume wall, this to be able to compare the velocities in the channel to the surrounding velocities. For each bump approximately 55 points were measured in

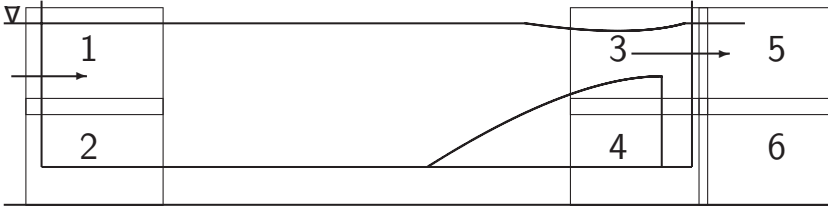


Figure 2.6: *A schematic figure of the six fields of view in the attraction channel. The planes overlap to give a smooth transition when evaluating the flow field.*

random order.

The velocity increase is measured as the mean velocity over the bump over the mean velocity on the flow on the outside of the channel (0.17 m/s for the reference case). The largest velocity increase, 38 % was achieved with the 80 mm bump. Figure 2.5 show the results from the measurements with the 80 mm bump and the reference measurement with no bump in the channel.

The blockage in the channel due to the bump, forces the water aimed for the channel to the outside. In the present setup where the channel takes one third of the flume width, this causes an increase of the water velocity on the outside of the channel, cf. Figure 2.5. As this is an effect of the lab setup the effect will be much smaller in full-scale where the attraction channel is small compared with the width of a river. The velocity out of the model channel is compared with the surrounding velocity in the case with no bump in the channel.

To further investigate the flow in the attraction channel it was studied with the 80 mm bump at three different water depths using PIV. The depths were measured as the water depth over the highest point of the bump and were 7, 13 and 20 mm. In the original setup using the LDV the water depth over the bump was 5.6 mm.

PIV is a field measuring technique and the attraction channel model was divided into 6 measuring fields that cover the inlet, the bump and the flow directly downstream the channel, cf. Figure 2.6. All measurements were conducted in the middle of the channel. Due to strong reflections at the bump surface and the surface of the water the velocities at the

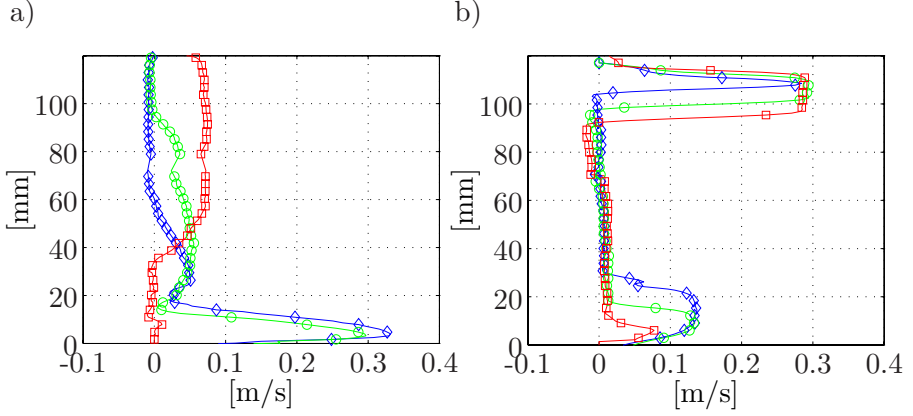


Figure 2.7: *Vertical velocity profiles at different positions in the attraction channel. \diamond = small depth. \circ = medium depth. \square = large depth. a) Velocity profiles 356 mm upstream the vertical edge of bump and b) the velocity profiles 1 mm downstream the vertical edge of the bump.*

highest point of the bump were hard to measure.

The results from the measurements with the PIV show that for the case with 7 mm depth over the bump the water velocity out of the channel is the same as for the measurement with LDV with the same setup. The PIV results from measurements in the attraction (Figure 2.8) reveal two different patterns. One pattern for the small and medium depth of the channel and one for the larger depth. When the depth of the channel is small or medium the flow circulates in the channel creating a small jet close to the bottom. When the depth in the channel is large the flow instead creates a jet at the surface, and the flow close to the bottom is nearly zero. For the LDV measurements the flow in the channel (Figure 2.5) is near the surface (for the same case with PIV the flow is at the bottom, Figure 2.10a). When reinvestigating the two setups it is found that the attraction channel in the PIV set up is tilting so the bottom of the channel is 7 mm deeper at the inlet compared with the outlet. The difference in the flow pattern due to this change in inlet conditions indicate that the flow in the channel is very sensitive to change. The sensitivity of the flow in the channel needs further investigation.

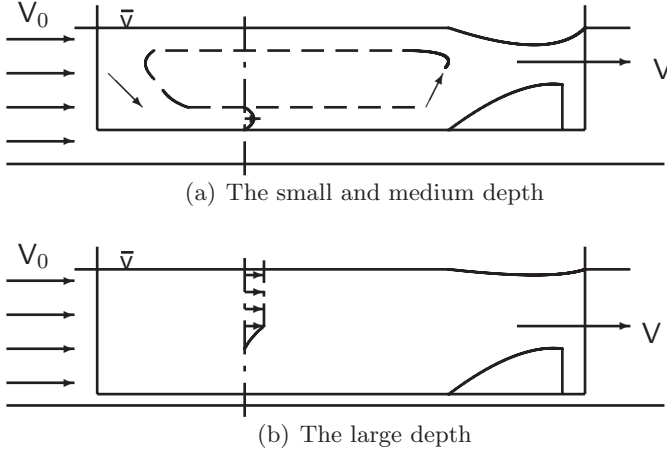


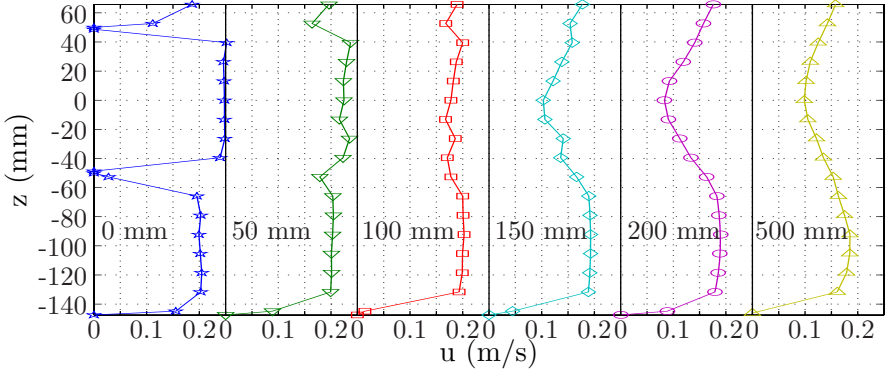
Figure 2.8: *A scaled presentation of velocity distributions in the attraction channel. In figure (a) is the recirculation and bottom jet shown. In figure (b) is the velocity distribution drawn in a cross section.*

2.5 The flow downstream the attraction channel

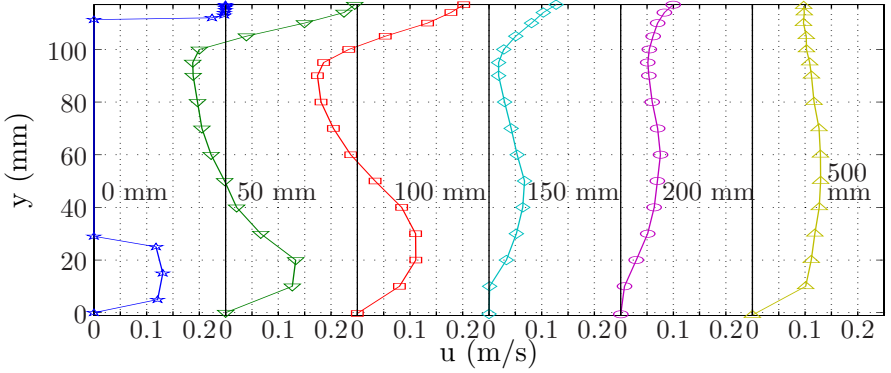
Fish swimming towards the attraction channel will encounter the flow downstream the channel. This is the attraction water that will guide the fish towards the inlet of the attraction channel. The velocity needs to be higher than the surrounding velocity (Weaver, 1963) and the velocity increase needs to be detectable as far downstream as possible.

To investigate the velocity downstream the attraction channel the flow was studied with LDV. An 80 mm bump was used and the depth in the attraction channel model was 88 mm (the same setup that gave the 38 % velocity increase). Velocity profiles were taken over the bump at 50, 100, 150, 200, 300, 400 and 500 mm downstream. Profiles were measured vertically in the middle of the flume and horizontally just below the water surface ($y = 114$ mm). The points were measured in random order.

The velocity profiles in Figure 2.9 show the results from the LDV measurements downstream the channel. The results show a jet flow (the attraction water) out of the channel with a mean velocity of 0.23 m/s. Below the jet a wake is formed. Between the jet and the wake a mixing



(a) Horizontal velocity profiles.



(b) Vertical velocity profiles.

Figure 2.9: *Water velocities downstream the attraction channel.*

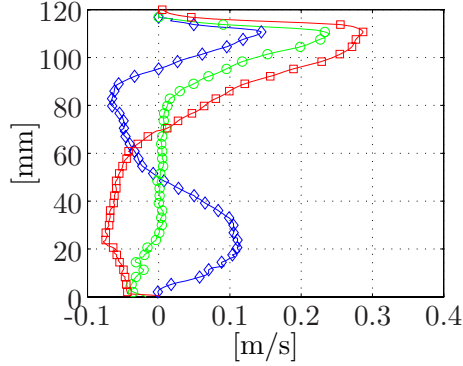


Figure 2.10: *Vertical velocity profiles 150 mm downstream the attraction channel, velocities acquired with PIV. \diamond = small depth. \circ = medium depth. \square = large depth*

layer is developed, as well as between the jet and the water flowing beside the channel. The area where the jet is detectable is where the fish will be attracted to the inlet, as suggested by Weaver (1963), who presented different water velocities to steelhead, chinook and silver salmon and showed that they choose to swim in the higher velocity. In the present set up the attraction water is detectable 100 mm downstream or 18 water depths over the bump (water depth over the bump is 5.7 mm).

The mixing layer is smoothed out with downstream distance. The surface horizontal profile is uniform 100 mm downstream. But the vertical profile is not uniform until 500 mm downstream. The reduction of the mixing layer in the vertical direction decreases the surface velocity so that it is slower than the surrounding velocities 500 mm downstream.

Measurements of the flow downstream the attraction channel has been visualized with PIV at three different water depths in the attraction channel. The fields of view investigated are shown in Figure 2.6 (position 5 and 6). The setup for the small depth is the same as for the setup with the LDV measurements. The results from the PIV measurements in Figure 2.10 show the same profile downstream the channel as for the LDV measurements. In Figure 2.12 the velocity field from the PIV measurements are shown. The wake downstream the channel is captured, it is seen that the water flow under the channel is directed upwards and some of the water is captured in the counter clock wise

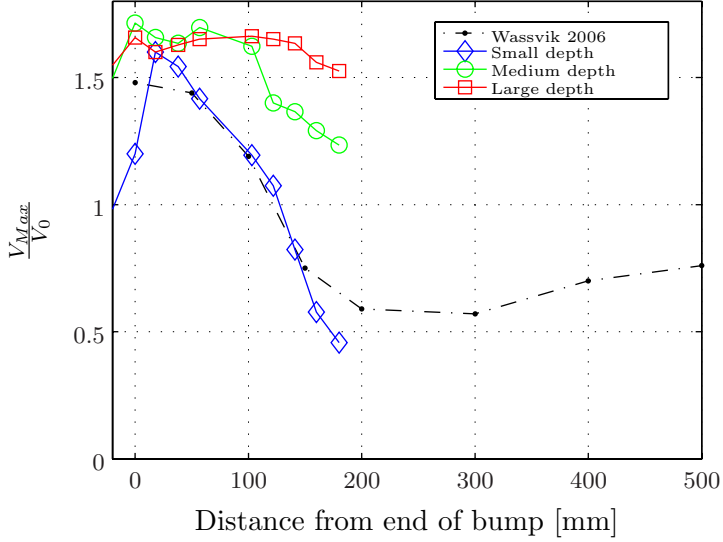


Figure 2.11: *Dimensionless maximum velocity downstream the attraction water. The downstream end of the attraction channel is at $x = 70$ mm.*

rotating eddy behind the bump, and some of the water is captured in clock wise rotating eddy further downstream the channel.

In Figure 2.11 the velocity increase measured with the LDV and PIV are compared, as the maximum surface velocity over the mean reference velocity. The measurements agree well 50 mm to 150 mm downstream the channel. The difference in the other parts is due to the measuring techniques. Over the bump the results from the PIV are difficult to extract due to strong reflections on the surface of the bump and in the water surface.

The result with different depths in the channel indicates that increasing the depth in the channel increases the traceability of the attraction water.

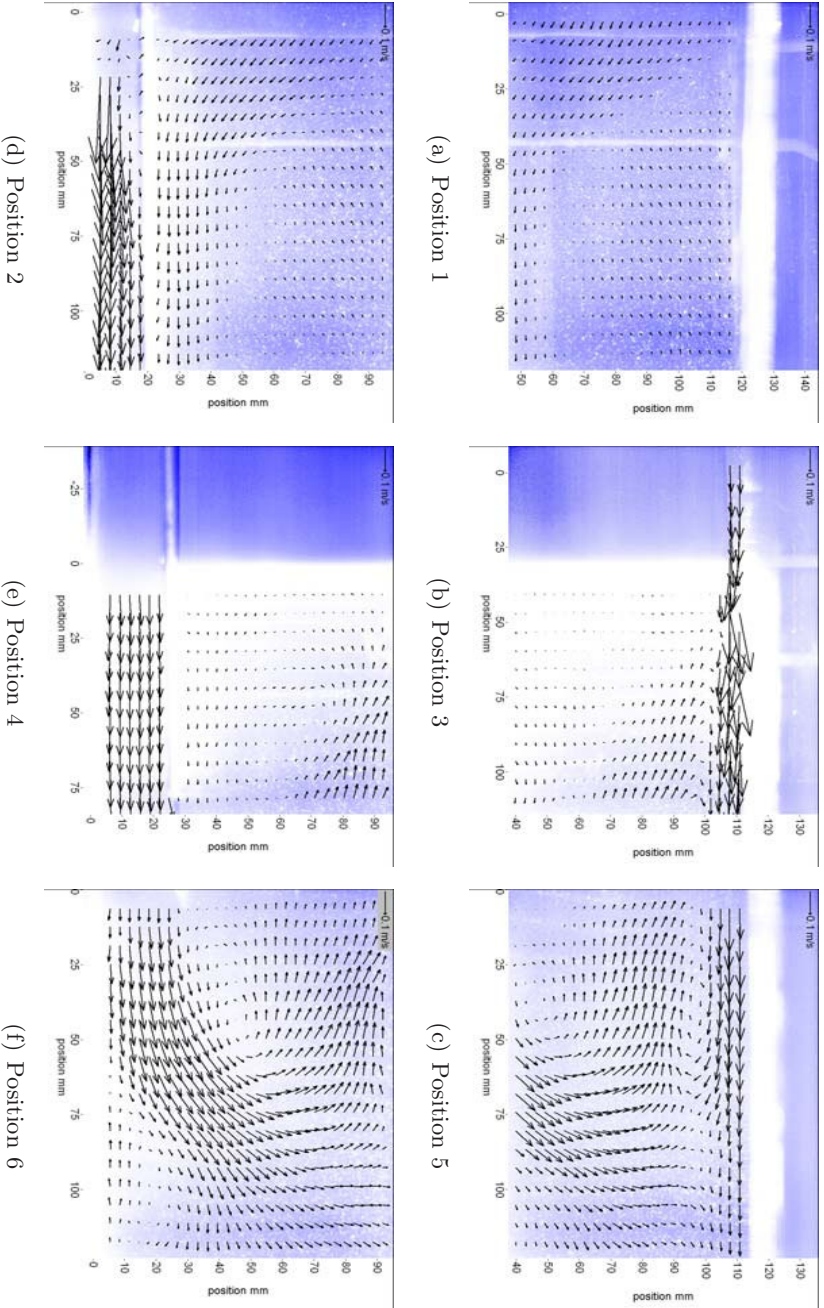


Figure 2.12: *PIV measurements of the flow in the attraction channel (cf. Figure 2.6) with 80 mm bump and 7 mm depth over the bump.*

CHAPTER 3

FIELD EXPERIMENTS

The concept of the attraction channel was investigated in full scale during the summers of 2004 and 2005 (**Paper D**). To investigate the fish attraction to the channel and the fish behaviour in the channel it was equipped with underwater cameras and monitored during three weeks each year during peak migration.

3.1 Study area

The study site during the field experiments was Sikfors hydropower plant in Piteå River in northern Sweden, see Figure 3.1. Sikfors is the only hydropower plant in the Piteå river and is situated 40 km upstream the coast. The mean annual discharge in the river is $158 \text{ m}^3/\text{s}$ and the power plant head is 19.5 - 21 m. The power plant is equipped with two 20 MW Kaplan turbines and the annual energy production is 185 GWh. The maximum flow rate through the power plant is $250 \text{ m}^3/\text{s}$ and excess flow is spilled through the spillways to the old river bed connecting the reservoir dam and the turbine outlet, cf. Figure 3.1a. From the turbines the water is transported via a tunnel to the outlet, ending in a 60 m vertical shaft. This results in a very complex and unsteady flow field in the turbine outlet area.

At the dam a pool and weir fishway helps the fish to pass the dam. To reach the fishway the fish need to swim 700 m up the old river, so during

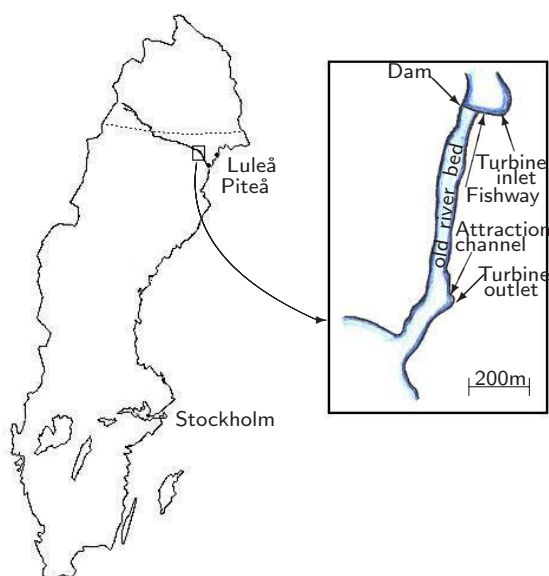


Figure 3.1: *Sikfors hydropower plant in Piteå river, Sweden. The attraction channel is located at the turbine outlet.*

fish migration (15 May - 15 October) a minimum of $15 \text{ m}^3/\text{s}$ is spilled over the dam, into the old river bed, cf Figure 3.1a. The fishway is 115 m long and has 45 pools, with a flow rate of $0.7 - 0.8 \text{ m}^3/\text{min}$. At the top of the fishway a fish counter records the fish passing through and the fish are via photographs manually species-defined. Other information from the fish counter is date, time and direction of the fish passing. The fish count in the fishway at the dam during 2004 and 2005 was (both salmon and sea trout) 1672 and 1446, cf Figure 3.1b and c.

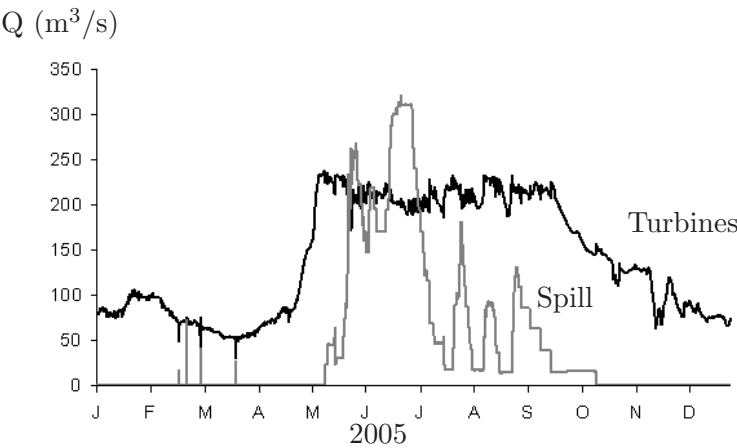
3.2 Attraction channel

The full scale attraction channel is a 3 m long aluminum U-shaped channel with a cross-section of $1.2 \text{ m} \times 1 \text{ m}$, cf. Figure 3.3. On the sides and under the bottom there are floating elements made of Styrofoam to reduce the need for lift support. In 2004 the channel was painted grey and in 2005 the channel was painted black. The channel was mounted on a concrete wall at the outlet from the power plant, cf. Figure 3.4. The channel was free to move in the vertical direction and locked in the horizontal direction.

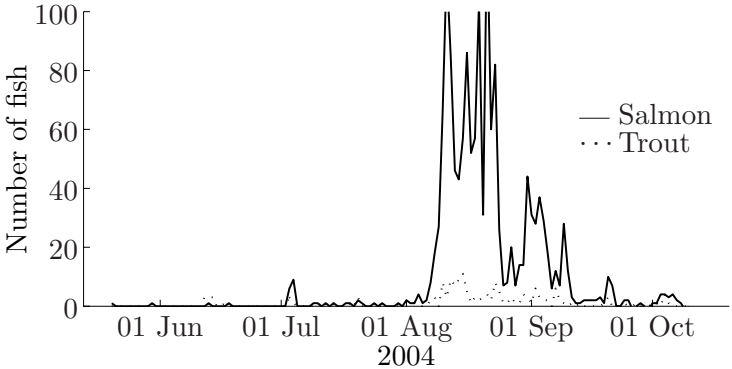
The bump in the downstream end of the channel is made of plywood and can easily be taken out for comparison test. The height of the bump was 0.51 m in 2004 and 0.65 m in 2005. Both bumps have a smooth shape and reach 1 m into the channel, cf. Figure 3.3. A small hand-driven crane was used to lift the channel in and out of the water to a platform on the river bank. The platform was used when working on the channel, the bump or cameras. Since the floating elements were not sufficient to keep the channel floating in the water the crane kept the channel at the right level in the water. In 2004 the channel was free to move in the upward direction when the flow from the turbines forced it in that direction, but in 2005 the channel was locked also in the vertical direction.

Instrumentation

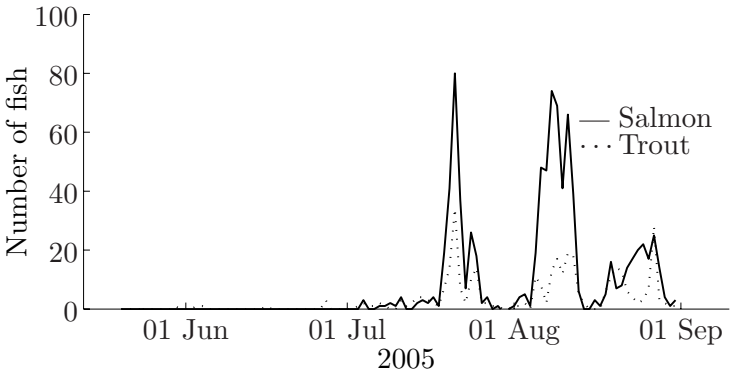
The channel was equipped with two digital underwater cameras to monitor the fish swimming through the channel; see Figure 3.3. One was mounted over the bump monitoring the inlet and one further upstream monitoring the whole channel. During the field tests cameras broke and were replaced; during parts of the project when only one camera was



(a) Flow rate through the hydropower plant and spillways in 2005.



(b) Number of salmon and sea trout passing the fishway in 2004.



(c) Number of salmon and sea trout passing the fishway in 2005.

Figure 3.2: *Flow rate and the number of salmon and sea trout passing the fishway at Sikfors hydropower plant in Piteå River, Sweden.*

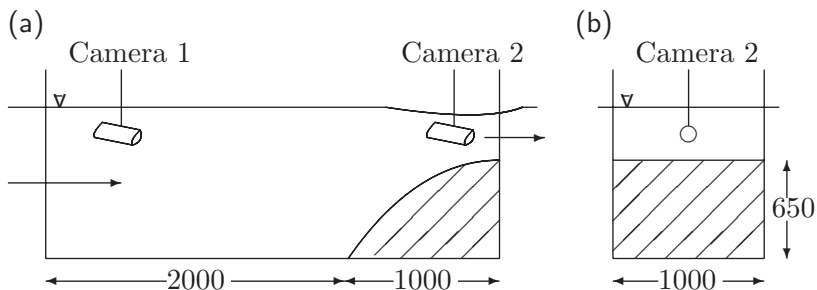


Figure 3.3: *Full scale attraction channel with underwater surveillance cameras (a) side view (b) front (entrance) view. All dimensions in mm.*

used it monitored the whole channel. Some of the cameras had infrared light, but under the prevailing conditions the infrared light had no effect on the quality of the recordings. No extra light was provided resulting in that no fish could be detected during the darkest hours (21.00 - 04.00). The cameras were continuously recording at three frames per second which were stored in a computer.

The water level at the turbine outlet was manually read on a fixed scale. Mean water level at the turbine outlet was 3.74 m (standard deviation of 0.11 m) during 2004 and 4.39 m (standard deviation of 0.3 m) during 2005. The flow and temperature data was provided by the power plant owner, Skellefteå Kraft. The air temperature was measured with a common outdoor thermometer. In 2005 the water visibility was measured with a white circular disk (diameter 4 cm) that was lowered in the water until it could not be seen, and the depth was recorded.

3.3 Measuring procedure and data processing

The channel was placed in the turbine outlet of Sikfors hydropower plant, with and without the bump, during three weeks each year, August 16 to September 5 in 2004 and August 9 to September 1 in 2005. During both years the measurements took place during peak migration in Piteå river (according to the fish counter at the dam, cf. Figure 3.1b and c). In 2004 the channel was in the water 6 hours per day. At 09.00 the channel was lowered into the water. The water depth in the channel was 22 cm over the bump. At 15.00 the channel was lifted out of the water. The bump was tested every second day and in between the channel was



Figure 3.4: *The full scale attraction channel in the turbine outlet at Sikfors hydropower plant.*

tested without bump, for comparison. The water depth in the channel without bump was 80 cm. In 2005 the channel was kept in the water for one week at a time. The test site was visited every other to third day and then the depth in the channel was adjusted; the water depth over the bump was 32 cm. The first and third weeks the channel was tested with the bump, the second week without the bump. The water depth in the channel without bump was 105 cm.

The recordings from the cameras were manually scanned for fish. For every fish entering the channel the date, time, swimming direction and fish direction was noted. Only fish swimming through the whole channel the right way (from inlet to outlet, head first) were counted. As the quality of the recordings is poor due to low visibility and the black attraction channel, salmon and trout could not be separated from each other. Occasional perch was not counted. The fish only spend a few seconds in the channel, and only a few spend longer time.

Since only cameras were used to monitor the fish and the fish just swam through the channel, the same fish could enter the channel repeatedly. Some of the fish had injuries that could be identified and at one occasion one of these fish swam through the channel several times.

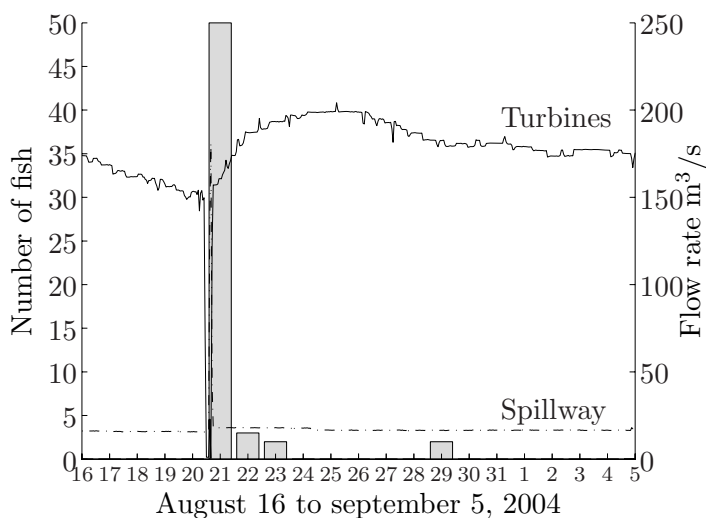


Figure 3.5: *Number of fish passing through the attraction channel in 2004 (bars) and the flow rate through the power plant and spillway.*

3.4 Results and observations

During the first field test in 2004 the attraction channel was painted grey and the camera houses were in aluminum. Most of the fish entering the channel that year did so during one day. On August 20 the power plant had an unplanned stop forcing all the water to the spillways and the old river bed; cf. Figure 3.5. The flooding in the old river bed caused the water to be turbid and in the turbid water 57 fishes swam through the attraction channel. During that day there were no bump in the channel. The observations from that year was that the fish only entered the channel during turbid conditions. This suggested that the channel was too light in color, or that the tests were performed when the fish were not actively migrating, since the channel was tested only during the day (09.00 - 15.00). However research indicates that salmon migrate between dusk and dawn or when the river is turbid (Laughton, 1989; Banks, 1969).

For the 2005 test the setup was painted black; channel, bump and cameras. And the test was conducted both day and night. This year a total of 471 fish passed through the channel, cf. Figure 3.6. The result is presented together with the amount of fish passing the counter in the

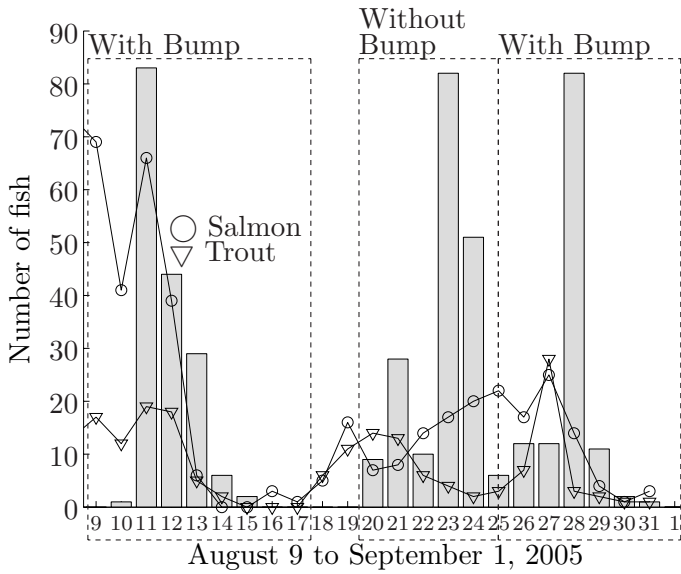


Figure 3.6: *Number of fish passing through the attraction channel in 2005 (bars) and the number of salmon and trout successfully passing through the fishway at the dam. 9-17/8 and 25/8-1/9 with bump in the channel, and 20-25/8 without the bump.*

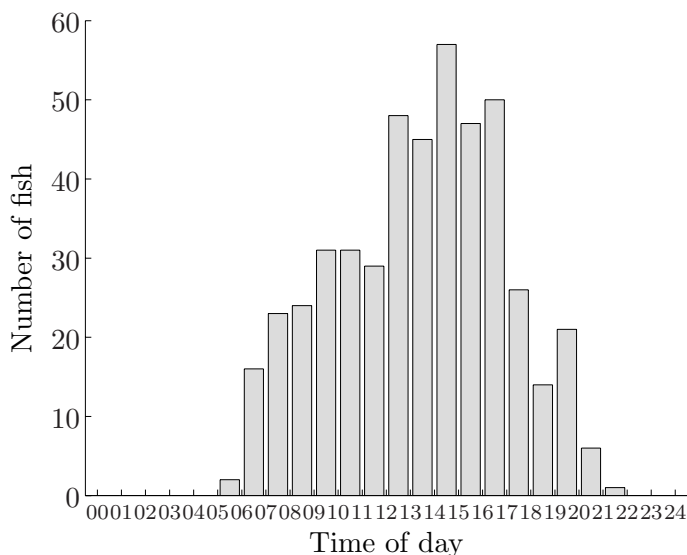


Figure 3.7: *Time of day when the fish passed through the attraction channel in 2005.*

fishway at the dam. It can be seen that the fish is swimming through the channel with good correlation to the number of fish using the fishway, and no difference can be seen between the days with and without the bump in the channel. If the inlet of the channel is considered there is a great difference between the two scenarios. When the bump is present in the channel the inlet depth is 32 cm, but without bump the inlet depth is 105 cm. This means that the number of fish per inlet area is bigger when the bump is in place. Both with and without the bump the fish swam through the channel close to the bottom floor.

The activity in the channel is shown in Figure 3.7. During the darkest hours no fish could be detected, but according to Figure 3.7 the peak activity in the channel is between 12.00 and 17.00, which means that the result from 2004 does not depend on the fact that the channel only was tested from 09.00 to 15.00. The greater number of fishes passing through the channel in 2005 is due to some other factor.

The visibility in the water was measured during 2005. The results indicate that the number of fish that swim through the channel does not correlate to the visibility in the water, cf. Figure 3.8. However, the results indicate that it is the color of the channel that makes the fish use

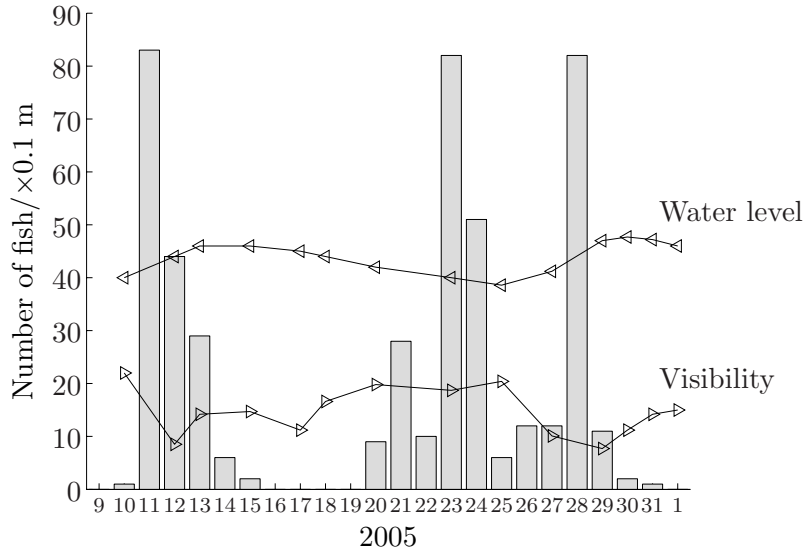


Figure 3.8: *Number of fish swimming through the attraction channel (bars) and the water level and visibility at the turbine outlet.*

the channel in 2005 and not in 2004.

CHAPTER 4

SIMULATIONS

The flow in the attraction channel has been studied using computational fluid dynamics (CFD). The numerical model was built from the model of the attraction channel used in laboratory testing. The goal was to investigate the blockage effect without the surrounding water flume, which influences the flow surrounding the attraction channel (**Paper E**).

The flow upstream Sikfors hydropower plant has also been numerically studied to evaluate the surface flow around a smolt guidance device (**Paper F**).

4.1 Computational fluid dynamics

Using numerical methods to determine a fluid flow has many advantages such as to be able to investigate problems where full- or model-scale measurements are difficult to perform, or not representative. Numerical methods are often more cost effective compared to full- and model-scale experiments. But one should have in mind that numerical solutions always are an approximation of the real case.

In computational fluid dynamics (CFD) the flow of interest is discretized and the partial differential equations (that in most cases can not be solved analytically) are solved iterative for the discrete points. When discretizing the fluid domain is subdivided into a number of

small control volumes by a grid (the finite volume method).

The solver used in this thesis is ANSYS CFX-11.0 where the unsteady Navier-Stokes equations are solved in their conservation form (CFX 11.0). These equations fully describe both laminar and turbulent flow without any additional information. But to be able to solve the flow for complex geometries with a reasonable grid size the equations must be averaged in such a manner that the unsteady structures of small scale is expressed as their mean effect on the flow in the so called Reynolds stresses. This is called the Reynolds Averaged Navier-Stokes (RANS) equation and the Reynolds stresses are modelled with a turbulence model. What kind of turbulence model appropriate to use depends on the flow studied. There are no universal turbulent model that work for all turbulence problems. The most common turbulence model is the $k-\varepsilon$ model where the Reynolds stresses are modelled with the velocity gradients of the flow and the eddy viscosity. The eddy viscosity is modelled with the two transport equations for k and ε , where k is the turbulent kinetic energy and ε is dissipation rate. Even though the model is robust, and can be used in a wide range of applications it has some weaknesses such as: poorly predicts mixing, flow separation, flow recovery following re-attachment, heat transfer, development of boundary layers etc. (Casey and Wintergerste, 2000). The shear stress transport model (SST) solves the $k-\omega$ at the wall and the $k-\varepsilon$ in the bulk flow (where ω is a frequency of the large eddys), which improves the prediction of separation.

The turbulence models most frequently used when studying a natural river is standard $k-\varepsilon$ or the Yakhot and Orszag (1986) RNG $k-\varepsilon$ turbulence model (Kiviloog, 2005; Rodriguez et al., 2004), where the RNG model performs better in flows with separation (Hargreaves et al., 2007).

Numerical simulations of river flows involve the modelling of the free surface. The surface can be heavily distorted as in a hydraulic jump, but in most cases the surface is relatively flat. Representing the surface can be done in many ways (Scardovelli and Zaleski, 1999), of which the simplest is to use a rigid lid approach where the water surface is represented by a wall with free slip (Meselhe et al., 2000). The rigid lid approach is acceptable to use when the surface elevations are smaller than 10 % of the depth (Rodriguez et al., 2004). Another common way of calculating the free surface is by the Volume-of-Fluid (VOF) method where the surface is represented by a volume fraction function equal to

1 in water and 0 in air, and the water surface is represented by numbers between 0 and 1 (Hirt and Nichols, 1981). A disadvantage when using the VOF approach is that the interface (surface) tends to be smeared out, so it is important to have a fine mesh at the surface.

Errors

The errors in a numerical solution can be divided in three parts (Ferziger and Perić, 2002):

Modelling error. For many phenomena where exact equations are not available or numerically feasible to use (e.g. turbulence) the solution will always be an approximation of reality. Modelling error also contain errors due to simplifying the geometry or boundary conditions.

Discretization error. The accuracy of a numerical solution always depend on the quality of the discretization. Discretization error is also called truncation error which is the difference between the discretized equation and the exact equation. The discretization error tends to zero as the grid spacing tends to zero. The solution should always converge to a grid independent solution.

Iteration error. The iterative method must always run for a long time to obtain the exact solution of the discretized equations.

If the equations are solved exactly (the discretization and iteration error negligible) the solution is still an approximation. To validate the model (evaluate the modelling error) the solution must be compared with experimental data or more accurate models.

The European Research Community On Flow, Turbulence And Combustion (ERCOTAC) has published a "Best Practice Guidelines" on quality and trust in industrial CFD (Casey and Wintergerste, 2000). Some of the recommendations are listed here:

- a solution is converged if the round-off error is reached.
- monitor the solution in at least one point in a sensitive area to see if the region has reached convergence.
- grid element angles should be between 40° and 140° . Tetrahedral elements should tend to have their four angles equal.

- the aspect ratio (between the longest and shortest edge on an element) should not be larger than 20 - 100 in important regions of the flow. In non-critical regions and in the boundary layer the restriction may be relaxed.
- a grid dependency study is necessary to estimate the numerical error. At least three significantly different grid resolutions should be used. To evaluate the study, Richardson extrapolation can be used.
- first order schemes are acceptable at the start of the calculation, as it is more robust; when the solution starts to converge switch to a higher order scheme.
- a constant turbulence length scale for internal flows can be derived from a characteristic geometrical feature.

The mesh quality in the Piteå river model was studied as how the maximum surface velocity at the narrowest part of the river changed with respect to the grid size. The convergence was evaluated with a second order trend line and Richardson interpolation; the approximate error due to the grid was 4.7 % and 2.3 %, respectively. The iterative convergence for the model of the Piteå River is 3-4 decades, following the suggestions of good convergence in CFX 11.0.

The mesh quality in the attraction channel model was studied using the depth and maximum velocity over the bump. The depth and velocity were compared with the results from the LDV measurements. The model differs 1 % in depth and 2 % in maximum velocity over the bump. The iterative convergence was judged using monitor points of the velocity over and behind the bump and under the channel. When the rms-values were 1×10^{-6} the monitor velocities were converged to the third decimal.

4.2 The attraction channel

When measuring the flow around the channel in the laboratory model, the flume influences the flow surrounding the attraction channel. Also, model experiments are very time consuming compared with numerical studies. The numerical setup aims to produce a model of the attraction channel which first is able to verify the experimental results, and then can be used to further investigate the flow in the channel. At first the

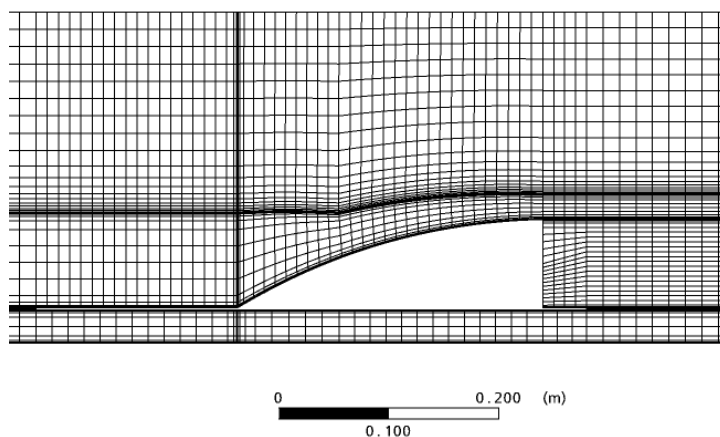


Figure 4.1: *The rough grid around the attraction channel (total number of nodes 588 996). In the model used the number of nodes was 1 698 828.*

influence of the flume walls is studied, but with a verified model of the channel other opportunities opens up. For example, the bump shape and operation of the channel can be optimized.

Model setup

The model of the attraction channel and the water flume used in the lab are modelled in scale 1:1. The numerical model stretches 1 m upstream the model attraction channel and 1 m downstream; the length of the channel is 0.5 m so the total length of the numerical model is 2.5 m. The cross-section of the model is 300 mm \times 300 mm, representing the 300 mm wide water flume and the water depth of 118 mm, plus air. The bump in the attraction channel is 80 mm high.

To investigate the effect of the flume on the blockage effect, the walls of the water flume are modelled with free slip. The walls are moved so the cross-section of the water is 8 and 16 times the cross-section of the attraction channel.

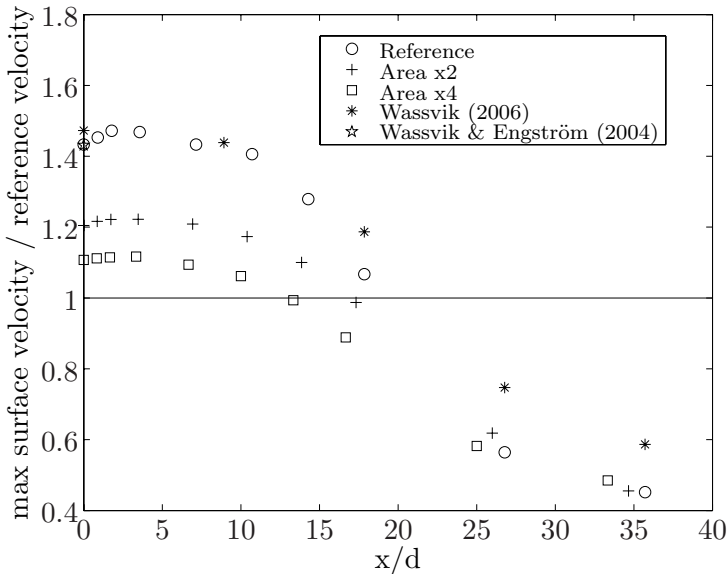


Figure 4.2: *Maximum surface velocity as a function of downstream distance. The velocity is normalized with a reference velocity for that case and the distance downstream is normalized with the depth over the bump.*

4.3 The attraction channel performance in a free stream

Figure 4.2 shows the results from the numerical calculations. The increase in velocity at the surface downstream the channel is shown as a function of downstream distance, normalized with the depth over the bump. The results indicate that the wider the free stream is compared with the width of the attraction channel the less amount of water flows through the attraction channel. As a consequence the water velocity out of the channel becomes lower.

4.4 Guiding downstream migrating smolt

At Sikfors hydropower plant in Piteå River (see chapter 3.1) a smolt guidance device is planned that will redirect the surface water away from the turbine inlets towards a surface spill (spillway B in Figure 4.3).

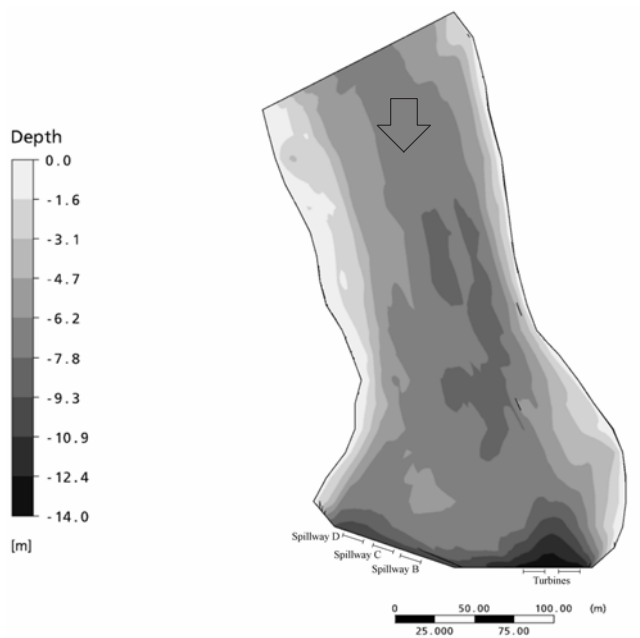


Figure 4.3: *Piteå River upstream Sikfors hydropower plant, flow from the top (inlet) to the bottom (outlets via turbines and spillways).*



Figure 4.4: *Smolt guidance device 1 and 10.*

The flow will be redirected with a non-permeable mechanical guiding device. The question is just: how should the device be designed to be able to guide the smolt? The mortality of smolt swimming through the turbines in Sikfors is about 20 % (Rivinoja, 2005). Ferguson (2008) calculated the mortality of smolt and kelt passing through turbines in Sikfors (Kaplan) and Stornorrfor (Francis) hydropower plants. The result shows that 90-95 % of the smolt and 55-75 % of the kelt survive the passage.

Downstream migrating smolt swim near the surface and follow the mainstream of the river (Moore et al., 1998). At Sikfors the smolt swim at a depth of 1-3 m (Rivinoja, 2005).

The smolt guidance device

To direct the flow towards the spillways, 10 different guiding devices are tested in a numerical flow model of the river upstream the power plant; device 1 and 10 are shown in Figure 4.4. The guiding devices have different length, depth and shape, but they are all tilted with 20° in the flow direction to mimic the flow induced force on the device, cf. Table 4.1. The criteria for the design of the guiding device are (the

Table 4.1: *Definition of the guiding devices investigated.*

Device	Length	Type	Depth	Surface water on the north side*
	[m]		[m]	[%]
1	80	Straight	2.5	31
2	80	Straight in sections	2.5	31
3	81	Bend in downstream end	2.5	31
4	98	Straight	2.5	32
5	101	Full bend with small radius	2.5	31
6	99	Full bend with large radius	2.5	30
7	133	Full bend with small radius	2	13
8	133	Full bend with small radius	1.7	11.5
9	123	Full bend with small radius	2	12
10	144	Full bend with small radius	2	8.5

*Measure of amount surface water (defined as the water surface and 2 m down) that passes the device between its upstream end and the northern (right) river bank.

surface flow is here defined as the free water surface and two meters down):

- I. the device should lead the surface flow towards the spillways in order to guide the smolt the same way.
- II. the device should be directed less than 45 degrees to the main direction of the surface flow. Bates and Vinsonhaler (1957) recommend an angle between 11.5° and 40° for louvers.
- III. there should be a prominent downwards acceleration of the water approaching the device. The scenario is then that the smolt will refuse to move under the device and instead migrate along it towards the spillways.
- IV. the acceleration of the flow on the upstream side of the device should otherwise be smooth and retardations should be avoided. This will facilitate the migration along the guiding device once the smolt have rejected to go under it.
- V. it should be practically possible to install the device in reality.

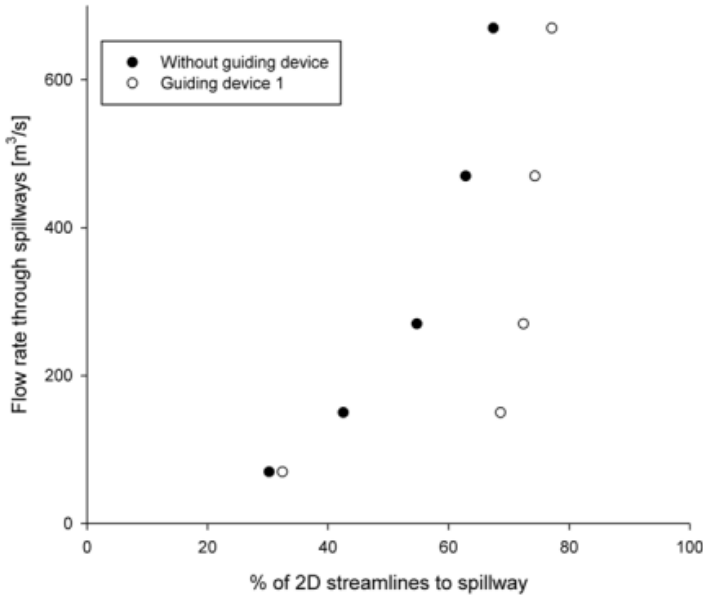


Figure 4.5: *Fraction of the surface flow that is directed towards the spillways for different flows, for guidance device 1 and without guidance device.*

Model setup

The river upstream Sikfors hydropower plant was modelled from measurements performed with a digital echo-sounder and GPS, (cf. Kiviloog, 2005). The flow was solved with ANSYS CFX-10 as a one-phase setup and the surface was represented with the rigid lid approach. The upstream inlet boundary condition and the outlets at turbine intakes and spillways are all modelled as plug flows. Five different flow scenarios were modelled ranging from a total flow of 320 m³/s to 920 m³/s, with at least 70 m³/s through the surface spillway B where the smolt is guided to. The average flow rate during smolt migration (May 20 to June 20) is 198 m³/s (Rivinoja, 2005).

4.5 The flow around the guidance device

When studying the results, two- and three-dimensional streamlines are used. The two-dimensional streamlines are assigned to a depth and represent the flow at that depth, three-dimensional streamlines denote the general flow in the domain. The two-dimensional streamlines are here used to resemble the smolt swimming path at a given depth. This is a rough way of representing the smolt motion, but gives an estimate of the effectiveness of the guidance device. The effectiveness is measured as the fraction of the surface flow that is directed towards the spillways. This is done by first looking for the dividing streamline between the flow headed for the turbines and the flow headed for the spillways and then measuring the upstream river width where streamlines (and smolt) head towards the spillways.

The flow around the simplest guidance device (device 1, cf. Table 4.1) show that the effectiveness depends on the flow rate in the river; cf. Figure 4.5. As the flow rate increases so does the guidance efficiency, both with and without guidance device. The focus is set on increasing the guidance efficiency for spilling 1, for which most can be gained with changing the design of the guidance device.

The most effective guidance device is device 10, for which the effectiveness is 93 %. The key to a successful guidance device can be shown by studying the interaction between the 3d streamlines and the device. Figure 4.6 shows the 3d streamlines for guidance device 10: it is seen that the streamlines touch the device. This means that smolt swimming along the device will end up in the streamlines headed for spillway B. The difference between the successful devices (4, 5, 7, 8 and 10 who all reach the streamlines headed for the spillways) is the distance between the upstream end of the device and the northern (right side in pictures) river bank, i.e. the longer the device the higher is the effectiveness.



Figure 4.6: *Flow around smolt guidance device 10, where 93 % of the upstream surface area directs smolt to the spillways. a) 2d streamlines at 1 m depth. b) 3d streamlines that end in spillway B.*

CHAPTER 5

SUMMARY

This thesis discusses an attraction channel, intended to further accelerate the attraction water out of a fishway and a smolt guidance device to direct downstream migrating smolt (and kelt).

The main purpose of the attraction channel is to increase the water velocity at fishway entrances, however other functions for the attraction channel could be to guide fish to an area where a fishway entrance is located or to use the same principle used in the channel and put a bump in a river bed in order to attract the fish to a river bypass.

The investigations regarding the attraction channel are divided in two major parts; how does the attraction channel work mechanically, and are the fish attracted to the channel? The work is based on the idea that salmon (and sea trout) are attracted to high water velocities. How and what fish are attracted to and what triggers the migratory behaviour is, however, not readily understood. Fish feel water velocities, pressure differences and temperature changes in the water very well (with the lateral line organ). What is known is that salmon are attracted to the outlet from hydropower plants (Arnekleiv and Kraabøl, 1996; Rivinoja et al., 2001) and if the salmon is presented to different water velocities they choose the higher one (Weaver, 1963). There are of course many other factors the salmon react to, such as water turbidity, cloud cover, wind direction etc. (Banks, 1969), and this makes it extra difficult to do experiments with fish, or any live animal. The field experiments in Sikfors gave two clear conclusions; firstly, the channel must be painted

dark, otherwise the fish won't use it. Secondly, the fish are attracted to the channel. The flow field at the turbine outlet in Sikfors is highly chaotic; the outlet tunnels from the power plant ends in a 60 m vertical shaft. When the channel is present in the outlet, it structures the flow even in the reference case with no bump. If this is why the fish used the reference channel or if this is the normal route of the fish is not clarified. Both during the reference run and the bump run the fish used the channel, even though the inlet height was only 0.32 m with bump compared with 1.05 m without. This gives an increase of three times more fish per area unit with the bump.

A model of the attraction channel was studied in a water flume using both LDV and PIV to explore the fluid mechanics of the channel. When studying the channel at a fixed depth with different heights of the bump the result show that the maximum velocity out of the channel compared to the surrounding velocity is achieved with an 80 mm bump. The increase is about 40 %, and a subsequent work showed that the velocity increase is present 18 water depth over the bump downstream the channel. However, when studying the same channel and the same bump at different depths the results indicate that the larger the depth is in the channel the longer is the velocity increase present downstream with preserved increase at the outlet of the channel. The larger momentum over the bump is probably why the traceability increases. In the model setup of the attraction channel the water flume is only three times wider than the attraction channel, which means that the blockage of the bump in the channel will force some of the water aimed for the channel to the outside of channel increasing the water velocity on the outside of the channel. To study the flow in the channel in an unbound environment, the channel and flume were modelled and the flow determined numerically. The walls of the flume were moved to create a larger cross-sectional area. The areas studied were 8 and 16 times larger than the cross-sectional area of the attraction channel. The results show that when increasing the surrounding area, less water flows through the channel and the water velocity out of the channel is lower. As a consequence of this the distance downstream where the velocity increase is present will also be shorter.

When studying the flow in the model channel at different depths, two patterns appear. For small and medium depth the flow circulates in the channel and the highest velocities are at the bottom; for the large depth there is a jet at the surface and the rest of the water is rather

stagnant. When measuring the velocities in the channel with LDV the pattern for large depth appears even though the depth was small. When reinvestigating the experiments it is found that the attraction channel is tilted in the PIV setup. This indicates that the flow pattern in the channel is sensitive to the angle. The fish that swam through the channel in the field experiment all swam close the bottom. If the fish did so because of the flow field is hard to tell, but as the fish is attracted to high velocities it is possible that they favored the high velocities there.

The attraction channel produces a surface-oriented water jet in the main flow direction and with low aeration. This should fit upstream migrating salmon and trout as they swim close to the surface (Rivinoja, 2005), are attracted to high water velocities (Weaver, 1963) and are discouraged by high aeration (Clay, 1995). A practical result is that the wider the channel is compared with the surrounding area the larger will the water velocity be out of the channel.

The results from the numerical model of the smolt guidance device show that it is possible to redirect the surface velocity towards a safer passage. The results were investigated by studying the dividing 2-dimensional streamline between the flow headed for the turbines and the flow headed for the spillways. In the most optimal design of the guiding device, 93 % of the river width will guide smolt towards the spillways and a safe route past the power plant. The results are based on the fact that smolt swim close to the surface and follow the main stream of the river if not disturbed. If this is the case the smolt movement can be compared with the 2-dimensional streamlines.

Questions that remain to be answered in the future are: How do we connect the channel with the fishway? What is the optimal design and operation of the attraction channel? This can be answered by studying the channel using for example the numerical model, but it can only be optimized to target variables such as velocity or turbulence level. This means that the fish favored flow must be known.

The smolt guidance device needs to be validated in a full-scale experiment, to see how the fish reacts when encountering it.

CHAPTER 6

DIVISION OF WORK

The division of work between the authors to the six papers are presented below. In August 2007 the author changed name from Wassvik to Lindmark.

Paper A

Model test of an efficient fish lock as an entrance to fish ladders at hydropower plants

Wassvik E.M. and Engström T.F.

Experimental work was performed by Wassvik. Error analysis was done by Engström. The paper was written by Wassvik and Engström.

Paper B

Attraction channel as an entrance to fishways - model assessment using LDV

Wassvik E.

All work was done by Wassvik under supervision of Gustavsson.

Paper C

Flow measurements in an attraction channel as entrance to fishways

Lindmark E.M., Green T.M., Lundström T.S. and Gustavsson L.H.

Planning and experimental setup was done by Lindmark and Green. Measuring was done by Green. Post-processing was mainly done by Green but in collaboration with Lindmark. The paper was written by all authors.

Paper D

Field study of an attraction channel as entrance to fishways

Lindmark E. and Gustavsson L.H.

The outline of the experiments was done by Lindmark and Gustavsson. The measurements, and post processing was done by Lindmark. The paper was written by Lindmark under supervision of Gustavsson.

Paper E

Numerical solution of the flow field in an attraction channel for migrating fish

Lindmark E.M.

All work done by Lindmark under supervision of Gustavsson and Marjavaara.

Paper F

Flow design of guiding device for down-stream fish migration

Lundström T.S., Hellström J.G.I. and Lindmark E.M.

Preprocessing and planning was done by Hellström and Lindmark. The simulations was done by Hellström, and postprocessing was mainly done by Lundström. The paper was written by all authors.

BIBLIOGRAPHY

- Adrian R. J. 1996. *Fluid Mechanics Measurements*, chapter Laser velocimetry, pages 175 – 299. Taylor & Francis, Washington, 2nd edition.
- Albrecht H.-E, Borys M, Damaschke N, and Tropea C. 2003. *Laser Doppler and Phase Doppler Measurement Techniques*. Springer, Berlin.
- Arnekleiv J. V and Kraabøl M. 1996. Migratory behavior of adult fast-growing brown trout (*Salmo Trutta*, L.) in relation to water flow in a regulated Norwegian river. *Regulated rivers: Research & Management*, **12**:39–49.
- Banks J. W. 1969. A review of the literature on the upstream migration of adult salmonids. *Journal of Fish Biology*, **1**:85–136.
- Bates D and Vinsonhaler R. 1957. Use of louvers for guiding fish. *Transactions of American Fisheries Society*, 86:38–57.
- Casey M and Wintergerste T. Best practice guidelines. Technical report, ERCOFTAC special interest group on "quality and trust in industrial CFD", 2000.
- CFX 11.0. ANSYS CFX release notes for 11.0.
- Clay C. H. 1995. *Design of Fishways and Other Fish Facilities*. CRC Press, Inc.: Boca Ranton.

- Ducharme L. J. A. 1972. An application of louver deflectors for guiding atlantic salmon (*salmo salar*) smolts from power turbines. *Journal Fisheries Research Board of Canada*, 29:1397–1404.
- Energy in Sweden. 2007. Energy in Sweden, facts and figures. Swedish Energy Agency, ET 2007:50.
- Erlandson E. 1988. *Lax & havsöring*. Naturia Förlag AB. ISBN 91-604-0147-8.
- Ferguson J. W. The behaviour and ecology of downstream migrating atlantic salmon (*salmo salar* l.) and anadromous brown trout (*salmo trutta* l.) in regulated rivers in northern sweden. Technical Report 44, Swedish University of Agricultural Sciences, 2005.
- Ferguson J. W. 2008. *Behavior and survival of fish migrating downstream in regulated rivers*. PhD thesis, No. 2008:23, Swedish University of Agricultural Sciences.
- Ferziger J. H and Perić M. 2002. *Computational methods for fluid dynamics*. Springer, Berlin, 3rd edition.
- Finnemore E. J and Franzini J. B. 2002. *Fluid mechanics with engineering applications*. McGraw-Hill, Boston.
- Forbes L. K and Schwartz L. W. 1982. Free-surface flow over a semicircular obstruction. *J. Fluid Mech.*, 114:299–314.
- Hargreaves D. M, Morvan H. P, and Wright N. 2007. Validation of the volume of fluid method for free surface calculation: the broad-crested weir. *Engineering Applications of Fluid Mechanics*, 1(2):136–146.
- Heggberget T. G. 1988. Timing of spawning in norwegian atlantic salmon (*salmo salar*). *Canadian Journal of Fisheries and Aquatic Sciences*, 45:845–849.
- Hirt C. W and Nichols B. D. 1981. Volume of fluid (vof) method for the dynamics of free boundaries. *Journal of Computational Physics*, 39:201–225.
- Johnson G. E, Adams N. S, Johnson R. L, Rondorf D. W, Dauble D. D, and Barila T. Y. 2000. Evaluation of the prototype surface bypass for salmonid smolts in spring 1996 and 1997 at lower granite dam on

-
- the snake river, washington. *Transactions of the American Fisheries Society*, 129:381–397.
- Kamula R. 2001. *Flow over weirs with application to fish passage facilities*. PhD thesis, University of Oulu.
- Kiviloog J. 2005. Three-dimensional numerical modelling for studying smolt migratin in regulated rivers. Licentiate thesis 2005:5, Chalmers University of Technology, Göteborg, Sweden.
- Laughton R. 1989. The movements of adult salmon within the river Spey. *Scottish Fisheries Research Report*, (41).
- Lundin B and Carles E. Protected nature 2004. Technical Report MI 41 SM 0501, Swedish enviromental protection agency and Statistics Sweden, 2006.
- Meselhe E. A, Weber L. J, Odgaard A. J, and Johnson T. 2000. Numerical modelling for fish diversion studies. *Journal of hydraulic engineering*, pages 365–374.
- Montén E. 1985. *Fish and turbines, fish injuries during passage through power station turbines*. Vattenfall, Stockholm.
- Montén E. 1988. *Fiskodling och vattenkraft*. Vattenfall,.
- Montgomery D. 2005. *Design and analysis of experiments*. John Wiley & Sons, Inc., Hoboken, 6th edition.
- Moore A, Ives S, Mead T. A, and Talks L. 1998. The migoratory behavior of wild atlantic sallmon (*salmo salar* l.) smolts in the river test and southampton water, southern england. *Hydrobiologia*, pages 295–304.
- Raffel M, Willert C. E, and Kompenhans J. 1998. *Particle image velocimetry, a practical guide*. Springer-Verlag, Berlin.
- Rivinoja P, McKinnell S, and Lundqvist H. 2001. Hindrances to upstream migration of Atlantic salmon (*Salmo Salar*) in a northern Swedish river caused by a hydroelectric power-station. *Regulated Rivers: Research & Management*, (17):101–115.

- Rivinoja P. 2005. *Migration problems of Atlantic salmon (Salmo Salar L.) in flow regulated rivers*. PhD thesis, No. 2005:114, Swedish University of Agricultural Sciences.
- Rodriguez J. F, Bombardelli F. A, García M. H, Frothingham K. M, Rhoads B. L, and Abad J. D. 2004. High-resolution numerical simulation of flow through a highly sinuous river reach. *Water Resources Management*, 18:177–199.
- Ruggles C. P and Ryan P. 1964. An investigation of louvers as a method of guiding juvenile pacific salmon. *The Canadian fish culturist*, 33:3–67.
- Scardovelli R and Zaleski S. 1999. Direct numerical simulation of free-surface and interfacial flow. *Annual review of Fluid Mechanics*, 31: 567–603.
- Schilt C. R. 2007. Developing fish passage and protection at hydropower dams. *Applied Animal Behavior Science*, (104):295–325.
- Taft E. P. 2000. Fish protection technologies: a status report. *Environmental Science & Policy*, pages 349–359.
- Vanden-Broeck J.-M. 1987. Free-surface flow over an obstruction in a channel. *Phys. Fluids*, 30(8):2315–2317.
- Čada G. 2001. The development of advanced hydroelectric turbines to improve fish passage survival. *Fisheries*, 26(9):14–23.
- Weaver C. R. 1963. Influence of water velocity upon orientation and performance of adult migrating salmonids. *Fishery Bull. Fish Wildl. Serv. U.S.*, **63**:97–121.
- Williams J. G. 1998. Fish passage in the Columbia river, USA and its tributaries: problems and solutions. In Jungwirth M, Schmutz S, and Weiss S, editors, *Fish Migration and Fish Bypasses*, pages 180–191. Fishing News Books.
- Yakhot V and Orszag A. 1986. Renormalization group analysis of turbulence. i. basic theory. *Journal of Scientific Computing*, 1(1):3–51.

Part II

Papers

PAPER A

Model Test of an Efficient Fish Lock as an Entrance to Fish Ladders at Hydropower Plants

Model test of an efficient fish lock as an entrance to fish ladders at hydropower plants

E.M. WASSVIK AND T.F. ENGSTRÖM

Division of Fluid Mechanics, Luleå University of Technology, SE-971 87
Luleå, Sweden

Abstract

Migrating fish that swim upstream in rivers for reproduction need to overcome obstructions, such as hydropower plants or similar. If a fish ladder is used to help the fish pass such an obstacle, water needs to be taken from the dam without first passing through the turbines. Also, the fish may have difficulties finding the fish ladder, due to the dominating flow from the turbine tailrace.

A fish lock, that uses turbine tailwater to entice the fish into the lock and further on to a fish ladder, is studied. The fish lock is a shallow open channel that uses a small fraction of the tailwater. A local acceleration of the flow is created by changing the cross sectional area of the lock channel.

Measurements are concentrated on how to design the lock so enough water passes through and a sufficient velocity increment is reached. This is investigated in a lab-scale model using laser Doppler velocimetry. A full-scale prototype will then be tested at the Sikfors hydropower plant in the Pite river in Sweden.

1 Introduction

Fish ways and fish locks are used to create a passage for migrating fish at obstructions in their path to or from their spawning ground. One such obstruction is hydropower plants, where the water for fish ways or locks is usually taken from the dam without first passing through

the turbines. Thus, this water can not be used to generate electricity. Another problem is that the fish have problem finding the entrance to the fish way or fish lock due to the dominating flow from the turbine tailrace.

The principle of the present fish lock is to operate without any water directly from the dam, using only water from the turbine tailrace, thus reducing the amount of water taken from the dam without passing the turbines. The lock is an open channel that will be partly submerged in the turbine tailrace so that water can flow through it, and around it. At the entrance (downstream in the lock) a bump will reduce the cross sectional area of the lock, creating an increased speed at this point, which will attract the fish. The water depth in the lock will be kept constant by letting the lock follow the water surface level. This means that the lock will be self-regulating when discharge and water level changes in the turbine tailrace.

The fish lock will work as an entrance and a subsequent project will deal with the transport from the lock to the dam. The current project concentrates on finding how the highest speed increase of the water at the entrance is reached, by creating a model of the fish lock and studying it in lab-scale.

Steady 2-d flow over submerged bodies is a well studied area. However, the focus has been on wave phenomena. For instance, the wave generation of a submerged semicircular body has been studied by Forbes and Schwartz (1982) and Vanden-Broeck (1987). Wave generation over other shapes has been studied by Faltas et al. (1989) and Hanna (1993).

The performance of the lock is compared with classic inviscid 2-d theory, where a bump that causes critical flow over it, will also create the highest velocity increase. In this case, where the fish lock only covers a small area of the tailrace, no damming of the water surface can occur. Instead, the flow rate will decrease inside the fish lock if the bump height is increased beyond the critical height.

The entrance speed to the lock must be related to the fish swimming capacity. The recommended speed at the entrance is 1.2 m/s for pacific salmon (cla). The fish lock in this project will be tested at the Sikfors hydropower plant (40 MW) in the Pite river in Sweden and the fish in that river, that use fish passages, are mainly salmon and salmon trout.

Fish swimming speed is categorised in three speeds; cruising, sustained and burst speed (cla). It is important that the flow speed at the entrance is as high as possible, compared to the surrounding flow speed,

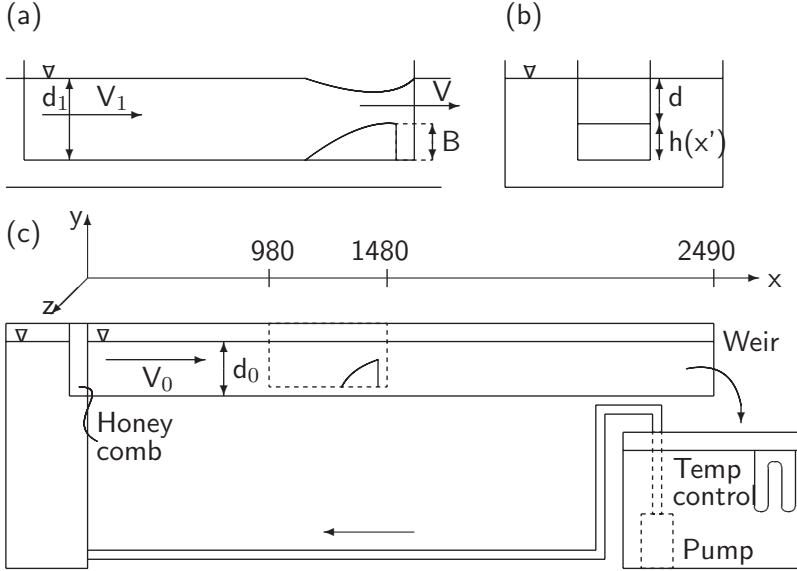


Figure 1: (a) Fish lock with bump. (b) Cross section of flume and fish lock. (c) Experimental setup of water flume with fish lock. All dimensions in mm.

in order for the fish to find it without being higher than the fish's burst speed.

2 Experimental setup

The method used to study this problem was to make a model of the fish lock and experimentally study its behaviour. The lock was partly submerged in a water flume representing the turbine tailrace. To study the behaviour, laser Doppler velocimetry was used to measure the velocity distribution in the water.

2.1 Water flume with fish lock

The water flume is a 2490 mm long, horizontal open channel made of 10 mm Plexiglas with a cross section of 200×300 mm, see Figure 1. At the inlet of the flume, there is a honeycomb to provide a more uniform velocity distribution. The honeycomb is 75 mm thick and the holes have

a diameter of 7.6 mm. At the outlet of the flume there is a V-notch weir to control the flow rate. The system was driven by a pump at the flow rate of $5.3 \times 10^{-3} \text{ m}^3/\text{s}$ ($\pm 1 \%$). The water depth, d_0 , was $118 \pm 1 \text{ mm}$ at $x = 2078$. The Reynolds number in the flume was $\text{Re} = U \times d_0 / \nu = 18000$.

The initial flow field in the flume was mapped with velocity profiles in the vertical and horizontal direction. The profiles were taken at $x = 459, 1097$ and 2154 , with no lock in the flume. The profiles showed a typical flow field for an open channel, with developing boundary layers.

The model of the fish lock is an open channel made of 1.7 mm glass, see Figure 1. The lock is 500 mm long with an inner cross section of $200 \times 96 \text{ mm}$. The lock was placed in the center of the flume, 30 mm over the bottom and 980 mm from the inlet. The area reduction in the lock is a bump made of Styrofoam with a plastic film glued to the top, to create a smooth surface. The shape of the bump is given by

$$h(x') = B - \frac{\tan^2(\pi/6)}{4B} x'^2 \quad (x' \geq 0, h \geq 0) \quad (1)$$

where B = the highest point of the bump. The bump is cut off at $x' = 0$ (Figure 1a), creating a steep end at the downstream end and a smooth slope at the up-stream end. The bump heights were 22, 34, 47, 70 and 80 mm. The bump was placed 40 mm from the outlet of the lock, to be able to measure the velocity over the bump using LDV.

2.2 Instrumentation

The flow rate in the channel was monitored with a V-notch weir, with the flow rate given by (ISO 1438/1-1980, 1980):

$$Q = \mu \sqrt{2g} \tan(\theta) \frac{8}{15} s^{5/2} \quad (2)$$

where μ = correction factor; θ = angle of the V-notch; and s = height of the water over the notch. The weir is made of 1.5 mm aluminium sheet, with a notch angle of $\theta = 75.3^\circ$. The correction factor $\mu = 0.74$, calibrated with a Danfoss MassFlo coriolis flowmeter (error $< \pm 0.5 \%$). The height of the water surface over the weir was measured with a calliper. The water temperature in the flume was controlled at $22.1 \pm 0.2 \text{ }^\circ\text{C}$ with a cooling system in the tank.

The velocities in the flume and lock were measured using laser Doppler velocimetry. The system is a two component setup from Dantec with

an 85 mm fiber optic probe. A beam expander (1.98) was fitted to the probe to reduce the measuring volume. The focal length of the front lens was 310 mm and the resulting measuring volume was 0.076×0.838 mm for the streamwise velocity component (514.5 nm) and 0.072×0.761 mm for the vertical velocity component (488 nm). The probe is fitted to a three-coordinate traverse system controlled by Dantec's BSAFlow software v.2 on a PC, that also controls the signal conditioning hardware. The seeding used in the water was polyamide particles with a mean diameter of $5 \mu\text{m}$ (Dantec's PSP-5). The system operated in backscatter mode and the hardware operated in non-coincident burst mode (spectrum analysis method).

2.3 Errors

Uncertainty in the measurements originates from the experimental setup and the measurement system. The setup has been carefully designed to yield stable experimental conditions. The measurement uncertainty is composed of uncertainty due to bias errors and precision errors. LDV measurements are associated with a variety of bias errors, such as error in the calibration factor, velocity bias, validation bias, angular bias and probe alignment/configuration bias. The system was setup to minimize the different bias errors. Velocity bias was compensated for by weighting each velocity sample with its residence time in the measuring volume.

The precision error was estimated by a repeatability test. Each profile was measured twice and the standard deviation of each pair of measurements was estimated to yield a 95 % confidence interval. The overall accuracy of the velocity measurements was $\pm 5 \%$, with locally larger errors close to the walls and the free surface.

2.4 Measuring procedure

Measuring points at the fish lock outlet were taken over the bump along a vertical line in the middle of the lock from the top of the bump to the water surface at $x = 1440$. At the same position along the x-axis, the data on the outside of the lock was collected from the bottom of the flume to the surface (between the lock and the flume wall) and under the lock along a vertical line in the middle of the flume. Measurements at the inlet of the lock were taken 48 mm from the inlet, inside the lock at $x = 1028$. Measurements were also taken along a horizontal line from the flume wall and through the lock.

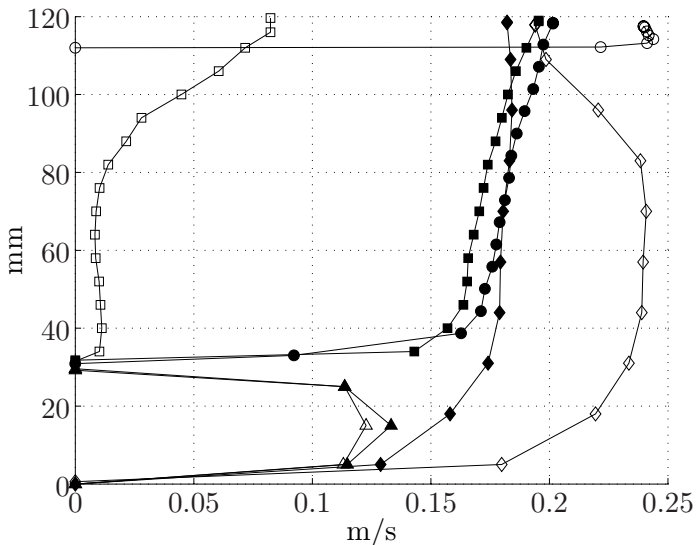


Figure 2: Velocity profiles for $B = 0$ mm (filled) and $B = 80$ mm. \diamond represents the velocities outside the lock, \triangle represents the velocities under the lock, \square represents the velocities at the inlet of the lock and \circ represents the velocities over the bump.

Approximately 55 points were acquired in random order for each bump. The sample time was 90-4500 s in each measuring point, and at least 10,000 samples were collected at each point.

3 Results and discussion

Results from two of the measurements are shown in Figure 2. The 80 mm bump, which gave the largest velocity increase, and the lock with no bump.

The velocity outside the lock, when there is no bump in the lock, is used as reference for measuring the velocity ratio over the different bumps. In the full scale test, the lock will only represent a small fraction of the total cross sectional area and the change in flow rate through the lock will not affect the velocity outside the lock significantly.

In Figure 2, it is seen that the velocity on the outside of the lock is higher for the 80 mm bump than for the measurements with no bump,

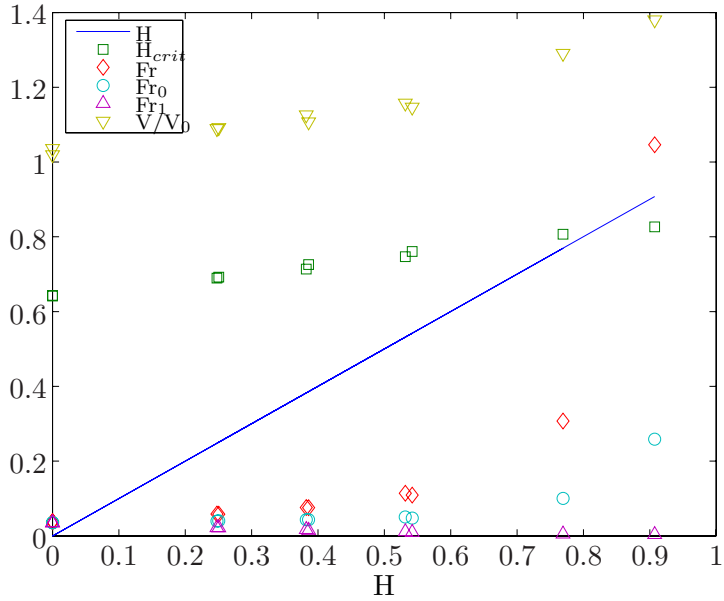


Figure 3: Results from the measurements where H is the dimensionless height of the bump and H_{crit} is the required height for critical flow over the bump based on Fr_1 , Fr , Fr_0 and Fr_1 are the Froude numbers over, beside and before the bump. V/V_0 is the speed ratio over the bump with respect to the speed outside of the lock without the bump.

due to the blockage effect by the lock that forces more water to the outside of the lock. The velocity at the upstream end of the lock also shows the blockage effect. The velocity is much lower for the 80 mm bump compared with the velocity for $B = 0$ mm. The upstream velocity is used to calculate Fr_1 , which can be used to theoretically calculate the height of the bump that gives critical flow over the bump.

The speed over the bump is the accelerated flow that the fish will be attracted to. As seen in Figure 2, the velocity for the 80 mm bump is significantly higher than the velocity on the outside of the lock for measurements with no bump, which indicates that the fish lock may produce an attractive flow for the fish.

In Figure 2 it can also be seen that the velocity under the lock does not change much for different bump heights.

The flow in the lock can be qualitatively described using the 2-d inviscid energy equation (Finnemore and Franzini, 2002)

$$\frac{\alpha_1 V_1^2}{2g} + d_1 = \frac{\alpha V^2}{2g} + (d + h) \quad (3)$$

where α , α_1 = kinetic energy correction factors; V , V_1 = mean velocities; d , d_1 = water depths and h = height of the bump, see Figure 1a,b. By using Equation 3 together with the continuity equation

$$q = V_1 d_1 = V d \quad (4)$$

and the upstream Froude number

$$Fr_1 = \frac{V_1^2}{g d_1}, \quad (5)$$

the height of the bump can be described as

$$H = 1 + \frac{\alpha_1 Fr_1}{2} - \frac{\alpha Fr_1}{2D^2} - D \quad (6)$$

where $H = h / d_1$ and $D = d / d_1$. Equation 6 has a maximum H_{crit} , where the flow over the bump is critical (local Froude number = 1). The maximum velocity ratio over the bump will be $V / V_1 = (\alpha \times Fr_1)^{-1/3}$.

For every bump, the critical height H_{crit} , of the bump is calculated. Figure 3 shows that H_{crit} increases as Fr_1 decreases with larger bump heights B , until critical flow is reached ($Fr = 1$). This is the point where

damming of the upstream water surface would occur, if the flow could only pass over the bump.

However, here the flow will be forced to the outside of the fish lock with maintained surface level upstream. An increase of the bump height at this point would decrease the flow rate through the fish lock. Even though the local acceleration would still increase, the overall acceleration would not. The maximum speed increase was 40 % for $B = 80$ mm (Figure 3). In the full-scale test it is important to take into consideration that the fish must be able to swim in to the lock, hence there must be a certain minimum water depth over the bump.

The blockage effect caused by the fish lock is partly due to the low Reynolds number in the model experiment. This effect will be smaller in the full-scale test, where the lock, and thus the Reynolds number, will be larger and the effect from the boundary layers will be smaller (the water velocity is approximately the same in the full-scale experiment as in the model test).

A small amount of damming occurs upstream the fish lock due to the blockage effect, which will counteract the deceleration inside the lock. This effect is considered small in the model test and will be insignificant in the full-scale test.

4 Conclusions

A model test of a new type of fish lock has been performed. Critical flow was reached over the bump and a significant acceleration of the flow was accomplished. Scale-up effects are thought to improve the performance of the fish lock.

References

- Faltas M, Hanna S, and el Malek M. A. 1989. Linearised solution of a free-surface flow over a trapezoidal obstacle. *Acta Mech.*, 78(3-4): 219–233.
- Finnemore E. J and Franzini J. B. 2002. *Fluid mechanics with engineering applications*. McGraw-Hill, Boston.

- Forbes L and Schwartz L. 1982. Free-surface flow over a semicircular obstruction. *J. Fluid Mech.*, 114:299–314.
- Hanna S. 1993. Free-surface flow over a polygonal and smooth topography. *Acta Mech.*, 100(3-4):241–251.
- ISO 1438/1-1980. 1980. Water flow measurement in open channels using weirs and venturi flumes - part 1: Thin-plate weirs.
- Vanden-Broeck J.-M. 1987. Free-surface flow over an obstruction in a channel. *Phys. Fluids*, 30(8):2315–2317.

PAPER B

Attraction Channel as an Entrance to Fishways -
Model Assessment Using LDV

Attraction channel as an entrance to fishways - model assessment using LDV

ELIANNE WASSVIK

Division of Fluid Mechanics, Luleå University of Technology, SE-971 87
Luleå, Sweden

Abstract

The flow field in an attraction channel, intended as an entrance to a fishway, is measured. The channel is open, U-shaped and uses a small fraction of the turbine tailwater. A local acceleration of the flow is created by decreasing the cross sectional area of the channel at its downstream end. The accelerated flow will attract the fish into the channel.

The flow field downstream the attraction channel is measured in a lab model using laser Doppler velocimetry. The results show that the velocity increase out of the channel can be detected up to 18 times the exit water depth of the channel. Further downstream, an interesting wake behavior in the near-surface region is observed.

1 Introduction

Fishways are used to create a passage for migrating fish at obstructions in their path to their spawning ground. One such obstruction is hydropower plants, where the water for fishways usually is taken from the dam without first passing through the turbines. Thus, this water can not be used to generate electricity. Another problem is that the fish have problems finding the entrance to the fishway due to the dominating flow from the turbine tailrace (Arnekleiv and Kraabøl, 1996; Rivinoja et al., 2001). This is especially the case when the fishway entrance is located away from the tailrace. The problem seems to be due to the preference of the fish to choose high velocity flows (Williams, 1998, adult salmon).

The principle of the attraction channel studied in this work is to operate with water directly from the turbine tailrace (or any other free stream), thus using all water for energy production. The channel is open at top (U-shaped) and is partly submerged in the turbine tailrace so that water can flow through and around it. At the flow exit a bump reduces the cross sectional area of the channel, creating an increased speed, which will (hopefully) attract the fish. The water depth in the attraction channel is kept constant by letting the channel adjust to the water level change in the turbine tailrace. The velocity increase over the bump in the attraction channel has previously been studied in the present model and showed an increase in water velocity of 38 % (Wassvik and Engström, 2004).

Steady 2-d flow over submerged bodies is otherwise a well studied area. The problem has been numerically studied by Forbes and Schwartz (1982), Vanden-Broeck (1987). Lamb (1932) describes the fundamentals of two-dimensional flow using the Bernoulli equation and this, together with the continuity equation, can be used when calculating the velocity over the bump (Forbes, 1988). But this will only work if all the water is passing through the attraction channel and over the bump. In this case, the water is free to also pass outside of the attraction channel. In fact, the device acts as a blockage to the uncoming stream if this has too low velocity. In addition, there is no consideration taken to friction in Forbes (1988) model.

For an attraction channel, the most interesting velocity field is downstream the channel since, this is what the fish will experience approaching the channel. Therefore, in this work we study the velocity field downstream the attraction channel and of particular interest is how far downstream the velocity increase is present. The study is done in a laboratory setup using the same model of the attraction channel as in earlier work (Wassvik and Engström, 2004) and laser Doppler velocimetry, to measure the flow field.

2 Experimental setup

A lab model of the attraction channel was built, and it was partly submerged in a water flume representing a free stream. To study the flow field, laser Doppler velocimetry was used to measure the velocity distribution in the water.

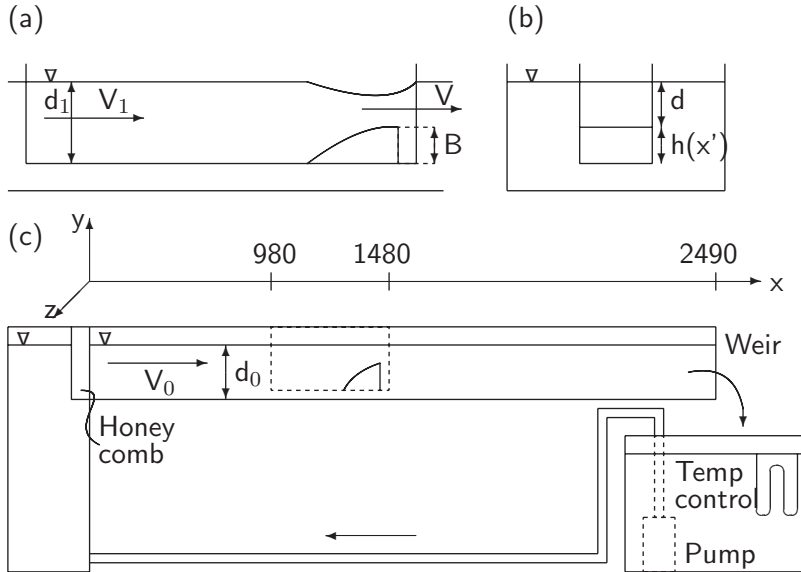


Figure 1: (a) Attraction channel with bump. (b) Cross section of flume and attraction channel. (c) Experimental setup of water flume with attraction channel and defining coordinate system. All dimensions in mm.

2.1 Water flume with attraction channel

The water flume is a 2490 mm long, horizontal open channel made of 10 mm Plexiglas with a cross section of 200×300 mm, see Figure 1. At the inlet of the flume, there is a honeycomb to provide a more uniform velocity distribution. The honeycomb is 75 mm thick and the holes have a diameter of 7.6 mm. At the outlet of the flume there is a V-notch weir to control the flow rate. The system was driven by a pump at the flow rate of $5.3 \times 10^{-3} \text{ m}^3/\text{s}$ ($\pm 1\%$). The water depth, d_0 , was 117 ± 1 mm at $x = 1530$. The Reynolds number in the flume was $Re = U \times d_0/\nu = 18000$. Profiles taken in the flume showed a typical flow field for an open channel, with developing boundary layers.

The model of the attraction channel is an U-shaped open channel made of 1.7 mm glass; see Figure 1(a). The channel is 500 mm long with an inner cross section of 200×96 mm. The channel was placed in the center of the flume, 30 mm over the bottom and 980 mm from the inlet; see Figure 1(c). The area reduction in the channel is a bump made of Styrofoam with a plastic film glued to the top, to create a smooth surface. The shape of the bump is given by

$$h(x') = B - \frac{1}{36B}x'^2 \quad (x' \geq 0, h \geq 0) \quad (1)$$

where B is the maximum height of the bump and x' originates at the peak and runs, in the negative x direction; cf. Figure 1(c). The bump has a smooth upstream slope and a vertical downstream end. The bump height, B , is 80 mm and its length 480 mm. The bump was placed 40 mm from the outlet of the attraction channel, so that the velocity over the bump could be measured with LDV. This is because both laser beams, measuring the streamwise velocity component, must pass through the wall of the channel.

2.2 Instrumentation

The flow rate in the flume was monitored with a Danfoss MassFlo coriolis flow meter (error $\pm 0.5\%$). The water temperature in the flume was controlled at 22.3 ± 0.3 °C by a cooling system in the tank. The velocities in the flume and attraction channel were measured using laser Doppler velocimetry. The system is a two component setup from Dantec with an 85 mm fiber optics probe. A beam expander (1.98) was fitted to the probe to reduce the measuring volume. The focal length of the

front lens was 310 mm and the resulting measuring volume was 0.076×0.600 mm for the streamwise velocity component (514.5 nm) and 0.072×0.569 mm for the vertical velocity component (488 nm). The probe is fitted to a three coordinate traverse system controlled by Dantec's BSAFlow software v.2 on a PC, that also controls the signal conditioning hardware. The seeding used in the water was polyamide particles with a mean diameter of $5 \mu\text{m}$ (Dantec's PSP-5). The system operated in backscatter mode and the hardware operated in non-coincident burst mode (spectrum analysis method).

2.3 Errors

Uncertainty in the measurements originate from the experimental setup and the measurement system. The setup has been carefully designed to yield stable experimental conditions. The measurement uncertainty is composed bias errors and precision errors. LDV measurements are associated with a variety of bias errors, such as error in the calibration factor, velocity bias, validation bias, angular bias and probe alignment/configuration bias. The system was set up to minimize the different bias errors. Velocity bias was compensated for by weighting each velocity sample with its residence time in the measuring volume. Parameter settings for the LDV system were optimized to achieve good signal quality and minimum bias on data.

The precision error was estimated by a repeatability test. The profile 50 mm downstream the model of the attraction channel was measured six times and the standard deviation of each pair of measurements was estimated to yield a 95 % confidence interval. The overall accuracy of the velocity measurements was $\pm 5 \%$ with lower accuracy in the low velocity areas in the mixing layer, where the velocities turn from positive to negative.

2.4 Measuring procedure

Velocity profiles in and around the attraction channel were taken at 0, 50, 100, 150, 200, 300, 400 and 500 mm downstream the channel in the water flume. At each position a vertical profile (in the middle of the flume) and a horizontal profile across the water flume (3 mm below the surface, at $y = 114$ mm) were captured. The vertical profile contains 15 measuring points, from 10 mm above the bottom to close to the water surface. The horizontal velocity profile contains 17 measuring

points. For the profile over the bump the measurements were taken from the wall of the water flume through the attraction channel and the last point was 8 mm outside the far side of the attraction channel. For the horizontal velocity profiles captured downstream the channel the same coordinates were used as in the profile over the bump. The vertical velocity profile captured under the bump contains three measuring points and the profile over the bump seven measuring points. Experimental data were extrapolated to all walls, assuming no-slip conditions.

The position of the walls was determined by placing the LDV measuring volume on the walls and using the coordinate system in the traverse system. The level of the water surface was measured similarly, but in this case the measuring volume was just below the water surface.

All measuring points were acquired in random order. The sample time was 120-360 s in each measuring point, and at least 10,000 samples were collected at each point.

3 Results and discussion

Figure 2 shows the velocity profiles in the attraction channel and water flume. The first profile represents water just out of the channel, over the bump. The mean velocity out of the model is 0.23 m/s. The surface velocity outside the attraction channel is 0.20 m/s, at the same position as the attraction water is 0.25 m/s; see Figure 2(b). With no attraction channel in the flume the mean velocity is 0.17 m/s, which compared to the mean attraction velocity of 0.23 m/s gives a increase in velocity of 35%. In Wassvik and Engström (2004) the increase was 38%. The increase in water velocity outside the channel is due to the blockage by the bump in the attraction channel, since the flow is subcritical in the channel. The blockage effect is accentuated in the lab test since the bump cross section is relatively large compared to the flume. However, in full scale, with the channel placed in a wide turbine tailrace, velocity increase outside the attraction channel will be small (Wassvik and Engström, 2004).

The flow out of the channel forms a jet at the water surface (this is the attraction water). Below the jet, a wake is formed and together they create a mixing layer in the vertical direction. At the same time a mixing layer is formed in the horizontal direction between the fast flowing jet out of the attraction channel and the lower velocities on the outside of the channel. The area where the jet is detectable is where

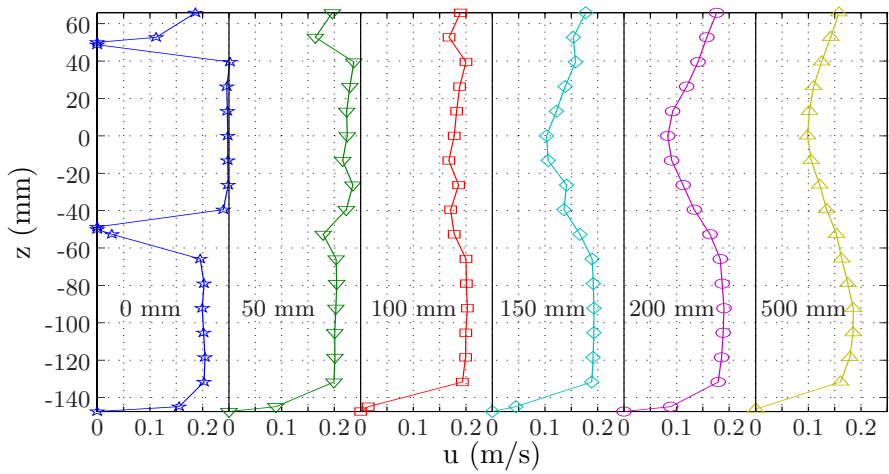
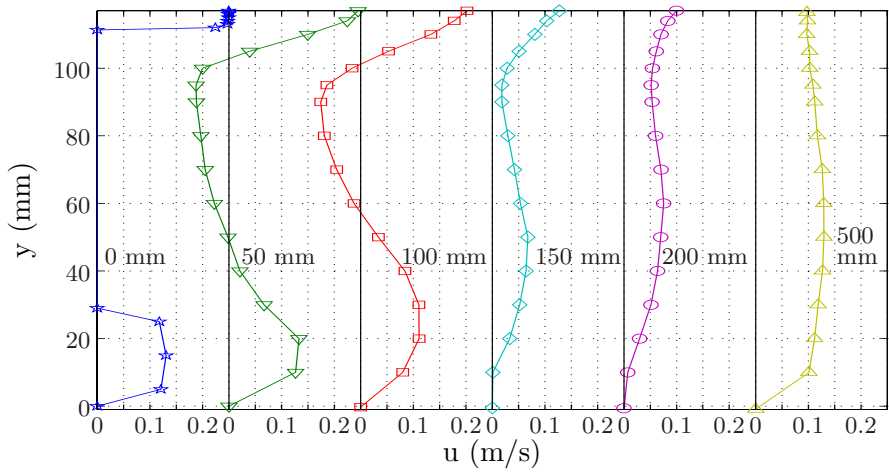


Figure 2: Velocity profiles over and downstream the bump.

the fish is supposed to be attracted to the channel, as motivated by Weaver (1963) who showed that steelhead, chinook and silver salmon choose the highest velocity if presented to water of different velocities. The jet is detectable 100 mm downstream the channel; cf. Figure 2(b), which corresponds to 18 times the water depth over the bump.

The mixing layers are smoothed out with downstream distance. First, the horizontal velocity becomes uniform 100 mm downstream the channel. But as the vertical profile does not become uniform until 500 mm downstream, the reduction of the mixing layer in the vertical direction decreases the surface velocity. A wake develops in the horizontal direction, this time with the center part (the former jet) slower than the rest.

Fishways in general work reasonably well if the fish finds the entrance (Northcote, 1998). Factors that stimulate the migration of fish are many, for example: flow rate, temperature, water quality, water depth, water turbidity and light (Banks, 1969). Clay (1995) states that highly aerated or turbulent water will discourage fish from entering a fishway. The present way of producing attraction water results in a smooth water jet with little aeration. The water in the jet is the same as in the surrounding water, so there is no temperature difference or quality change that will disturb the fish.

The attraction channel will only create accelerated flow near the surface. When migrating adult salmon approaching an outlet tunnel of a hydropower plant, they swim at a depth of one to four meters and most of them at one meter depth (Rivinoja, 2005). To generate a high velocity out of the attraction channel it is important to get as much water in the channel as possible. To maximize the amount of water the channel needs to be positioned in the streamwise direction. Karppinen et al. (2002) suggests that an inlet in the same direction as the main flow would increase the number of fish finding the inlet of a fishway. Due to the subcritical flow in the channel there is a blockage effect, and the velocity in the channel upstream the bump is very low (Wassvik and Engström, 2004). It is of interest, however, that despite this blockage there are portions of the existing flow with a higher velocity than the oncoming flow. How large this acceleration effect can be and how it is distributed calls for a more general study of blockage effects. Also, the channel needs to be tested in full scale to see if fish actually are attracted to it.

4 Conclusions

An attraction channel as entrance to a fishway is studied. The channel is U-shaped and partly submerged in a turbine tail race. To attract fish to the channel, the water is locally accelerated in the channel. This is done with a bump placed in the channel which reduces the cross-sectional area.

The downstream flow of the channel has been measured in a laboratory experiment using laser Doppler velocimetry. The results show that an increase in water velocity can be detected about 18 times the water depth at the bump of the channel.

The attraction channel has also been tested in full-scale at the outlet from Sikfors hydropower plant in the Pite river. The results of these tests will be reported separately.

Acknowledgements

The research presented in this paper has been done within the Swedish R&D programme “Hydropower - Environmental impact, remedial measures and costs in existing regulated waters”, which is financed by Elforsk, the Swedish Energy Agency, the National Board of Fisheries and the Swedish Environmental Protection Agency.

The author would like to thank Prof. Håkan Gustavsson and Dr. Fredrik Engström, Division of Fluid Mechanics, Luleå University of Technology, for helpful input on experimental setup and analysis of the results.

References

- Arnekleiv J and Kraabøl M. 1996. Migratory behavior of adult fast-growing brown trout (*Salmo Trutta*, L.) in relation to water flow in a regulated Norwegian river. *Regulated rivers: Research & Management*, **12**:39–49.
- Banks J. 1969. A review of the literature on the upstream migration of adult salmonids. *Journal of Fish Biology*, **1**:85–136.
- Clay C. 1995. *Design of Fishways and Other Fish Facilities*. CRC Press, Inc.: Boca Ranton.

- Forbes L. 1988. Critical free-surface flow over a semi-circular obstruction. *Journal of Engineering Mathematics*, 22:3–13.
- Forbes L and Schwartz L. 1982. Free-surface flow over a semicircular obstruction. *J. Fluid Mech.*, 114:299–314.
- Karppinen P, Mäkinen T, Erkinaro J, Kostin V, Sadkovskij R, Lupandin A, and Kaukoranta M. 2002. Migratory and route-seeking behaviour of ascending Atlantic salmon in the regulated river Tuloma. *Hydrobiologia*, 483:23–30.
- Lamb H. 1932. *Hydrodynamics*. Cambridge University Press, sixth edition.
- Northcote T. G. 1998. Migratory behaviour of fish and its significance to movement through riverine fish passage facilities. In Jungwirth M, Schmutz S, and Weiss S, editors, *Fish Migration and Fish Bypasses*, pages 3–18. Fishing News Books.
- Rivinoja P, McKinnell S, and Lundqvist H. 2001. Hindrances to upstream migration of Atlantic salmon (*Salmo Salar*) in a northern Swedish river caused by a hydroelectric power-station. *Regulated Rivers: Research & Management*, (17):101–115.
- Rivinoja P. 2005. *Migration problems of Atlantic salmon (Salmo Salar L.) in flow regulated rivers*. PhD thesis, No. 2005:114, Swedish University of Agricultural Sciences.
- Vanden-Broeck J.-M. 1987. Free-surface flow over an obstruction in a channel. *Phys. Fluids*, 30(8):2315–2317.
- Wassvik E and Engström T. 2004. Model test of an efficient fish lock as an entrance to fish ladders at hydropower plants. In *the Proceedings of the Fifth International Symposium on Ecohydraulics, September 12-17, Madrid, Spain*.
- Weaver C. 1963. Influence of water velocity upon orientation and performance of adult migrating salmonids. *Fishery Bull. Fish Wildl. Serv. U.S.*, **63**:97–121.
- Williams J. 1998. Fish passage in the Columbia river, USA and its tributaries: problems and solutions. In Jungwirth M, Schmutz S, and Weiss S, editors, *Fish Migration and Fish Bypasses*, pages 180–191. Fishing News Books.

PAPER C

Flow Measurements in an Attraction Channel as
Entrance to Fishways

Flow measurements in an attraction channel as entrance to fishways

*E.M. LINDMARK, T. M. GREEN, T. S. LUNDSTRÖM
and L. H. Gustavsson

Division of Fluid Mechanics, Luleå University of Technology, SE-971
87 Luleå, Sweden

*email: elianne.lindmark@ltu.se telephone: +46 920 491045 fax: +46
920 491047

Abstract

Upstream migrating fish need to find ways around obstacles, such as hydropower plants, on their route to the spawning grounds. To facilitate such passages different types of fishways have been developed. Although such devices by themselves are functional the up-stream migration is often stopped since the fish seem to be indifferent to the entrance of the fishway and instead move towards the turbine outlet where they fail to move forward. To avoid this scenario it has previously been suggested to employ a U-shaped attraction channel that accelerates a small fraction of the tailwater, or any free stream, to catch the attention of the fish to the fishway. The attraction channel has been successfully evaluated in field tests and it is therefore of importance to optimise further its performance. The local acceleration of the water is created by means of a bump which decreases the cross sectional area in the main flow direction. The flow through the channel is subcritical and the bump that accelerates the water may under certain circumstances also block some of the water flowing into the channel. In order

to find the optimum geometry a down-scaled model channel is placed in a water flume and flow fields in vertical planes directed along the flow are visualised using Particle Image Velocimetry (PIV). Results show that increasing the depth over the bump has little effect on the maximum velocity obtained while it makes the attraction water more perceptible downstream the channel.

Keywords: Fishway, Attraction water, Salmon, Migration, PIV

1 Introduction

When migrating fish, such as Atlantic salmon (*Salmo salar*) and sea trout (*Salmo trutta*), swim upstream rivers to spawn they encounter several barriers including water falls, weirs and hydropower plants. To guide the fish around such obstructions different kinds of fishways are often used. The problem with fishways is that the fish have problem finding the entrance (Northcote, 1998; Rivinoja et al., 2001; Williams, 1998). Common explanations for this are that the entrance of the fishway is poorly placed (i.e. not based on knowledge of fish preferences) and that the fish is attracted to the rapid water current from the power plants instead of the weaker current leaving the guidance device (Arnekleiv and Kraabøl, 1996; Webb, 1990). It has been shown that if chinook salmon, steelhead trout and silver salmon is subjected to two water velocities within a certain range, they choose the higher one (Weaver, 1963). The velocity can of course not exceed the fish maximum swimming capability and for Pacific salmon the recommended velocity of the attraction water is between 1.2 and 2.4 m/s (Clay, 1995).

One common solution applied in order to increase the attraction of a fishway is thus to increase the spilling from it. This, however, reduces the efficiency of the hydropower plant and it does not necessarily increase the velocity of the attraction water. The flow

characteristics behind three common fishways have been studied by Kamula (2001) who show that the flow behind the pool-and-weir fishway dives to the bottom while the flow from Denil and vertical slot fishways is more surface oriented. An alternative route is to increase the speed of the water without using any extra energy (i.e. no extra water will be supplied to the fishway). Such a route was taken in Wassvik and Engström (2004) by studying the flow in an attraction channel. The concept is that parts of the tail water from a hydropower plant, or any free stream, is lead into an open U-shaped channel where the water is accelerated by means of a contraction in the downstream end of the channel. This creates a water jet having a higher velocity than the surrounding water. For round water jets directed along, and located close to free surface it has been shown that the free surface do increase the decay rate of the jets as compared to unconfined ones (Madnia and Bernal, 1994; Liepmann, 1995). Still, the detailed flow around such jets, is not completely revealed although measuring techniques such as Particle Image Velocimetry exists (Murzyn et al., 2006). In particular very little is known about the behaviour of planar jets in this context. Such jets are obtained in Reichl et al. (2005) when the flow around a cylinder being close to a free surface is studied with Computational Fluid Dynamics. One result is that the average velocity between the cylinder and the free surface decreases with the Froude number. Another and even more interesting result is that this velocity has a maximum as to the distance between the cylinder and the free surface that is dependent of the Froude number. This shows that it is a potential to optimize the planar jet generated in the attraction channel in focus in this paper.

With the design tested it was shown that the speed of the water can be increased with as much as 38 % compared to the surrounding water velocity (Wassvik and Engström, 2004). Field tests of the attraction channel showed that fish do swim through the channel (Lindmark and Gustavsson, 2008). One observation made during the field experiments was that fish swimming through the channel did so close to the bottom of the channel; this will later be discussed in terms of the results in this report. In previous work on

the attraction channel the focus has been on the attraction water and not the surrounding water. Also the water flowing into the channel is blocked by the contraction; this blockage effect needs to be scrutinized in order to fully understand how the attraction channel works. It is therefore important to investigate further the function of the attraction channel and how it can be improved. Hence, in this work focus is set on how the depth of the channel influences the speed of the attraction water and how the detailed flow field within and down-stream the channel is composed. This is done by measurement in lab-scale using Particle Imaging Velocimetry (PIV). With PIV it is possible to capture instant velocity fields in arbitrary planes in the fluid. The technique is rather computational heavy and has therefore developed with the development of computer capacity. The technique has therefore lately been used to study complex flow fields around fish (Sakakibara et al., 2004; Siddiqui, 2007) and for instance detecting vortices in the wake region behind the fish. PIV has also been applied to open channel flow (Hyun et al., 2003; Agelichaab and Tachie, 2008) showing that PIV yields new results for the cases studied. The technique has however not to the authors knowledge been applied to study flow designs for fish migration.

2 Experimental setup

In order to measure the water velocity and to visualise the flow field in the attraction channel a model of it was constructed and placed in a water flume. The flume is 7.5 m long and has a cross-section of 295 mm \times 310 mm; see Figure 1. To create a uniform velocity distribution in the pure flume, i.e. the flume without the attraction channel model in place, a polymer honeycomb and a metal net were placed at the inlet. The honeycomb is 75 mm thick and the holes have a diameter of 7.6 mm. The net is made of 0.8 mm thick steel wire that is woven with a thread spacing of 2.5 mm \times 2.5 mm. The water depth in the flume was kept at 118 ± 1 mm with a weir at the outlet of the water flume. The water temperature was controlled to $20.1 \pm 0.6^\circ$ C and was supplied to

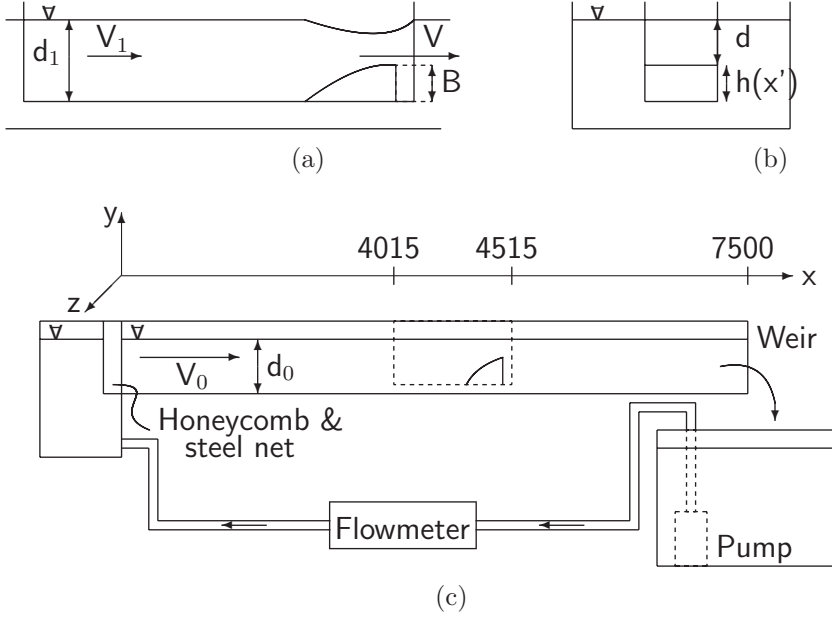


Figure 1: Schematic presentation of the experimental setup; all dimensions in mm. (a) The attraction channel with the bump. (b) Cross section of the water flume and attraction channel. (c) The flume as seen from the side.

the flume by a pump at the flow rate of $0.0056 \text{ m}^3/\text{s}$ resulting in an average speed of 0.2 m/s in the flume. The temperature and flow rate were monitored with a Danfoss MassFlo Coriolis flowmeter (error $< \pm 0.5 \%$); see Figure 1(c).

2.1 The attraction channel

The down-scaled model of the attraction channel is made from 1.7 mm window glass. The channel is 500 mm long, 100 mm wide and the sides of the channel are 200 mm high; see Figures 1(a)

and 1(b). At the downstream end of the channel a bump, made of Styrofoam, is placed to create the increase in water velocity that is of interest. A plastic film is glued on top of the bump to create a smooth surface and painted in a matt black colour to reduce reflections from the laser sheet. The channel was placed in the middle of the water flume and could be set at any depth in the flume. The bump has the shape of

$$h(x') = B - \frac{x'^2}{12B} \quad (x' \geq 0, h \geq 0) \quad (1)$$

where B is the highest point of the bump and x' originates at the highest part of the bump and runs upstream. According to Wassvik and Engström (2004), $B = 80$ mm gives the largest acceleration of the attraction water and is therefore used in this study. As seen in Figure 1(c) the bump has a vertical downstream end that is located 70 mm from the channel outlet. The attraction channel is placed 4015 mm downstream the steel net at the flume inlet.

2.2 Instrumentation

An attractive method to visualise and measure fluid flows in a two-dimensional plane is Particle Image Velocimetry, PIV. A simple PIV setup consists of a light source that illuminates the fluid flow of interest in the form of a thin light sheet. Seeding the fluid with tracer particles the fluid flow can be recorded as the particles pass the light sheet. Each of two recordings is divided into small interrogation windows where cross-correlation based on FFT is performed between respectively interrogation windows in the two pictures. The cross-correlation results in a velocity vector field of the entire measured plane, with every vector representing the statistical mean velocity for the corresponding interrogation window (Raffel et al., 1998). In order for the cross-correlation scheme to work optimally the tracer particles should not move more than 1/4 of the length of the interrogation window (Goldstein, 1996).

The PIV-system used is a commercially available system from LaVision GmbH. It consists of a Litron Nano L PIV laser, i.e. a

double pulsed Nd:YAG with a maximum repetition rate of 100 Hz, and a LaVision FlowMaster Imager Pro CCD-camera with a spatial resolution of 1280×1024 pixels per frame. The laser is mounted on a traverse so that the laser sheet and camera can be repositioned up to 500 mm in x-, y- and z-directions.

The tracer particles used, hollow glass spheres with a diameter of $6 \mu\text{m}$ from LaVision GmbH, are sufficiently small and have a density near to that of water allowing them to closely follow the motion of the fluid (Raffel et al., 1998). To get a sufficient spatial resolution an interrogation window size of 64×64 pixels with three multi-passes and decreasing window size to 32×32 pixels and 75 % overlap were used. The flow rate in the channel is about 0.2 m/s, hence the repetition rate of the laser is set to 50 Hz to satisfy the tracer particle motion condition for the selected size of the interrogation window.

2.3 Measuring procedure

The flow in the pure flume was characterised as to repeatability and velocity profile. The results of this served as a guide for the placement of the attraction channel. From the PIV measurements also the overall flow rate could be calculated. The measurements were performed for three depths of the attraction channel. The depths are given as the distance between the free surface and the highest point of the bump; see d in Figure 1(b). The depths were 7 mm, 13 mm and 20 mm. Further on these cases will be referred to as the small, medium and large depth.

The flow fields presented here are obtained in the middle of the attraction channel and for each water depth three positions in the channel are studied: the water inlet into the channel, the water outlet over the bump and the velocity field downstream the channel. To cover the whole area between the surface and the bottom of the flume it was necessary to reposition the camera at each depth which resulted in a total of six fields of view; see Figure 2.

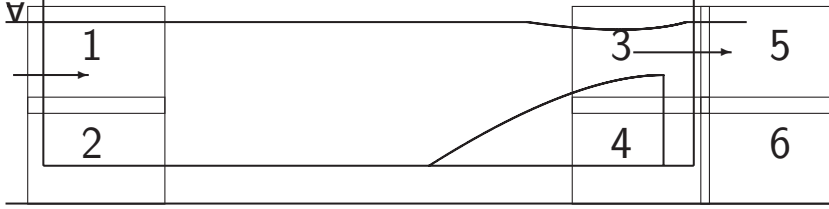


Figure 2: A schematic figure of the six fields of view in the attraction channel. The planes overlap to give a smooth transition when evaluating the flow field.

2.4 Errors

Due to instabilities of the free surface near the bump, and reflections from the light sheet in the surface, precise measures near the surface were rare. This artefact was compensated for by masking the area close to this border. This implies that this area is excluded from the vector calculations.

Since PIV is a statistical method, the sampling size matters and a larger number of pictures generally results in more accurate measurements. For these experiments the sampling size was empirically determined during the mapping of the flume to be 250 pictures. A control of the precision error was made by a repeatability test at three separate times.

3 Results and discussion

The measurements in the pure flume showed a developing velocity profile from the inlet and onwards. At $x = 4015$ mm the profile was found to be stable and repeatable enough (see Figure 3), indicating that measurements with the attraction channel could be made at this position.

The flow field naturally changes when the attraction channel is put into the flume. Main feature valid for all depths of the bump are that a jet is formed at the bottom of the flume under

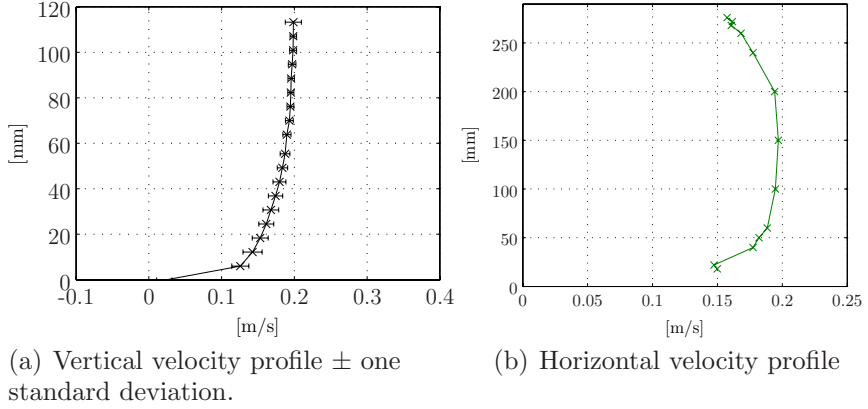


Figure 3: Velocity profiles in the pure flume 4015 mm downstream the net.

the attraction channel (although very weak for the largest depth), that an even stronger jet is formed over the bump and that the strength of the jets decreases in the flow direction, see Figure 4. The measurements also show that for the small depth there is a recirculation zone from the water inlet to the bump; see Figure 4 and 5(a). The recirculation hinders the water to freely enter the channel creating a blockage that forces the water to form a jet along the bottom of the channel. This blockage effect was also noticed for the medium depth, although not so distinguishable as for the small one. The jet formed along the bottom may explain that fish prefer to move near the bottom of the channel as observed in field tests by Lindmark and Gustavsson (2008). For the large depth the characteristics of the blockage was changed. The recirculating pattern has ceased allowing the water near the surface to flow more easily into the attraction channel; see Figure 5(b) and 6(a). Still the mean velocity is lower in the attraction channel than what it is in the pure flume.

When examining the downstream velocity profile near the bump (Figure 6(b)) it can be seen that the velocity profile peaks near the surface for all three depths. Interestingly, for the small depth,

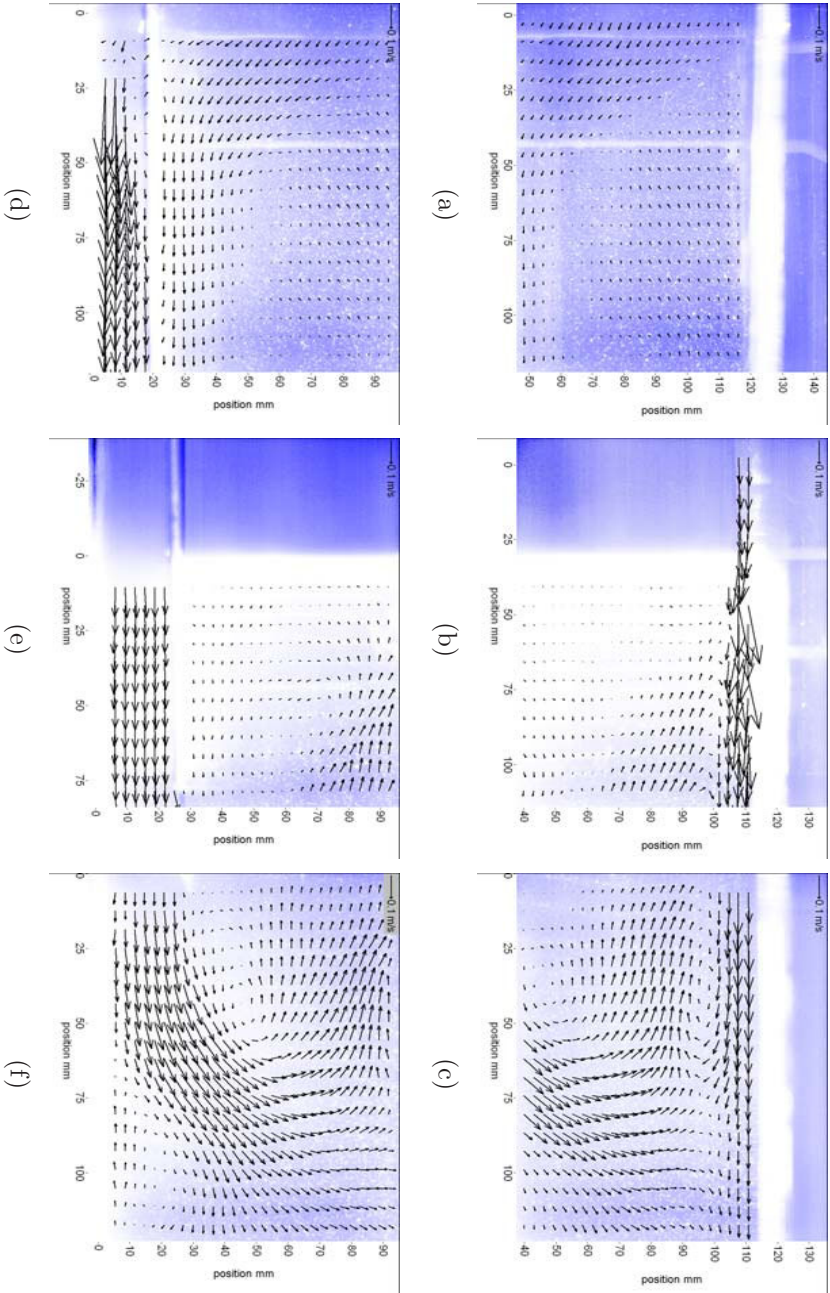


Figure 4: PIV measurements of the flow in the attraction channel (see Figure 2) with 80 mm bump and 7 mm depth over the bump.

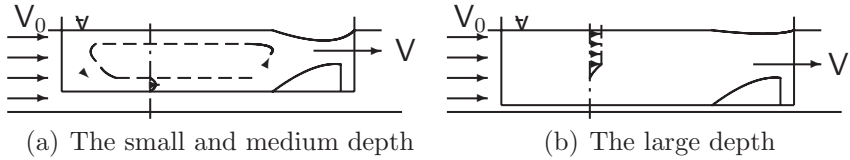
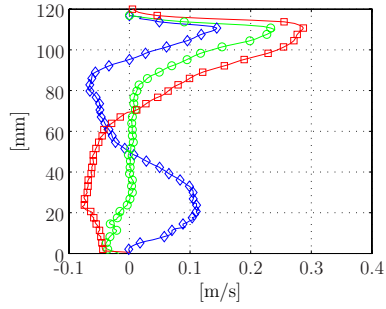
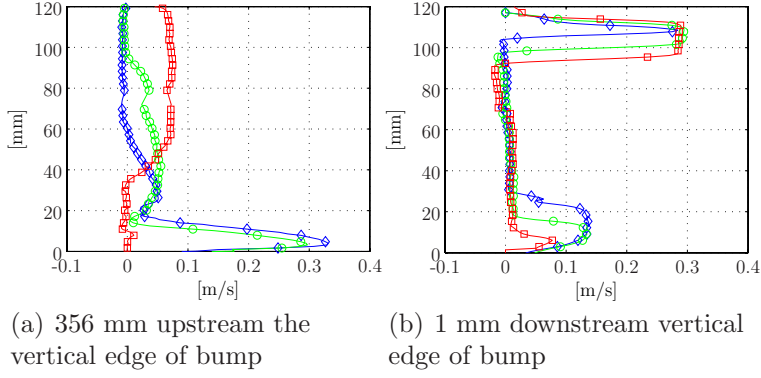


Figure 5: A scaled presentation of velocity distributions in the attraction channel. In figure (a) is the recirculation and bottom jet shown. In figure (b) is the velocity distribution drawn in a cross section.

150 mm downstream the bump some of the water moves opposite to the main flow direction; see Figure 6(c). If the hypothesis holds, that salmonids are attracted to high velocities, then this upstream flow would have a negative influence on the migrating fish if caught in that area. For the large depth this negative flow also appears but at a larger depth. Consequently, the attraction water has a larger area that entices the fish to swim through the attraction channel.

In order to quantify the speed of the jet leaving the attraction channel the maximum velocity is plotted as a function of position; see Figure 7 where the dimensionless form is obtained by dividing the maximum velocity at position x by the mean velocity before the attraction channel, $\frac{V_{Max}}{V_0} = f(x)$. As clearly seen the small depth is perceptible about 125 mm downstream the bump, corresponding to 18 times the depth over the bump (d in Figure 1(b)). Due to limitations in the traverse system the length of traceability could not be decided for the medium and large depth. It is however obvious that increasing the depth increases the downstream perceptibility of the attraction water. Decreasing the depth of the attraction channel even further would eventually result in that the jet becomes weaker as indicated in Reichl et al. (2005). Hence, a large depth should be chosen to obtain a larger perceptible area for the attraction water; see figure 6(c). In field the depth of the entrance (and the attraction water) should correspond to the swimming depth of the fish. For Atlantic salmon this has been studied by Rivinoja (2005), and the result showed upstream migrating salmon at a depth of one



(c) 150 mm downstream vertical edge of bump

Figure 6: Vertical velocity profiles at different positions in, and downstream the attraction channel. \diamond = small depth. \circ = medium depth. \square = large depth

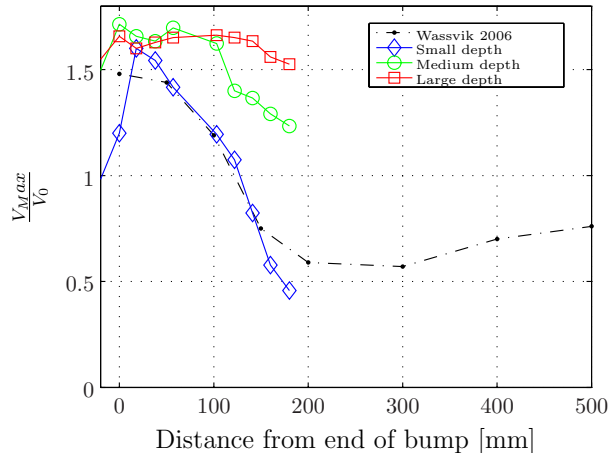


Figure 7: Dimensionless maximum velocity downstream the attraction water. The downstream end of the attraction channel is at $x = 70$ mm.

meter. This is consistent with Clay (1995) who recommends an entrance depth of 1.2 m for Pacific salmon. The measurements in Figure 7, obtained from Wassvik and Engström (2004) were performed at the same conditions as for the small depth case but with Laser Doppler Velocimetry, LDV. The deviation between the measurements from $x = -20$ to 50, where the jet is narrow, and 140 to 180 mm, where the jet is weak, in Figure 7 is due to differences in measuring techniques. LDV is a point measuring technique with good temporal resolution while PIV measurements yield instant velocity fields with good spatial resolution. Hence the LDV is more accurate representing the average speed in one point. Otherwise the velocity measurements from the techniques match supporting results in Hyun et al. (2003).

For the scaling of the model it is important to notice that gravity and inertial forces dominate. The Froude number is a dimensionless number, given by

$$Fr = \frac{V^2}{gd}, \quad (2)$$

describing the relation between these forces. Using Froude scaling

means that the Froude number is kept constant between the model and the full scale case. The Reynolds number is another dimensionless number depicting the ratio between the inertial and viscous forces. When using Froude number scaling it is important that the Reynolds number is sufficiently high (Cederwall and Larsen, 1976; Finnemore and Franzini, 2002). What a sufficiently high Reynolds number means is case dependent. Here, the Reynolds number in the model and the full scale model is 36 000 and 500 000, respectively. Hence it is judged that the criteria is fulfilled in this case.

To exemplify usage of Froude scaling on the attraction channel in a river with the surface velocity 0.5 m/s an attraction flow of 0.7 m/s is obtained using an attraction channel that is 1 m deep and has a bump height of 0.44 m.

4 Conclusion

A model test of an attraction channel as entrance to a fishway was conducted using PIV. The results show that the depth over the contraction does not affect the maximum velocity generated. On the other hand it is shown that the depth over the contraction has a significant effect on the downstream traceability of the attraction water. Increasing the depth over the contraction makes the attraction water perceptible further downstream from the attraction channel. It is even possible to trace the acceleration as far downstream as 18 times the depth over the contraction in conformity with previous results produced with LDV. It is also shown that the depth affects the characteristics of the blockage at the upstream inlet and the flow pattern inside of the attraction channel. Further tests are needed to investigate how the attraction channel will perform in an unbounded surrounding.

5 Acknowledgements

The research presented in this paper has been done within the Swedish R&D programme "Hydropower - Environmental impact,

remedial measures and costs in existing regulated waters”, which is financed by Elforsk, the Swedish Energy Agency, the National Board of Fisheries and the Swedish Environmental Protection Agency.

References

- Agelinchab M, Tachie M. F. 2008. Piv study of separated and reattached open channel flow over surface mounted blocks. *Journal of Fluids Engineering*, 130:205–206.
- Arnekleiv J. V, Kraabøl M. 1996. Migratory behavior of adult fast-growing brown trout (*Salmo Trutta*, L.) in relation to water flow in a regulated Norwegian river. *Regulated rivers: Research & Management*, **12**:39–49.
- Cederwall K, Larsen P. 1976. *Hydraulik för väg- och vattenbyggare*. LiberLäromedel. ISBN 91-40-54300-5.
- Clay C. H. 1995. *Design of Fishways and Other Fish Facilities*. CRC Press, Inc.: Boca Ranton, 2nd edition. ISBN 1-56670-111-2.
- Finnemore E. J, Franzini J. B. 2002. *Fluid Mechanics with Engineering Applications*. McGraw - Hill Higher Education, 10 edition. ISBN 0-07-112196-X.
- Goldstein R. J, editor. 1996. *Fluid mechanics measurements*. Taylor & Francis, 2 edition. ISBN 1-56032-306-X.
- Hyun B. S, Balachandar R, Yu K, Patel V. C. 2003. Assessment of piv to measure mean velocity and turbulence in open-channel flow. *Experiments in Fluids*, 35:262–267.
- Kamula R. 2001. *Flow over weirs with application to fish passage facilities*. PhD thesis, University of Oulu.

- Liepmann D. 1995. Why do streamwise vortices form at the top and bottom of a round jet moving parallel to a free surface? *Journal of Fluids Engineering*, 117:205–206.
- Lindmark E, Gustavsson L. H. 2008. Field study of an attraction channel as entrance to fishways. *River Research and Applications*, 24:564–570.
- Madnia K, Bernal L. 1994. Interaction of a turbulent round jet with the free surface. *Journal of Fluid Mechanics*, 261:305–332.
- Murzyn F, Mouaze D, Chaplin J. R. 2006. Flow visualization and free surface length scales measurements in a horizontal jet beneath a free surface. *Experimental Thermal and Fluid Science*, 30:703–710.
- Northcote T. G. 1998. Migratory behaviour of fish and its significance to movement through riverine fish passage facilities. In Jungwirth M, Schmutz S, Weiss S, editors, *Fish Migration and Fish Bypasses*, pages 3–18. Fishing News Books.
- Raffel M, Willert C, Kompenhans J. 1998. *Particle image velocimetry: a practical guide*. Springer. ISBN 3-540-63683-8.
- Reichl P, Hourigan K, Thompson M. C. 2005. Flow past a cylinder close to a free surface. *Journal of Fluid Mechanics*, 533:269–296.
- Rivinoja P. 2005. *Migration problems of atlantic salmon (Salmo salar L.) in flow regulated rivers*. PhD thesis, Swedish University of Agricultural Sciences.
- Rivinoja P, McKinnell S, Lundqvist H. 2001. Hindrances to upstream migration of atlantic salmon (salmo salar) in a northern swedish river caused by a hydroelectric power-station. *Regulated rivers: research & management*.
- Sakakibara J, Nakagawa M, Yoshida M. 2004. Stereo-piv study of flow around a maneuvering fish. *Experiments in Fluids*, 36: 282–293.

- Siddiqui M. H. K. 2007. Velocity measurements around a freely swimming fish using piv. *Measuring Science and Technology*, 18: 96–105.
- Wassvik E. M, Engström T. F. 2004. Model test of an efficient fish lock as an entrance to fish ladders at hydropower plants. In de Jalón & P. Vizcaíno D. G, editor, *the Proceedings of the Fifth International Symposium on Ecohydraulics, September 12-17, Madrid, Spain*, volume 2, pages 915–920. IAHR.
- Weaver C. R. 1963. Influence of water velocity upon orientation and performance of adult migrating salmonids. *Fishery Bull. Fish Wildl. Serv. U.S.*, **63**:97–121.
- Webb J. 1990. The behaviour of adult atlantic salmon ascending the rivers tay and tummel to pitlochry dam. Technical report, Scottish Fisheries Research Report.
- Williams J. G. 1998. Fish passage in the Columbia river, USA and its tributaries: problems and solutions. In Jungwirth M, Schmutz S, Weiss S, editors, *Fish Migration and Fish Bypasses*, pages 180–191. Fishing News Books.

PAPER D

Field Study of an Attraction Channel as Entrance
to Fishways

Field study of an attraction channel as entrance to fishways

ELIANNE LINDMARK & L. HÅKAN GUSTAVSSON

Division of Fluid Mechanics, Luleå University of Technology, SE-971 87
Luleå, Sweden

Abstract

A flow device that accelerates turbine tail water (or any free stream) to act as an attraction for migrating fish, is field tested. The device consists of an open (U-shaped) channel which accelerates the incoming flow by a local constriction of the cross-sectional area. The velocity increase has previously been investigated in a lab-scale model and an increase of 38% has been established. In the summers of 2004 and 2005, a full-scale prototype of the attraction channel was tested at the Sikfors hydropower plant in the Pite river in Sweden. The channel was equipped with underwater cameras to monitor and record the fish swimming through it. The tests show that the fish do swim through the attraction channel. During the same time period in 2004 and 2005, 57 and 471 fishes swam through the channel, respectively. The major change of the channel between the two years was that it was painted black for 2005.

1 Introduction

When migrating fish swim upstream in rivers to reach there spawning grounds they may be obstructed by hydropower plants or regulation dams. In order to pass these, fishways are often used. Because migrating adult salmon tend to seek out areas with higher velocities (Banks, 1969) this behavior is used to attract fish to the entrance of the fishway (Katopodis, 1990). It is important that the fish easily finds the fishway in order to reduce stress on the fish (Clay, 1995).

Due to the dominating flow from the turbine tailrace fish may have problems finding the entrance to the fishway (Arnekleiv and Kraabøl, 1996). In order for fish to find the entrance it is important where it is located. Clay (1995) points out the importance of placing the inlet as close to the obstruction as possible. Also the velocity of the attraction water is important. Weaver (1963) showed that steelhead, chinook and silver salmon choose the higher velocity if presented to different alternatives.

In this work the capacity of an attraction channel that uses a small fraction of a turbine tailrace (or any other free stream) to attract fish, is studied. The channel is U-shaped having an area reduction (a bump) in the downstream end. The water flowing through the channel is accelerated over the bump and fish are supposedly attracted to swim into the channel.

The flowfield in and around the attraction channel has previously been measured in a lab-model. The results showed an increase of 38% in water velocity compared to the oncoming free stream. (Wassvik and Engström, 2004). A subsequent work with the same model showed that the increase in velocity is detected downstream at a distance roughly 18 times the minimum water depth in the channel.

In the summers of 2004 and 2005 the channel was tested in full-scale, at the Sikfors hydropower plant in Pite river in Sweden. The migratory fish in this river are mainly Atlantic salmon (*Salmo salar*) and brown trout (*Salmo trutta*). The goal of this work is to determine if fish are attracted to the increase in water velocity produced by the channel.

2 Experimental setup

The attraction channel was tested in full-scale at Sikfors hydropower plant, Pite river, Sweden; cf. Figure 1. To monitor the fish in the channel underwater cameras were used.

2.1 Study area

Sikfors hydropower plant in the Pite river in northern Sweden is the only power plant in the river and is located 40 km from the coast. The power plant is equipped with two 20 MW Kaplan turbines, with a yearly production of 185 GWh. The head is 19.5 m and the maximum flow rate through the turbines is 250 m³/s. Excess flow pass through the spillways and into the old river bed. From the turbines the water is transported in

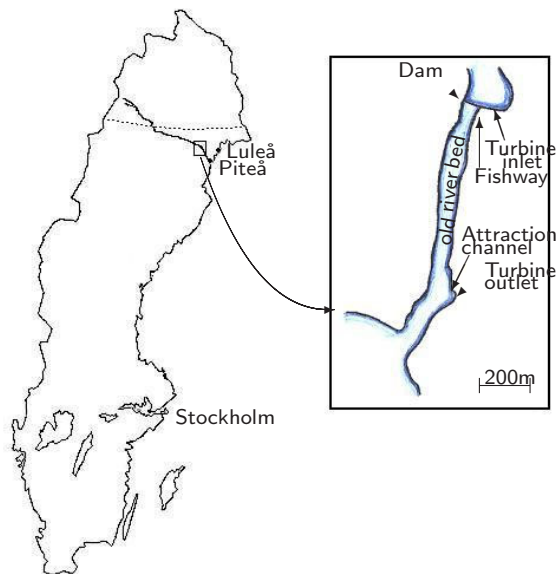


Figure 1: Sikfors hydropower plant, Pite river. The attraction channel is located at the turbine outlet.

a tunnel towards the outlet. The tunnel ends with a 60 m long vertical shaft. This results in a very complex and unsteady flow field at the outlet.

The outlet is located 700 m from the dam construction. At the dam there is a pool and weir fishway with a fish counter at the top. The fishway is 115 m long and has 45 pools. The flow rate in the fishway is 700-800 l/min. It is open from May 15 to October 15. During this time a minimum flow of 15 m³/s is released through the spillways. The spillway flow is needed to guide the fish up the old river bed into the fishway. Fish trapped in the old river bed, after the fishway is closed, is net-fished at the end of September and released back in the river.

Five photos are taken of every fish passing the counter in the fishway, and the fish is manually species defined. Other information available from the counter are date, time and direction of the fish passing. The operation of the fishway is the responsibility of the power plant owner, Skellefteå Kraft.

In 2004, 1513 salmon and 159 brown trout successfully passed Sikfors hydropower plant and in 2005 there were 1012 salmon and 434 brown trout.

2.2 The attraction channel

The attraction channel is an U-shaped aluminum construction. It is 3 m long, 1 m wide and 1.2 m deep; cf. Figure 2. Under the bottom and on the sides there are floating elements made of Styrofoam, to reduce the need for lift support. In 2004 the inside of the channel was painted grey and in 2005 the whole channel was painted black. The channel was mounted on a concrete wall at the outlet from the power plant. The channel was free to move in the vertical direction and locked in horizontal directions.

The bump at the downstream end of the channel is made of plywood and can easily be taken out for comparison test. In 2004 the bump was 0.51 m high and in 2005 it was 0.65 m high. Both bumps have a smooth shape on the upstream end and stretch 1 m into the channel; cf. Figure 3(a).

A small hand driven crane was used to lift the channel in and out of the water. Since the floating elements were not sufficient to keep the channel floating the crane kept the channel at the right water level. During 2004 this made the channel free to move upwards when the flow



Figure 2: The attraction channel mounted at the turbine outlet in 2005.

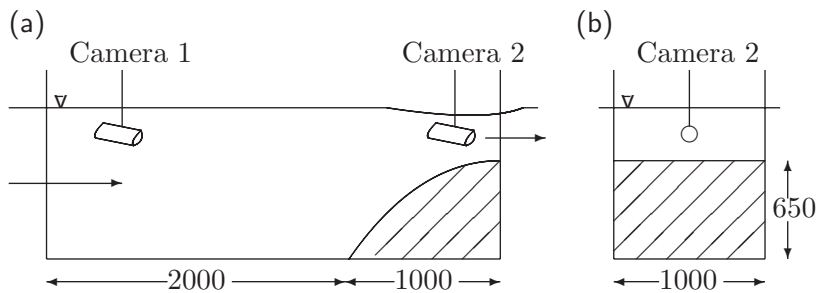


Figure 3: The attraction channel, side view (a) and front view (b). All dimensions in mm.

from the turbine outlet pressed the channel in that direction. In 2005 the channel was locked in position and was no longer moving vertically in the water.

2.3 Instrumentation

The attraction channel was equipped with underwater cameras. One camera was mounted monitoring the fish inlet (camera 2), and the other was mounted monitoring the whole channel (camera 1); cf. Figure 3. During the work some of the cameras broke and were replaced. During the parts of the project, when only one camera worked, it monitored the whole channel (camera 1). Some of the cameras used were equipped with infrared light, but under the prevailing conditions there was no effect of the light on the quality of the movie. The cameras were continuously recording three frames per second and were connected to a PC for storing. Since no extra light was provided (except the infrared light on some of the cameras) no fish could be detected during the darkest hours (21.00 - 04.00). The recordings were manually scanned at four times the actual speed. Only the fish that swam through the channel against the current, and did not turn around, were counted.

The water level at the turbine outlet was manually read on a fixed scale. Water temperature and flow rate, both through the power plant and through the spillways was provided by the power plant owner, Skellefteå Kraft. The air temperature was measured with a common outdoor thermometer.

During the work in 2005 the water transparency was measured by a visibility test. A white circular disc with a diameter of four centimeters was lowered in the water until it could not be seen, and the depth was noted (Laine et al., 1998).

2.4 Measuring procedure

The test was performed each year during three weeks of the migration season of salmon and brown trout. In 2004, the channel was in place from August 16 to September 5, six hours per day, from 09.00 to 15.00. It was tested alternating with and without bump, changing every day. In 2005 the channel was kept in place for one week at a time, from August 9 to September 1. The first and third week the channel was tested with a bump and the second week the test was performed without bump. In

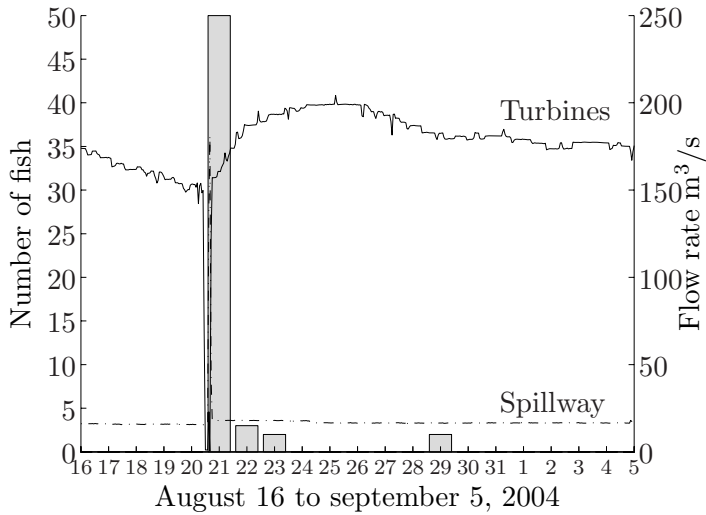


Figure 4: Number of fish passing through the attraction channel in 2004 (bars) and the flow rate through the power plant and spillway.

2004 the test site was visited every day and in 2005 the site was visited every other or third day.

The water depth in the channel was kept constant throughout the test. It was set to 80 cm at the flow inlet in 2004 and to 105 cm in 2005. The depth was set after testing different depths and measuring the lowering of the water level over the bump. In 2004 the depth at the bump was 22 cm and in 2005 it was 32 cm.

3 Results and discussion

Figure 4 shows the amount of fish passing through the attraction channel in 2004, together with the flow from the turbine outlet and spillway. A total of 57 fish passed through the channel in 2004. Most of the fish passed during one day, August 21. That day there was no bump in the channel. The day before (August 20) a stop in the power plant directed all the water in the river over the spillway (from 11.00 to 17.00); cf. Figure 4.

The days when fish were swimming through the channel the water was turbid and that suggested that the channel may be too light in color,

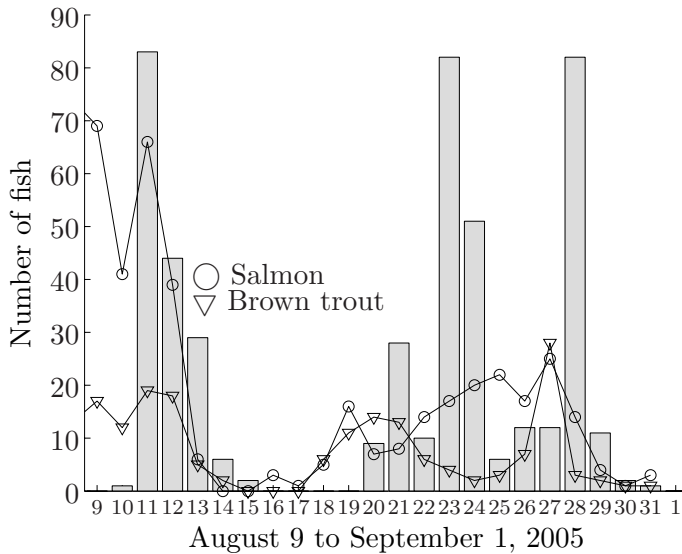


Figure 5: Number of fish passing through the attraction channel in 2005 (bars) and the number of salmon and brown trout successfully passing the fishway. 9-17/8 and 25/8-1/9 with bump in the channel, and 20-25/8 without the bump.

or maybe the test was preformed when fish was not actively migrating. Research indicates that salmon migrate between dusk and dawn or when the river is turbid (Laughton, 1989; Banks, 1969)

In 2005 the attraction channel was painted black and the bump was 0.65 m high, making it possible to use a depth of 1.05 m at the flow inlet. The results from 2005 are shown in Figure 5 together with the amount of salmon and brown trout passing the counter in the fishway. A total of 471 fish passed through the channel in 2005. During the test period in 2004, 884 salmon and 56 brown trout passed through the fish counter in the fishway (56 % of the total amount of fish passing that year). In 2005 the amount was 398 salmon and 174 brown trout (40 % of the total amount). The fish is now swimming through the channel with good correlation with the number of fish using the fishway at the dam. The activity during the day is shown in Figure 6; the peak in activity is between 12.00 and 17.00. This shows that the fish are most active during the day and the low number of fish passing in 2004 could not be explained

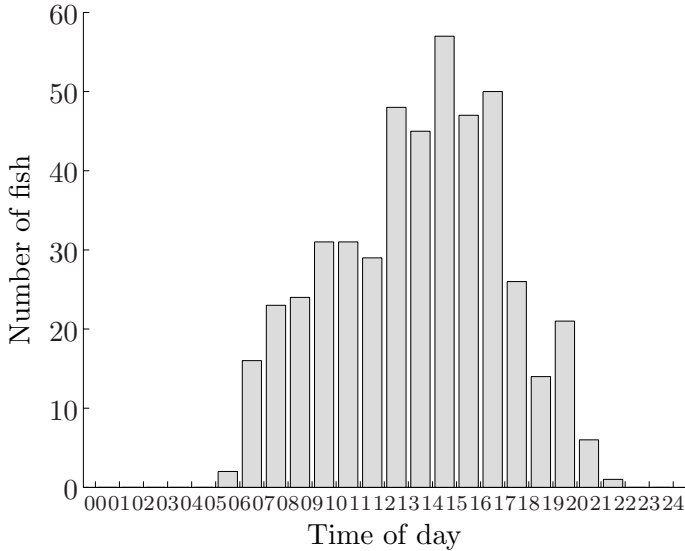


Figure 6: Time of day when the fish passed through the attraction channel in 2005.

with the fact that the fish was not actively migrating during the time of the test (09.00-15.00), so there must be some other explanation for the greater number of fish in 2005. During 2005 the visibility in the water was measured with a white circular disc and the mean sight in the water was measured to 1.46 m, with a standard deviation of 0.45 m; cf. Figure 7. The visibility does not correlate to the number of fish swimming through the channel. However the results suggest that it is the color of the attraction channel that makes the fish used the channel in 2005 and not in 2004.

Since only cameras were used to monitor the fish and the fish just swam through the channel, the same fish could enter the channel repeatedly. Some of the fish had injuries that could be identified and at one occasion one of these fish swam through the channel several times.

In 2005 there is no difference between the test with and without the bump. This despite the fact that the fish inlet depth differ from about 0.32 m with bump and 1.05 m without bump. Even the test without the bump affects the flow downstream the channel. In the chaotic flow from the turbines the channel provides a more structured flow both through and downstream the channel.

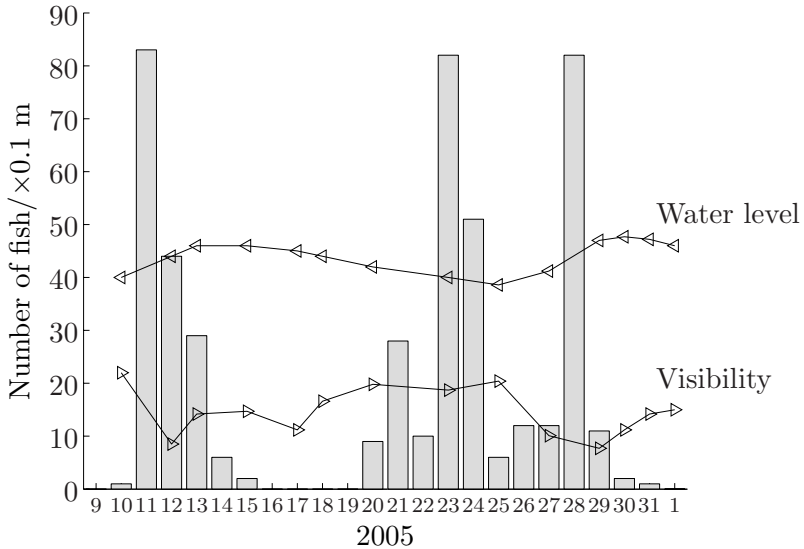


Figure 7: Number of fish swimming through the channel (bars) and the water level at the turbine outlet and visibility in the water.

When counting the fish swimming through the channel only fish that swim through in the right direction (against the current) is counted. Some of the fish enter the channel and then backs out and some enter the channel at the upstream end and swims through in the wrong direction (tail first). When they swim through it takes a few seconds and only very few spend longer time in the channel.

The mean water level at the turbine outlet during the test in 2004 was 3.74 m (standard deviation of 0.11 m) and during 2005 it was 4.39 m (standard deviation of 0.3 m).

4 Conclusion

An attraction channel, that uses a fraction of the tailwater to entice fish to swim through it, has been tested in full-scale. The channel works by locally accelerating the water to attract fish. The test was preformed during two summers in the Pite river in Sweden. The results show that the color of the channel is of importance. The fish used the black painted channel with and without the acceleration of the water velocity. Further

tests are needed to elucidate the role of the bump for attracting the fish. Also, techniques to guide the fish from the channel to a regular fishway need to be developed.

Acknowledgements

The research presented in this paper has been done within the Swedish R&D programme “Hydropower - Environmental impact, remedial measures and costs in existing regulated waters”, which is financed by Elforsk, the Swedish Energy Agency, the National Board of Fisheries and the Swedish Environmental Protection Agency.

The author would also like to thank Prof. Håkan Gustavsson and Dr Fredrik Engström, Division of Fluid Mechanics, Luleå University of Technology for helpful input on experimental setup and analysis of the results. Thanks goes also to Allan Holmgren, Jan-Erik Almqvist, Markus Larsson and Claes Oderstad for help with construction and monitoring of the channel, and postprocessing of the movies.

Thanks to Skellefteå Kraft for access to the location and providing helpful personnel.

References

- Arnekleiv J and Kraabøl M. 1996. Migratory behavior of adult fast-growing brown trout (*Salmo Trutta*, L.) in relation to water flow in a regulated Norwegian river. *Regulated rivers: Research & Management*, **12**:39–49.
- Banks J. 1969. A review of the literature on the upstream migration of adult salmonids. *Journal of Fish Biology*, **1**:85–136.
- Clay C. 1995. *Design of Fishways and Other Fish Facilities*. CRC Press, Inc.: Boca Ranton.
- Katopodis C. 1990. Advancing the art of engineering fishways for upstream migrants. In *the Proceedings of the Fifth International Symposium on Fishways '90, October 8-10, Gifu, Japan*, pages 19–28.
- Laine A, Ylinärä T, Heikkilä J, and Hooli J. 1998. Behaviour of upstream migrating Whitefish, *Coregonus lavaretus*, in the Kukkolankoski rapids, northern Finland. In Jungwirth M, Schmutz S, and Weiss

S, editors, *Fish Migration and Fish Bypasses*, pages 33–44. Fishing News Books.

Laughton R. 1989. The movements of adult salmon within the river Spey. *Scottish Fisheries Research Report*, (41).

Wassvik E and Engström T. 2004. Model test of an efficient fish lock as an entrance to fish ladders at hydropower plants. In *the Proceedings of the Fifth International Symposium on Ecohydraulics, September 12-17, Madrid, Spain*.

Weaver C. 1963. Influence of water velocity upon orientation and performance of adult migrating salmonids. *Fishery Bull. Fish Wildl. Serv. U.S.*, **63**:97–121.

PAPER E

Numerical Solution of the Flow Field in an
Attraction Channel for Migrating Fish

Numerical Solution of the Flow Field in an Attraction Channel for Migrating Fish

ELIANNE M. LINDMARK

Division of Fluid Mechanics, Luleå University of Technology, SE-971 87
Luleå, Sweden

Abstract

Atlantic salmon and sea trout migrate upstream rivers to spawn. In regulated rivers the fish is hindered by the hydropower plants and fishways are often used to help the fish pass the power plants. But the fish have problems finding the entrance to the fishway, due to the dominating flow from the turbine outlet. An attraction channel has previously been studied in both laboratory and field. The device works by increasing the water velocity at the fish inlet attracting fish to swim into the channel and further on to the fishway. In this paper a numerical model is made of the attraction channel. The model is validated using results from previous laboratory experiments and the model is used to study the blockage in the channel. The results show that the water velocity out of the attraction channel decrease as the area surrounding the channel increase.

1 Introduction

Fish such as Atlantic salmon (*Salmo salar*) and sea trout (*Salmo trutta*) migrate upstream rivers to spawn. In regulated rivers the fish are obstructed by hydropower plants or other man-made structures. Even though the plant is equipped with a fishway to help the fish pass the plant, few fish find the entrance to the fishway (Northcote, 1998; Rivinoja et al., 2001; Williams, 1998). Migrating salmon and trout are attracted to high water velocities when migrating upstream (Weaver, 1963;

Williams, 1998) and are often attracted to the dominating flow from the turbine tail race (Arnekleiv and Kraabøl, 1996; Rivinoja et al., 2001). In order to reduce stress on the fish it is important that the fish find the entrance fast and the delay in migration is kept to a minimum (Clay, 1995).

One way to improve the attraction to a fishway entrance is to increase the water velocity. In this paper, an attraction channel that increases the water velocity is studied. The device is an open U-shaped channel that is partly submerged in the turbine tailrace, or any free stream. At the downstream end of the channel a bump accelerates the water. The channel has previously been studied in model-scale (Wassvik and Engström, 2004; Wassvik, 2006) and the results show that the attraction channel may increase the water velocity by approximately 40 % and that the attraction is preserved at least 18 water depths (over the bump) downstream. Also, Lindmark et al. (2008) suggest that an increase in water depth in the channel increases the length of the attraction with preserved velocity increase at the fish inlet. The models in the quoted papers were all studied in a water flume three times wider than the model. As the bump in the attraction channel blocks water from flowing into the channel, the water redirected to the outside of the channel increase the velocity there, thus affecting the performance of the channel. In this paper, the flow in the attraction channel is studied numerically to further investigate the blockage in the channel and the effect of the water flume.

Steady, 2d flow over submerged bodies is a well studied area. The problem has been studied numerically by Forbes and Schwartz (1982), Vanden-Broeck (1987). Lamb (1932) describes the fundamentals of 2d flow using the Bernoulli equation together with the continuity equation to calculate the velocity over the bump (Forbes, 1988). However, this only describes the flow over the bump. In the present setup the water is free to flow through the attraction channel and beside it. As the flow is subcritical in the channel the blockage caused by the bump will force water aimed for the channel to the outside. A 3d model is therefore necessary to determine this flow.

The model of the attraction channel and water flume in Wassvik and Engström (2004) is studied with the commercial code ANSYS CFX-11.0, which uses the volume-of-fluid (VOF) to represent the free surface of the water (Hirt and Nichols, 1981). The effect of the water flume is studied by moving the walls of the model, increasing the cross-sectional area of

the model by two and four times and representing the wall by free slip to resemble a free stream.

2 Model setup

The flow in the attraction channel and water flume used in Wassvik and Engström (2004) is modelled. The attraction channel is 500 mm long and 98 mm wide (inner width). The original model is made of 1.7 mm window glass and in the numerical model the walls are 2 mm thick. The flow field is set 1 m upstream and 1 m downstream the attraction channel. The total length of the numerical model is thus 2.5 m; cf. Figure 1. The cross section of the numerical model is 300 mm wide (same as the real water flume) and 300 mm high. The water depth in the flume was set to 118 mm. The upper part of the model is modelled as air. In the attraction channel a 80 mm high bump is placed; the shape of the bump follows the second order curve

$$h(x') = B - \frac{1}{36B}x'^2 (x' \geq 0, h \geq 0) \quad (1)$$

where B denotes the maximum height of the bump (80 mm) and x' originates at the highest part of the bump and runs in the negative x direction; see Figure 1. The rear end of the bump is placed 40 mm from the flow outlet, as in the real setup.

The flow field was solved using ANSYS CFX-11.0 with RANS equations. The surface method used is volume-of-fluid (VOF) introduced by Hirt and Nichols (1981). The method uses an extra variable, the volume fraction, to keep track of the surface. Volume fraction 1 represents water and 0 represents air; anything in between is the free surface. This method tends to smear out the surface, so a fine grid is necessary to resolve the interface.

The turbulence model used is SST which uses the $k-\varepsilon$ turbulence model in the bulk flow and $k-\omega$ near the walls (CFX 11.0); this improves the prediction of separation compared with ordinary $k-\varepsilon$. The SST model requires a grid size of $y^+ = 1$ near the walls.

The problem is first solved with a first order scheme to get an initial guess for the second order scheme. The iterative convergence in the solutions are 1.0×10^{-6} (rms) and ten times higher for the maximum values. A solution is fully converged if the values reach the round-off error of the computer (Casey and Wintergerste, 2000), but maximum

values of 1.0×10^{-5} is a very tight convergence according to CFX 11.0. The convergence was also assessed by studying the velocity at monitor points in the domain. These were located over the bump, directly behind the bump in the wake, and under the attraction channel. When the rms-values reach their target the velocities in the monitor points were converged to the third decimal.

The flow domain is discretized using hexahedral elements, cf. Figure 2. The elements close to the walls are 0.1 mm thick, which gave a y^+ values of 1-2 on the wall. In the air, the y^+ values are even lower. The aspect ratio between the longest and the shortest edge of the element is 115 (near the wall) and the expansion rate between the elements is 100. Casey and Wintergerste (2000) recommend an aspect ratio of 100, but in the boundary layer the restriction is relaxed.

A grid convergence study was performed using four different grids with 588 996, 1 086 410, 1 698 828 and 3 673 608 nodes. The parameters studied are the maximum velocity and the water height over the bump in the middle of the channel. The water surface is set at volume fraction 0.5. The parameters are compared with the results from measurements. For the three finest grids the error compared with results from LDV are 1 % for the water depth and 2 % for the maximum velocity. The second finest grid (1 698 828 nodes) is used to further investigate the flow in the channel.

2.1 Boundary conditions

For the reference case where the flume and channel is modelled as in Wassvik (2006) the walls and the bump are modelled as smooth surfaces with no slip. The top boundary is modelled as an opening, where the air freely moves in and out of the domain. The outlet is modelled with zero pressure in the air and hydrodynamic pressure in the water. At the inlet, a profile representing the water velocity in the water flume is used. The stream wise velocity component in a cross-section of the flume was measured when the flume used in the above mentioned papers was characterized. The profile was slightly adjusted to create a smoother profile. The flow rate is $0.0052 \text{ m}^3/\text{s}$ and the mean velocity in the middle of the flume is 0.17 m/s . The profile extends up in the air.

To study the attraction channel in a free stream half the water flume is modelled with a symmetry plane in the middle of the channel. The walls of the flume are modelled with free slip. Three different cross-

sectional areas were tested where the water area in the flume is 8 and 16 times larger than the cross-sectional area of the attraction channel. The velocity at the inlet is 0.17 m/s (modelled as plug flow), which is the mean velocity in the velocity profile used in the flume.

3 Result & Discussion

A model of an attraction channel and water flume has been made to numerically calculate the flow field in and around the channel. The model is first validated using results from previous studies on the channel (Wassvik and Engström, 2004; Wassvik, 2006) and then studied in a free stream to see how the blockage in the channel is affected by the water flume.

3.1 Validation of the model

To validate the numerical model of the attraction channel a replica of the laboratory test on the channel was made. The calculated reference flow is shown in Figure 3. Comparing the numerical result with results from the LDV measurements of Wassvik and Engström (2004), it is seen that the numerical model captures the flow over the bump and the recirculation zone downstream the bump very well; cf. Figure 4b. But the form of the velocity profile into the channel (Figure 4a) and the form of the profile outside the channel (Figure 4c) are less well represented.

It is seen in Figure 4c that the velocity profile outside the channel is not uniform as in the real setup, where the profile is more plug-like. This means that the boundary layer on the attraction channel does not develop properly in the numerical model. The channel inlet velocity profile (Figure 4a) has a more uniform shape in the simulations than in the real case. The inlet profile is taken 40 mm into the channel both for the measured and calculated profile. The water depth over the bump is 5.6 mm in the model, measured from the highest part of the bump to the point where the water volume fraction is 0.5. In the real set up in Wassvik and Engström (2004) the depth was also 5.6 mm.

The model of the attraction channel gives a good representation of the flow in the water flume and attraction channel. In particular, when considering the velocity out of the attraction channel and downstream the channel. This can be seen when comparing the flow field downstream

the channel with PIV measurements of the flow, cf Figure 5 (Lindmark, 2008).

For the validation test above the whole cross-section of the flume is represented in the calculations, but in the further calculations a symmetry plane in the middle of the flume makes it possible to calculate the flow field only in half the flume. This saves computation time as only half the amount of grid cells is used. A comparison between the results from the whole flume and the flume with symmetry plane show the same results.

3.2 Attraction channel in a free stream

To simulate the attraction channel in a free stream the boundary condition on the flume walls was set to free slip. The walls of the flume were moved both in y and z directions (equal distance) so the cross-section area of the water became 8 and 16 times larger than the cross-section area of the attraction channel, or 2 and 4 times the original area, respectively.

To study how the blockage effect changes when the surrounding of the channel changes, the maximum velocity in the surface region downstream the channel is studied. This region extends from the water surface and down to $y = 112$ mm (the highest part of the bump ends at $y = 112$ mm). The free surface is set to where the volume fraction is 0.5. Figure 6 shows the maximum surface velocity as a function of downstream distance, where the velocity is normalized with the mean velocity in the free stream (0.17 m/s) and the downstream distance is normalized with the water depth over the bump.

The results show that the larger the surrounding area is the lesser amount of water flows into the attraction channel, and the velocity out of the channel becomes smaller. The distance downstream where the water increase is present also changes when the surrounding area changes. The lesser the momentum out of the channel the lesser the increase is present.

Figure 7 shows the flow surrounding the attraction channel when the surrounding area is four times larger than the reference case. Beside and under the channel separation zones are visible. In Figure 4c the flow beside the channel (reference case) is compared with measurements at the outlet of the channel. In that case the numerical model indicates a larger boundary layer than the measurements. How large the real separation zone is in the case with a larger surrounding area can only

be speculated.

As the attraction channel is positioned in the flow direction and the attraction flow out of the channel flows in the same direction as the main flow only fish swimming in that area will be attracted to the channel. With this in mind it is important where to place the attraction channel and how to design it. A wider channel increases the area where the fish feel the increase in water velocity and the wider the channel is compared with the free stream the more water will flow through the channel increasing the water velocity of the attraction water.

Also, the attraction channel produces a surface oriented jet with low aeration. This should fit upstream migrating salmon and trout as they swim close to the surface (Rivinoja, 2005), are attracted to high water velocities (Weaver, 1963) and are discouraged by high aeration (Clay, 1995). Kamula (2001) investigated the flow downstream the entrance of different fishways. The result show that the flow from a pool-and-weir fishway dives while the flow from Denil and vertical slot fishways are more surface oriented. According to Laine et al. (2002) larger salmon seem to favor pool and weir fishways with a water fall at the entrance.

The attraction channel has been studied in field and salmon did swim through the channel (Lindmark and Gustavsson, 2008). The channel was placed at a wall, probably forcing some of the water trough the channel. A placement near a wall or shoreline would therefore be beneficial for the performance of the channel; not only would it force more water through the channel but fish also tends to follow the shorelines when migrating upstream (Williams, 1998).

In the future the numerical model can be used to optimize the design of the channel, or it can be used when scaling the channel to full-scale.

4 Conclusions

A numerical model of an attraction channel has been made. The model represents the water flow downstream the channel well. The model is used to investigate the blockage in the channel when the surrounding environment change. The result show that the larger the area of water surrounding the channel is the lower the attraction water out of the channel will be. The channel will probably benefit from a placement near a wall or a shoreline, as the water aimed for the channel will be forced through it.

Acknowledgements

The author would like to thank Prof. Håkan Gustavsson and Dr. Daniel Marjavaara, Division of Fluid Mechanics, Luleå University of Technology, for helpful input on experimental setup and analysis of the results.

References

- Arnekleiv J. V and Kraabøl M. 1996. Migratory behavior of adult fast-growing brown trout (*Salmo Trutta*, L.) in relation to water flow in a regulated Norwegian river. *Regulated rivers: Research & Management*, **12**:39–49.
- Casey M and Wintergerste T. Best practice guidelines. Technical report, ERCOFTAC special interest group on "quality and trust in industrial CFD", 2000.
- CFX 11.0. ANSYS CFX release notes for 11.0.
- Clay C. H. 1995. *Design of Fishways and Other Fish Facilities*. CRC Press, Inc.: Boca Raton.
- Forbes L. K. 1988. Critical free-surface flow over a semi-circular obstruction. *Journal of Engineering Mathematics*, **22**:3–13.
- Forbes L. K and Schwartz L. W. 1982. Free-surface flow over a semi-circular obstruction. *J. Fluid Mech.*, **114**:299–314.
- Hirt C. W and Nichols B. D. 1981. Volume of fluid (vof) method for the dynamics of free boundaries. *Journal of Computational Physics*, **39**:201–225.
- Kamula R. 2001. *Flow over weirs with application to fish passage facilities*. PhD thesis, University of Oulu.
- Laine A, Jokivirta T, and Katopodis C. 2002. Atlantic salmon, *salmo salar* L., and sea trout, *salmo trutta* L., passage in a regulated northern river - fishway efficiency, fish entrance and environmental factors. *Fisheries Management and Ecology*, **9**:65–77.
- Lamb H. 1932. *Hydrodynamics*. Cambridge University Press, sixth edition.

- Lindmark E and Gustavsson L. 2008. Field study of an attraction channel as entrance to fishways. *River Research and Applications*, 24: 564–570.
- Lindmark E. M. 2008. *Flow design for migrating fish*. PhD thesis, No. 2008:55, Luleå University of Technology, Luleå, Sweden.
- Lindmark E, Green T, Lundström T, and Gustavsson L. 2008. Flow measurements in an attraction channel as entrance to fishways. *Submitted to River Research and Applications*.
- Northcote T. G. 1998. Migratory behaviour of fish and its significance to movement through riverine fish passage facilities. In Jungwirth M, Schmutz S, and Weiss S, editors, *Fish Migration and Fish Bypasses*, pages 3–18. Fishing News Books.
- Rivinoja P, McKinnell S, and Lundqvist H. 2001. Hindrances to upstream migration of Atlantic salmon (*Salmo Salar*) in a northern Swedish river caused by a hydroelectric power-station. *Regulated Rivers: Research & Management*, (17):101–115.
- Rivinoja P. 2005. *Migration problems of Atlantic salmon (Salmo Salar L.) in flow regulated rivers*. PhD thesis, No. 2005:114, Swedish University of Agricultural Sciences.
- Vanden-Broeck J.-M. 1987. Free-surface flow over an obstruction in a channel. *Phys. Fluids*, 30(8):2315–2317.
- Wassvik E. Attraction channel as entrance to fishways. Licentiate thesis 2006:30, Luleå University of Technology, Luleå, Sweden, 2006.
- Wassvik E. M and Engström T. F. 2004. Model test of an efficient fish lock as an entrance to fish ladders at hydropower plants. In *the Proceedings of the Fifth International Symposium on Ecohydraulics, September 12-17, Madrid, Spain*.
- Weaver C. R. 1963. Influence of water velocity upon orientation and performance of adult migrating salmonids. *Fishery Bull. Fish Wildl. Serv. U.S.*, **63**:97–121.
- Williams J. G. 1998. Fish passage in the Columbia river, USA and its tributaries: problems and solutions. In Jungwirth M, Schmutz S, and Weiss S, editors, *Fish Migration and Fish Bypasses*, pages 180–191. Fishing News Books.

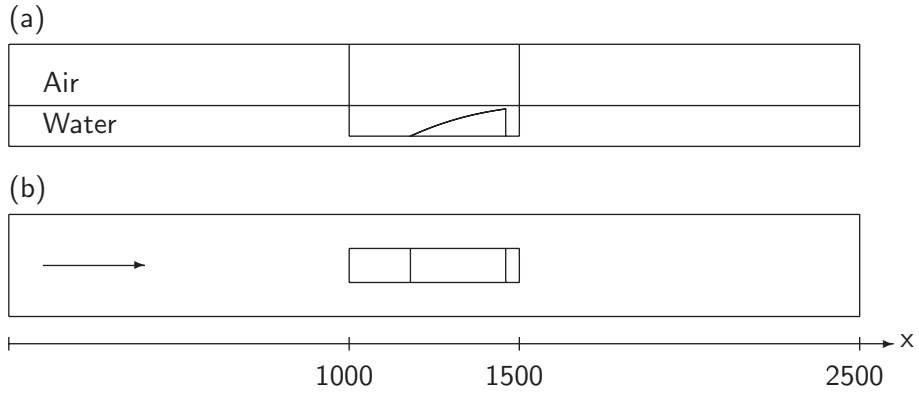


Figure 1: Model of the water flume with attraction channel. All dimensions in mm.

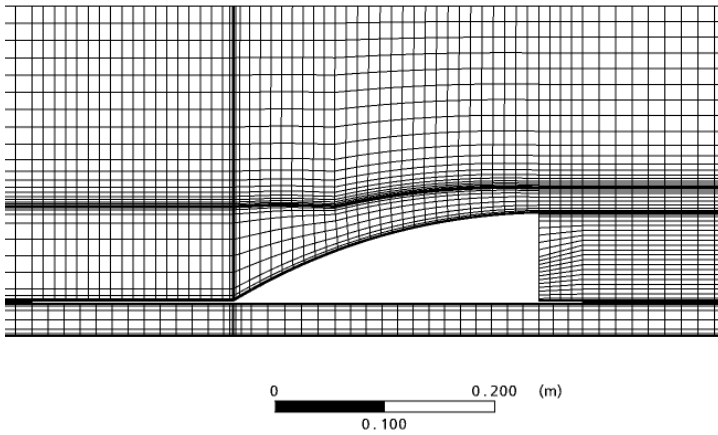
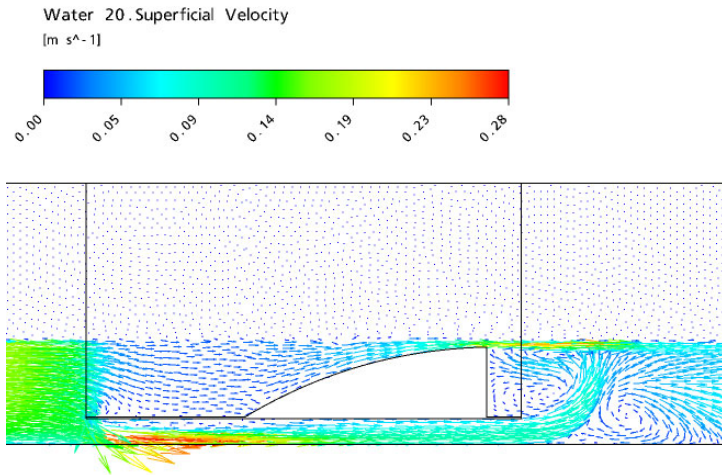
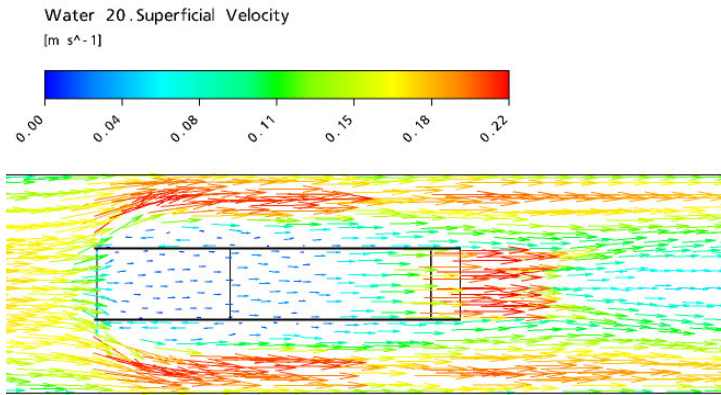


Figure 2: The structure of the grid around the attraction channel shown with 588 996 nodes; in the model 1 698 828 nodes was used.



(a) Velocities in the middle of the water flume.



(b) Velocities just below the water surface

Figure 3: Reference flow in the water flume.

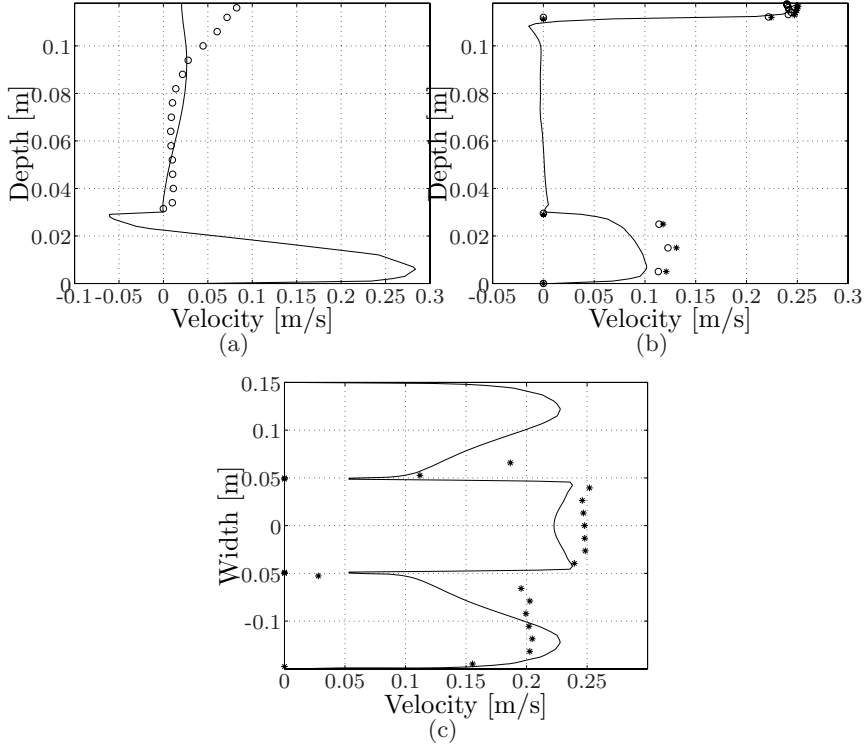
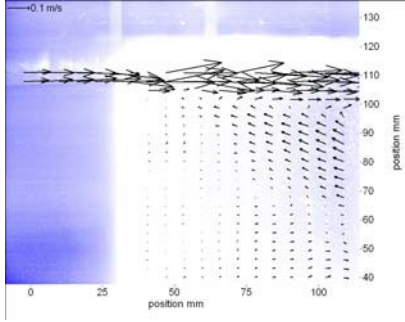
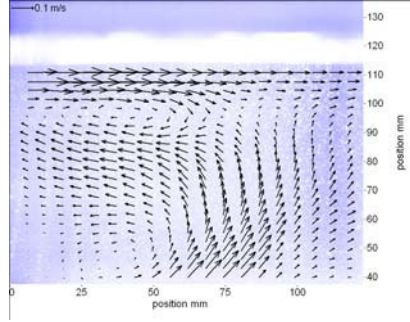


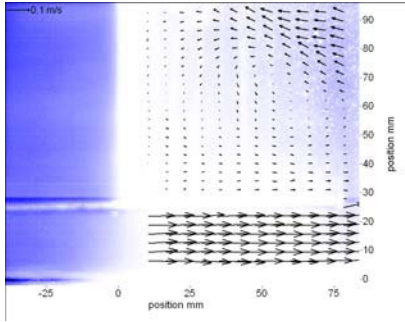
Figure 4: Velocity (u) profiles from measurements (\circ from Wassvik and Engström (2004) and $*$ from Wassvik (2006)) and simulations (solid line). a) Velocity profile at the flow inlet of the channel, channel bottom at $y=30$ mm. b) Velocity profile at the highest part of the bump. c) Velocity profile at the highest part of the bump just below the water surface.



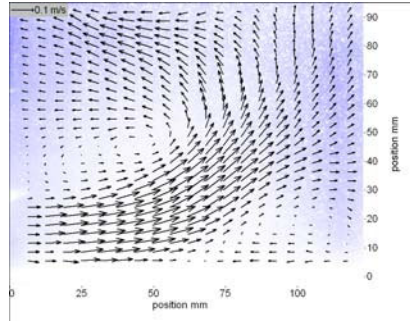
(a) Flow over the bump



(b) Surface flow behind the bump



(c) Flow under the bump



(d) Bottom flow behind the channel

Figure 5: PIV measurements of the flow in and behind the channel for the reference case (Lindmark, 2008).

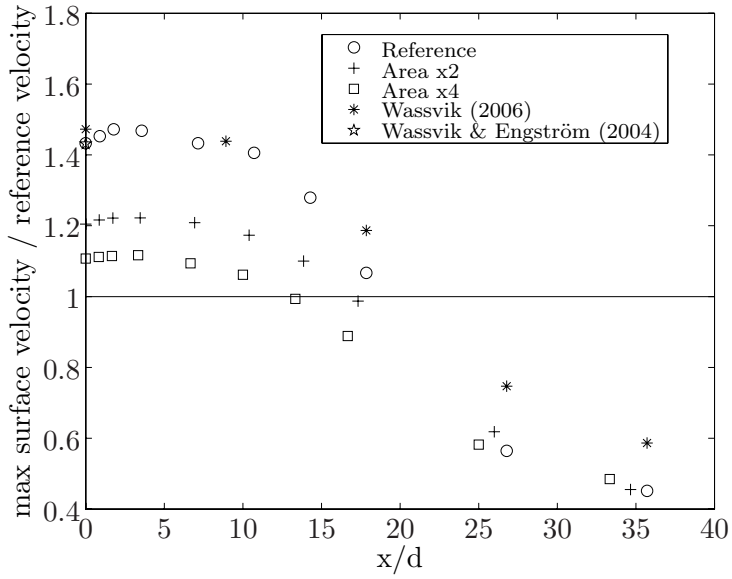
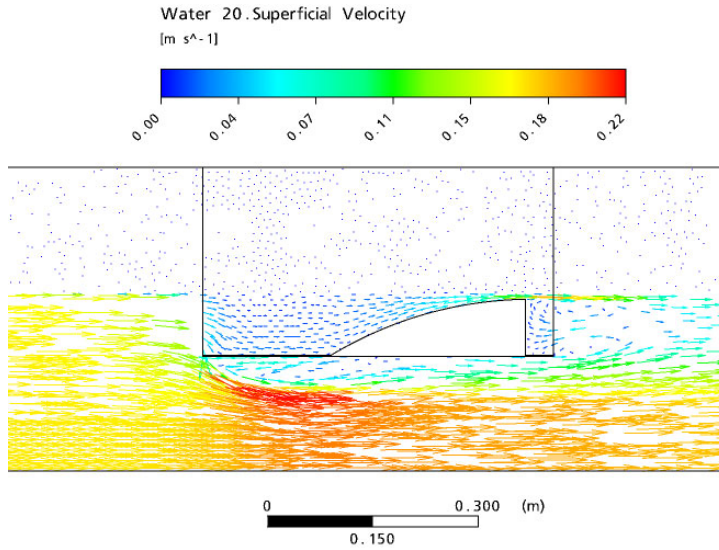
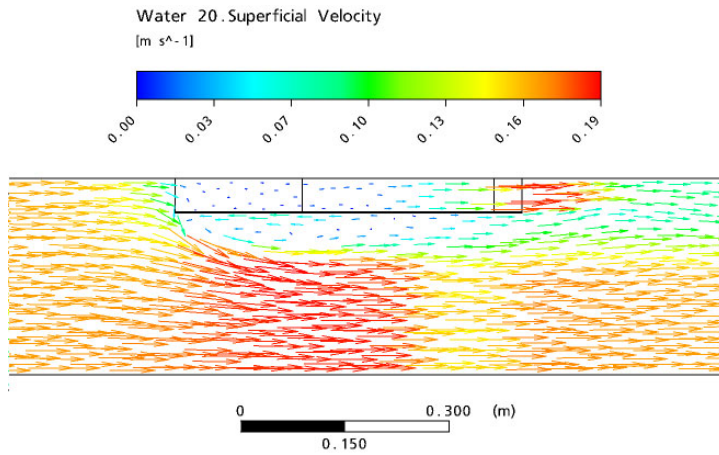


Figure 6: Maximum surface velocity as a function of downstream distance. The velocity is normalized with a reference velocity and the distance downstream is normalized with the depth over the bump.



(a) Velocities in the middle of the water flume.



(b) Velocities just below the water surface

Figure 7: Flow around the attraction channel in the model with 4 times larger cross-section area.

PAPER F

Flow Design of Guiding Device for Downstream
Fish Migration

Flow Design of Guiding Device for Downstream Fish Migration

T. Staffan Lundström, J. Gunnar I. Hellström and Elianne M. Lindmark
Division of Fluid Mechanics
Department of Applied Physics and Mechanical Engineering
Luleå University of Technology

Abstract

Downstream migrating smolt should be guided around hydropower plants to avoid fish mortality in the turbines. In Piteå River, an already regulated river, spillways are open to serve this purpose but too few fishes find this route. Hence, actions must be taken to enhance downstream fish migration. One way to attract the fish to the spillways is to direct the surface flow towards them with a guiding device. The hydrodynamic design of one such type of device is here outlined by means of numerical calculations of the flow upstream the spillways and by assuming that the fish move near the surface of the water. By starting from a straight impermeable barrier that extends from the water surface and two meters down and stretches over a part of the river a number of geometries are evaluated. A major result is that it is possible to redirect the surface water towards the spillways at very low spilling rates and thus with high energy efficiency. It is also found that the device should stretch over a major part of the river. For optimal functionality, the spilling should match the guiding device geometry. A high spilling implies that the guiding has low impact while for a low spilling the geometry is crucial for a successful down-stream migration.

Introduction

A successful downstream migration is fundamental for the survival of migrating species such as Atlantic salmon (*Salmo salar*) and sea trout (*Salmo trutta*). Fish mortality in connection to human made barriers such as hydropower plants in particular must be minimized. Often the only migration path in rivers with hydropower is via the turbines with two devastating scenarios as a result: i) The fish are severely injured or killed during their passage through the turbines, mortality mostly depending on the type of turbine and size of the fish (Clay, 1995). ii) The fish move towards the turbine intakes but refuse to enter and therefore remain upstream the dam, sometimes for several days (Schilt, 2007). It may of course also happen that the fish move via the turbines without being hurt or killed, or they find alternative routes around the dam. In the Columbia River (USA) the mortality is in the range of 81 – 92 % (Kaplan turbines; Ferguson, 2005).

As long as the smolts are migrating in fresh water they tend to follow the main stream while using as little energy as possible (Moore et al., 1998). They also have a propensity to keep to the water surface and to avoid strong accelerations or retardations, (Johnson et al., 2000; Taft, 2000). As an indirect indication of this, it has been shown that the geometry of a weir strongly effect the number of smolt that move over it (Haro et al., 1998). The trend is that the smoother geometry and thus the less acceleration the more fish is passing the weir. Kemp (2006) let Pacific salmon smolts encounter two different weirs in an open flume (two accelerations, 0.26 m/s^2 and 1.23 m/s^2 , or 0.4 s^{-1} and 1.72 s^{-1}) and though fish passed the weirs the hesitation was longer before passing through the higher acceleration. When the smolts (Chinook, Steelhead, Coho and Sockeye) in the same flume encountered a non-constricted or constricted part (acceleration in the constricted part 1.27 and 1.84 m/s^2 , or 1.4 s^{-1} and 1.65 s^{-1}) most smolts chose the non-constricted part (Kemp, 2005). With this in mind there are several passive and

active ways to guide the smolts to a certain route such as bar racks, barrier nets, screens, louver systems, fish pumps, sound and lights (Taft, 2000). At the power station Sikfors in the Piteå River in Sweden, the fish may pass the dam via the spillways, which are opened during the period of smolt migration. Investigations in the Piteå river show that the smolts follow the main flow in the river at a depth of 1-3 m, and most of the smolts pass the power plant via the turbines, with a mortality of 19 % and no smolts pass the dam via the spillways (Rivinoja, 2005).

In order to increase the percentage of smolts surviving the passage of Sikfors power station in the Piteå River it has been proposed to build a non permeable mechanical fish guiding device that directs some of the surface water towards the spillways. This hydro power plant is the only one in the Piteå river and has a head of 19.1 – 21.0 m and an annual mean flow of 158 m³/s. The power plant is equipped with two Kaplan turbines at 20 MW each. The surface water is here defined as the water located from the free air-water surface and two meters down. The concept has been tested for permeable devices such as louvers at several rivers and extensive work has been carried out to confirm their effectiveness, (Ruggles and Ryan, 1964; Ruggles et al., 1993; Scruton et al., 2003). The main conclusion of these studies is that using a louver to guide smolts towards a bypass is a convenient way to increase smolt survival but that the design of the guiding device must be carefully done for an optimal functionality.

Simulations of the flow upstream Sikfors has been preformed with ten appearances of the guiding device for five flow scenarios with the aim to investigate the influence on the flow through the reservoir from the guiding device. Of particular interest is to what extent it is possible to direct the surface flow to the spillways. The flow upstream Sikfors hydropower plant has previously been studied by Kiviloog (2005) with the purpose to compare the flow field with the position of downstream migrating smolt. In the study smooth wall was used for the river bed and the water surface was represented with a zero-shear slip lid. The numerical results were compared with field measurements of the velocity and the agreement was best in the middle of the river where the velocities are the highest. The usage of smooth walls might be discussed but is actually supported by results in Hardy et al. (2005) indicating that the surface roughness has limited effect on the mean flow when roughness was represented by cubes with a height of 0-10 % of the depth while it matters for other phenomena such as sedimentation. In the present numerical model of Piteå River a rigid lid is used as the free surface. This is called the rigid-lid approach, and is acceptable when the elevations of the surface are smaller than 10 % of the channel depth (Rodrigues et al., 2004). In the Piteå River case it is for energy efficient reasons of course of interest that the smolts are guided towards the spillways with as little flow over it as possible. Hence, in this work the flow around some designs of non-permeable guiding devices will be visualised as a function of flow rate over the spillways.

Numerical set-up

The geometry of the upstream river was obtained in the form of positions in space, the measurements were performed with a digital echo-sounder (Simrad EQ32Mk11) and a differential GPS (Trimble Pro XR), cf. Kiviloog (2005). The software Matlab was then used to sort this data so that the points belonging to the part of the river closest to the dam could be selected and too shallow areas could be excluded, see Figure 1. The areas excluded are indeed shallow, typically less than 0.05 m but were actually expelled so that problems with isolated regions and the mesh quality (bad angles) could be avoided. The 3D-points are then linearly interpolated onto a well structured grid, in order to get a simple and well structured array of

values for the geometry. From the interpolated points, 24 curves (18 m distance between each other) were approximated and from these curves cross-sections were formed and a 3D virtual geometry of the river was created in the CAD-software I-deas. The geometry was next divided into a number of finite volumes in the form of tetrahedrons in ANSYS ICEM-CFD, as exemplified Figure 2. The mesh quality obtained is presented in Table 1 for guiding device 10, the too warped elements, too small angles and too large element volume ratio are all located in the shallow areas of the river and it is assumed that they do not influence the main results. The position of the two turbine intakes and the three spillways are displayed in Figure 3 where also the depth of the reservoir is displayed showing that the maximum depth is 14 m and the mean is 7 m. In addition, the total simulated water volume is 270 000 m³. In order to investigate what mesh-resolution to employ a mesh-study was performed with a number of nodes varying from 450 033 to 4 851 914 for the setup without the guiding device and the downstream boundary condition corresponding to spilling 1, see Table 2. The parameter chosen for the mesh-study was the maximum velocity at the surface of the narrowest section of the river. The grid convergence was evaluated in two ways; first with a trendline of second order and secondly with Richardson extrapolation (Roache 1997), cf. Figure 4. The grid chosen for the simulations consists of 1 412 685 nodes corresponding to a volume-averaged number of nodes of 0.58. When comparing the chosen grid with the forecasted value from the trendline, corresponding to an infinitely fine grid, an error of about 4.7 % is obtained while the error resulting from the Richardson extrapolation is about 2.3 %.

A total number of *ten guiding devices* as defined in Table 3 and shown in Figure 5 were investigated. The basic criteria used for the designs are that:

- I. the device should lead the surface flow towards the spillways in order to guide the smolts the same way.
- II. the device should be directed less than 45 degrees to the main direction of the surface flow. Bates and Vinsonhaler (1957) recommend an angle between 11.5° and 40° for louvers.
- III. there should be a prominent downwards acceleration of the water upstream the device. The scenario is then that the smolts will refuse to move under the device and instead migrate along it towards the spillways, (Johnson et al., 2000; Taft, 2000).
- IV. the acceleration of the flow on the upstream side of the device should otherwise be smooth and retardations should be avoided. This will facilitate the migration along the guiding device once the smolts have rejected to go under it (Kemp, 2005; Kemp, 2006).
- V. it should be practically possible to install the device in reality.

The guiding device was tilted 20° from a vertical axis and in the flow direction in order to mimic its response to the hydrodynamic forces generated by the flow.

In this context it is worth pointing out that focus, in this study, was set on the flow in the reservoir and flow characteristics resembling the motion of the fish are therefore required. One potential measure is two-dimensional (2D) streamlines located in planes parallel and close to the free surface of the reservoir. Such lines follow the main flow but do not leave the plane they are assigned to, e.g. they do not dive under a guiding device. Another measure is naturally 3D streamlines denoting the general flow throughout the whole volume of the reservoir.

The simulations were performed in a one-phase mode with ANSYS CFX-10 and the free water surface was assumed to be flat and therefore modelled as a wall with free-slip. The bottom of the river and the guiding device were also modelled as walls but with no-slip conditions and the walls were considered smooth, cf. Rodrigues et al. (2004), Kiviloog (2005) and Hardy et al. (2005). This is a rather crude assumption for the shallow areas. It can, however, be assumed that these areas do not seriously affect the main flow patterns in the reservoir being of interest in this investigation. At the in-flow at the upstream end of the river and at the intake to the turbines and the spillways, velocity boundary conditions of plug flow type were applied, see Figure 3 and furthermore Table 2 where 5 spillings are defined with increasing amount of water-spill. The 10 years average spill during smolt migration, 20 May to 20 June, is $198 \text{ m}^3/\text{s}$ (Rivinoja, 2005). The procedure is that all spillings are studied with device 1 while for the rest of the devices focus is set on spilling 1 (total flow $320 \text{ m}^3/\text{s}$) since most can be gained from a redesign of the guiding device at this spilling. The iterative convergence for the simulations is 3-4 decades, following the suggestion in ERCOFTACs "Best Practice Guidelines" (Casey and Wintergerste, 2000). Too stiff upstream and downstream boundary conditions, assumed stationary conditions or problems with the cells in the shallow areas are probable reasons for not having even better convergence.

Measures were taken to obtain better iterative convergence by applying pressure and flow rate boundary conditions. The resulting flow field for the tested case was similar as for the stiffer conditions but the simulations were much more time-consuming. The reason for this is that in an initial stage, so called opening conditions must be set. This implies that the water can move in both directions over the boundary. The condition is then transformed into an outlet condition with a discretization scheme of first order. To get reliable results the scheme is finally upgraded to second order. Preliminary non-stationary simulations have also been carried out with indications of a better converged solution that yields similar results as the stationary simulations. This topic, however, requires further investigations.

Results and discussion

The simulations for the plain reservoir show that most of the water moves straight-forward from the model inlet through the reservoir and to the spillways and turbine intakes. This is exemplified in Figure 6, showing two-dimensional (2D) streamlines at depths of 1 m and 2.5 m at spilling 1 and 5 (total flow $320 \text{ m}^3/\text{s}$ and $920 \text{ m}^3/\text{s}$), respectively, and confirmed by velocity contour plots. Notice that the 2D stream-lines presented in Figure 6 emerge at the upstream inlet boundary of the reservoir. These streamlines are practically the same at the two depths studied for respectively spilling, bearing in mind that the width of the reservoir decreases with its depth, see Figure 6. An important conclusion from Figure 6 is furthermore that a *minority* of the 2D streamlines that start at the model inlet move to the spillways for spilling 1 while for spilling 5 a *majority* of them take this route. These scenarios can be quantified by defining a dividing streamline or in other words a percentage of the streamlines at the inlet that moves to the spillway which in these cases is measured to be 30 % and 67 %, respectively. When adding a guiding device the flow field naturally becomes more intricate. Still, different scenarios can be found from studies of the 2D and 3D streamlines. For guiding device 1 and spilling 1 the flow moves around the device while by increasing the spilling the 2D streamlines move from the guiding device and to the spillways, see Figure 7. When scrutinizing the 3D streamlines passing through spillway B it is also obvious that device 1 has no function at spilling 1 while at spilling 3 it has a great potential to lead the smolts to the stream going to spillway B, see Figure 7. In conformity with these observations it is found

that the percentage of the 2D streamlines that move to the spillway increases with the spilling as well as the use of guiding device 1, see Figure 8.

If now focus is set on spilling 1, for which most can be gained with a change in design of the spillway, it is found that the fraction of the 2D streamlines moving to spillway B is directly linked to the design of the device, see Figure 9. Several guiding devices (1, 2 3, 6 and 9) have marginal effect on this measure while with device 10 the fraction of streamlines increases up to as much as 93 %, see Figure 9 and the upper two plots in Figure 10. Other successful designs according to this criterion are devices 4, 5, 7 and 8. This observation is reinforced by a study of the interaction between the devices and the 3D streamlines moving to spillway B. To illustrate, the downstream end of device 10 reaches these streamlines, see Figure 10. Hence, any object keeping to the surface, i.e. smolts, will probably be captured by the water moving to the spillway rather than by the water aiming for the turbine intakes. This picture also holds for devices 4, 5, 7 and 8 while the downstream ends of devices 1, 2 3, 6 and 9 are far from the 3D streamlines of interest and the flow goes around the devices on there downstream sides towards the turbine intakes. The efficiency of the devices leading the 2D streamlines to the spillway (4, 5, 7, 8 and 10) is solely set by the distance between their upstream end and the right-side river bank. Hence the longer the device is the better functionality, cf Table 3 and Figure 9.

Now that the main principles of the guiding devices are set it is in place to scrutinize further the results with focus on the flow field near guiding device 10. This device is chosen since it, so far, has the best performance. For this study the velocity gradients along the principal axes, x , y and z are scrutinized, being directed nearly perpendicular to the devices, normal to the surface of the reservoir and nearly along the devices, respectively. At a depth of 1 m there is a downwards acceleration of about 0.1 s^{-1} close to the device, see Figure 11. At the same depth there is, as expected, a deceleration of the water in the direction perpendicular to the device as the water approaches it, see Figure 12 and the plot of the gradient of the velocity component u in the x -direction. The change in velocity along the device is considerably less than in the other directions as demonstrated by the gradient of the velocity component w in the z -direction, see figure 13. This acceleration is also much less than those investigated in (Kemp 2006, 2007). Hence any object or species such as smolts that wishes to avoid huge alterations in velocity in general and downwards accelerations in particular (Johnson et al., 2000; Taft, 2000) will probably prefer to go along with the guiding device towards the spillways. It may also be noted that the 2D streamlines parallel to the free surface at a depth of 2.5 m are not affected by the guiding devices as exemplified in Figure 10.

One main drawback with impermeable guiding devices, as the ones studied here, is that the force on them can be relatively large. This force is strongly related to the wetted area of the devices. To exemplify, CFD calculations yield that the force in the x -direction (being close to main flow direction) on device 7 is 75 % of the force on device 8. These devices are geometrically equal with one exception being that the depth of device 7 is 1.7 m while it is 2.0 m for device 8. Interestingly, although the force differs the flow field around these guiding devices is only marginally affected by the difference in depth of them as exemplified in Figure 14. In this Figure the velocity component perpendicular to the surface of the water at a depth of 2.5 m is shown. There is even a noticeable downwards velocity component at a depth of 4.5 m for both devices, see Figure 15. Hence, this study also reveals that the guiding devices here modelled influence the out of plane flow to a much larger depth than their own height. It must however be noticed that the 2D streamlines, on their hand, are only marginally affected at depths deeper than the guiding device, cf Figure 10.

All calculations presented have been carried out by assuming a stiff boundary condition on the surface of the water. The result of this is a non zero pressure distribution on the surface instead of alterations in elevation. This may naturally influence the results. The levels of the pressures obtained near the guiding devices are, however, relatively low. By using the rigid-lid approach (Booker, 2003; Bhuiyan et al., 2007) elevations of less than 0.2 m are obtained in the area around device 10 which can be compared to the averaged depth of the water in the reservoir, 7 m, see Figure 16.

Conclusions

This work demonstrates that it is possible to guide downstream migrating smolts towards a turbine by-pass such as a spillway at minor spilling rates and thus high energy efficiency by following the observation that the smolts move close to the surface of the water. It is also found, for the particular case studied, that the device should be stretched over a major part of the river and that it is possible to design the device in such a way that the downwards acceleration at the device is much larger than accelerations or retardations along it. While the impact on the in-plane velocity components is weak at depths larger than the device there is a noticeable downwards velocity component even at a water depth more than twice the depth of the device. A general conclusion is furthermore that, for optimal functionality, the spilling should be matched to the guiding device geometry. A high spilling implies that the guiding has low impact while for a low spilling the geometry is crucial for a successful down-stream migration. Even more conclusions on the detailed geometry of the guiding device could be made if the simulations were refined regarding for instance, outlet geometries, boundary conditions and numerical mesh. Future work involves also detailed simulations of the flow field near the spill-ways and an extensive experimental study once the guiding device is in place.

Acknowledgement

This work was sponsored by Skellefteå Kraft AB and the authors acknowledge the discussions with, Mr. Martin Johansson, Skellefteå Kraft AB, Mr. Karl Rytters, Second and Prof. Håkan Gustavsson, Luleå University of Technology, they furthermore send their gratitude to Mr. Mårten Strömberg, at Umeå University and Prof. Hans Lundqvist at the Swedish University of Agricultural Sciences who provided the geometry of the river.

References

- Bates, D.W. and Vinsonhaler, R. 1957. Use of louvers for guiding fish. *Transactions of American Fisheries Society* 86: 38-57.
- Bhuiyan, A.B.M.F. and Hey, R. 2007. Computation of three-dimensional flow field created by weir-type structures. *Engineering Applications of Computational Fluid Mechanics* pp. 350-360
- Booker, D.J. 2003. Hydraulic modelling of fish habitat in urban rivers during high flows. *Hydrological processes* 17: pp. 577-599
- Casey M, WintergersteT, 2000. ERCOFTAC Special Interest Group on "Quality and Trust in Industrial CFD" Best Practice Guidelines
- Clay, C.H. 1995. Design of fishways and other fish facilities. Second ed. CRC Press, Inc., Boca Raton.
- Ferguson, J.W. 2005. The behaviour and ecology of downstream migrating Atlantic salmon (*Salmo salar* L.) and anadromous brown trout (*Salmo trutta* L.) in regulated rivers in northern Sweden. Report no 44, Swedish University of Agricultural Sciences
- Hardy, R.J., Lane, S.N., Lawless, M.R., Best, J.L., Elliott, L. and Ingham, D.B. 2005. Development and testing of a numerical code for treatment of complex river channel topography in three-dimensional CFD models with structured grids. *Journal of Hydraulic Research* 43(5): pp. 468-480
- Haro A, Odeh M, Norieka J, Castro-Santos T. 1998. Effect of water acceleration on downstream migratory behavior and passage of Atlantic salmon smolts and juvenile American shad at surface bypasses. *Transactions of the American Fisheries Society* 127: 118-127.
- Johnson GE, Adams NS, Johnson RL, Rondorf DW, Dauble DD, Barila TY, 2000. Evaluation of the prototype surface bypass for salmonid smolts in spring 1996 and 1997 at Lower Granite Dam on the Snake River, Washington. *Transactions of the American Fisheries Society*, 129: 381-397.
- Kemp PS, Gessel MH, Sandford BP, Williams JG, 2006. The behaviour of Pacific salmonid smolts during passage over two experimental weirs under light and dark conditions, *River Research and Applications*, 22: 429-440
- Kemp PS, Gessel MH, Williams JG, 2005. Fine-scale behavioral responses of Pacific salmonid smolts as they encounter divergence and acceleration of flow, *Transactions of the American Fisheries Society*, 134: 390-398
- Kiviloog, J. 2005. Three-dimensional numerical modelling for studying smolt migrating in regulated rivers. Licentiate theses 2005:5, Chalmers University of Technology, Göteborg, Sweden
- Moore A, Ives S, Mead TA, Talks L, 1998. The migratory behaviour of wild Atlantic salmon (*Salmo salar* L.) smolts in the River Test and Southampton Water, southern England. *Hydrobiologia*, 372: 295-304
- Östergren J, 2006. Migration and genetic structure of *Salmo salar* and *Salmo trutta* in northern Swedish rivers, *Acta Universitatis agriculturae Sueciae*, 2006:112
- Rivinoja P, 2005. Migration problems of Atlantic salmon (*Salmo salar* L.) in flow regulated rivers, *Acta Universitatis agriculturae Sueciae*, 2005:114
- Roache, P.J. 1997. Quantification of uncertainty in computational fluid dynamics. *Annual review of Fluid Mechanics*, Vol. 29, pp. 123-160.
- Ruggles CP, Robinson DA, Stira RJ, 1993. The use of floating louvers for guiding Atlantic salmon smolts from hydroelectric turbine intakes. In Proceedings of the Workshop on Fish Passage at Hydroelectric Developments, 26-28 March 1991, St. John's, Newfoundland Williams UP, Scruton DA, Goosney RF, Bourgeois CE, Orr DC, Ruggles CP (eds). *Canadian Technical Report of Fisheries and Aquatic Sciences* 1905: 87-94

- Ruggles CP, Ryan P, 1964. An investigation of louvers as a method of guiding juvenile Pacific salmon, *Canadian Fish Culturist*, **33**: 3–67.
- Schilt C.R., 2007. Developing fish passage and protection at hydropower dams. *Applied Animal Behaviour Science* 104: pp. 295-325
- Scruton DA, McKinley RS, Kouwen N, Eddy W, Booth RK, 2003. Improvement and optimization of fish guidance efficiency (FGE) at a behavioural fish protection system for downstream migrating Atlantic salmon (*Salmo salar*) smolts, *River Research and Applications*, **19**: 605–617
- Taft EP, 2000. Fish protection technologies: a status report, *Environmental Science Policy*, **3**: 5349–5359

Table 1. Mesh quality quantities.

Quantity	Mesh for device 10	CFX-manual recommended values
Max face angle (degrees)	136	< 170
Min face angle (degrees)	5	> 10
Max edge length ratio	13	< 100
Connectivity number	78	< 50
Element volume ratio	140	< 30
Number of nodes	$1.35 \cdot 10^6$	
Number of elements	$7.45 \cdot 10^6$	

Table 2. Downstream boundary conditions

Spilling	Turbines [m ³ /s]	Spillway B [m ³ /s]	Spillway C [m ³ /s]	Spillway D [m ³ /s]	Total [m ³ /s]
1	250	70			320
2	250	150			400
3	250	270			520
4	250	270	200		720
5	250	270	200	200	920

Table 3. Definition of the guiding devices investigated.

Device	Length	Type	Depth	Surface water for spilling 1 [*] ,
	[m]		[m]	[%]
1	80	Straight	2.5	31
2	80	Straight in sections	2.5	31
3	81	Bend in downstream end	2.5	31
4	98	Straight	2.5	32
5	101	Full bend with small radius	2.5	31
6	99	Full bend with large radius	2.5	30
7	133	Full bend with small radius	2	13
8	133	Full bend with small radius	1.7	11.5
9	123	Full bend with small radius	2	12
10	144	Full bend with small radius	2	8.5

**Measure of amount surface water (defined as from the water surface and two metres down) that passes the devices between its up-stream end and the northern river bank.*

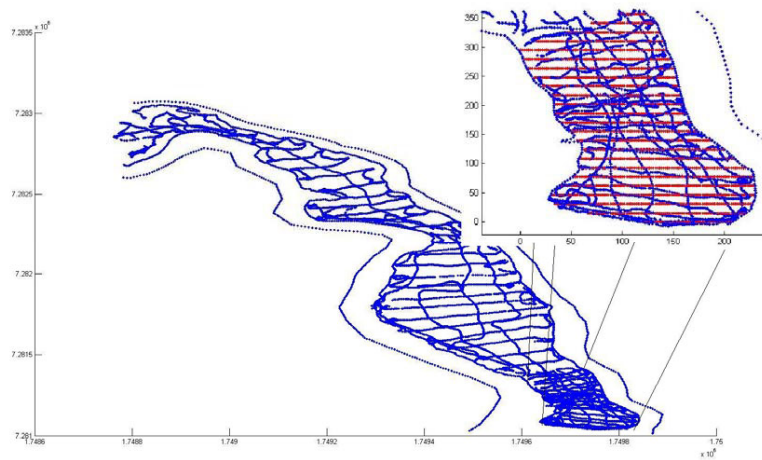


Figure 1 . Top view of the river geometry. The blue points show the locations of the measurements and the red ones interpolated data points.

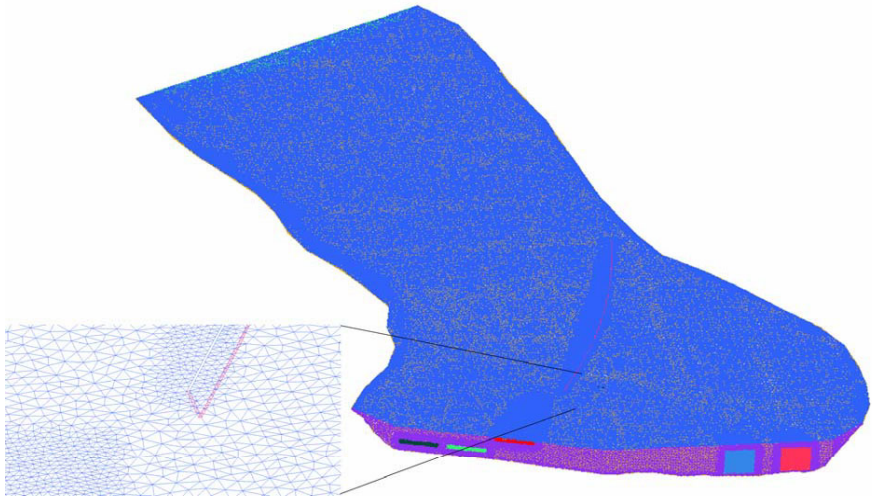


Figure 2. Example of virtual geometry divided into finite volumes.

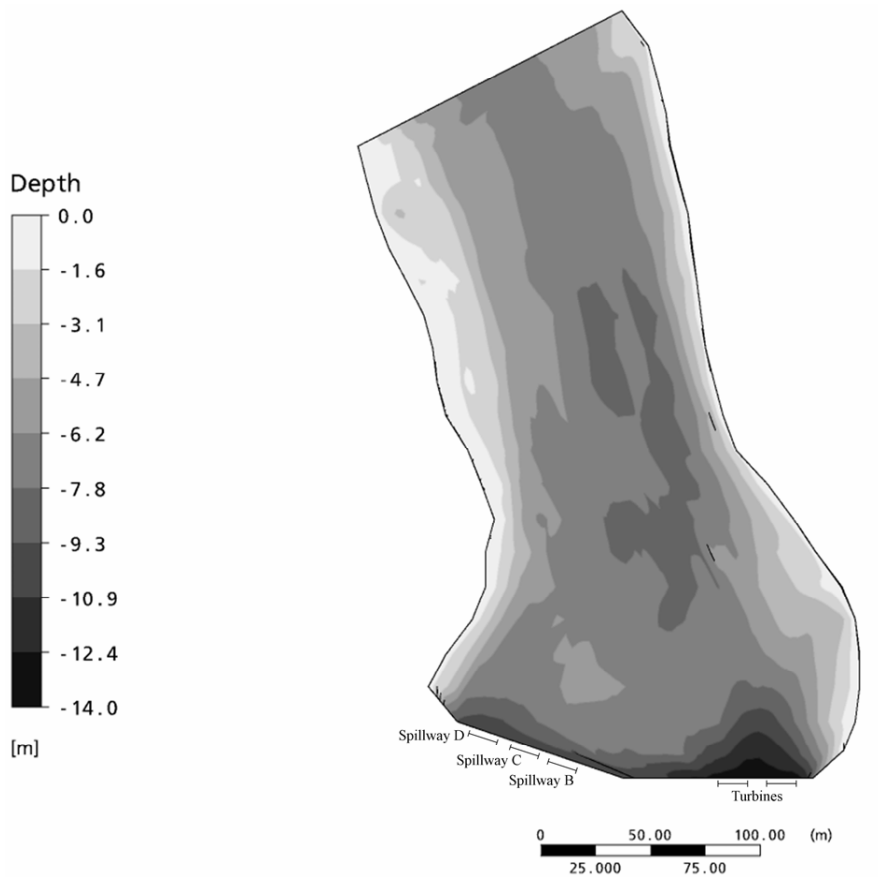


Figure 3. Indications of the position of the two turbine intakes, the three spillways and depth contours.

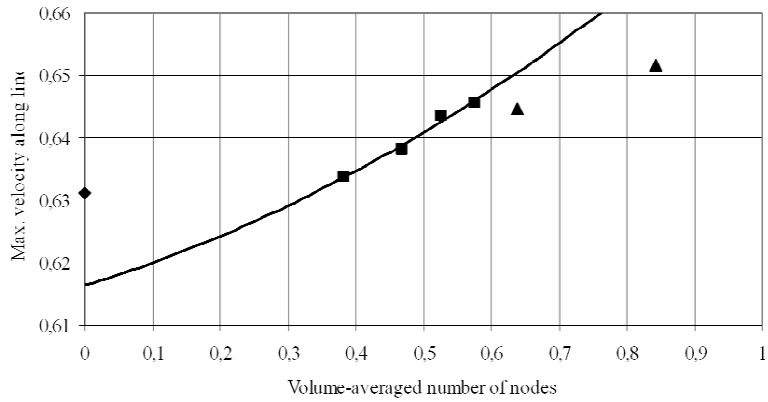


Figure 4. Extrapolated values of the max velocity along a line perpendicular to the main flow direction located at the narrowest section of the reservoir. Richardson extrapolation yields a value just above 0.63 m/s and a trend-line a value just below 0.62 m/s. Both methods are applied on results from the four finest grids, the squares.



Figure 5. Geometry and position of the ten guiding devices investigated. In the top row devices 1-3 are presented, in the second row devices 4-6, in the third row devices 7-9 and in the final row device 10. The scale in the bottom of each figure has a total length of 100 m.

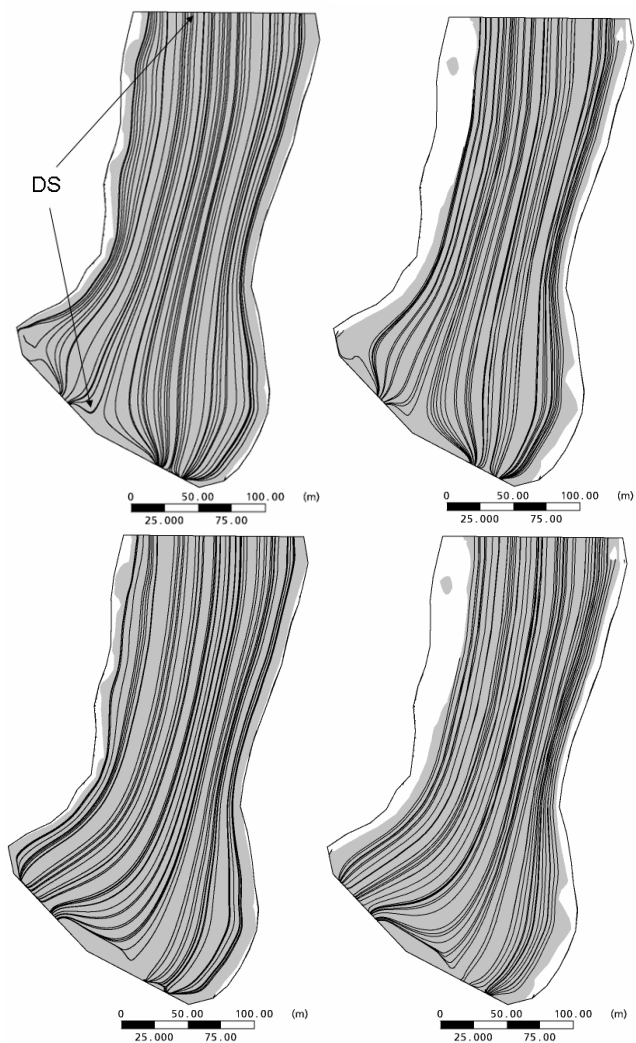


Figure 6. Plotted 2D-streamlines in the plain reservoir at a depth of 1 m to the left and at a depth of 2.5 m to the right. The too shallow areas are indicated in white. The upper figures shows the case for spilling 1, flow rate $320 \text{ m}^3/\text{s}$, and the lower ones for spilling 5, flow rate $920 \text{ m}^3/\text{s}$. DS indicates dividing streamline.



Figure 7. Streamlines for device 1. The upper two figures shows 2D streamlines at a depth of 1 m and the lower figures illustrate 3D-streamlines passing through spill-way B. The left-wing figures shows spilling 1, total flow rate $320 \text{ m}^3/\text{s}$, and the right-wing figures spilling 3, total flow rate $520 \text{ m}^3/\text{s}$.

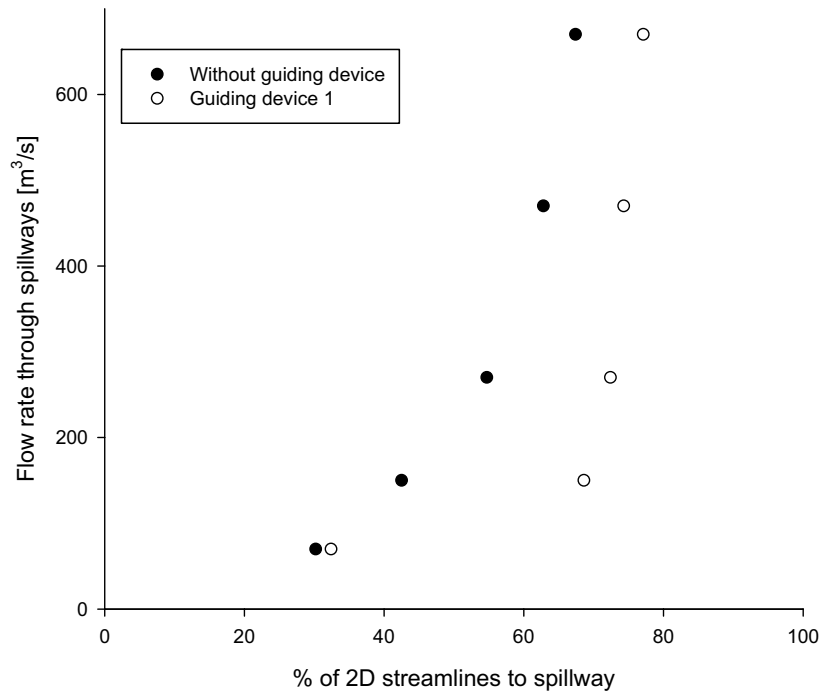


Figure 8. Plot of dimensionless dividing streamline at a depth of 1 m at the entrance of the model as a function of flow rate through the spillways. In essence the x-axis denote the fraction of these streamlines that goes through the spillways.

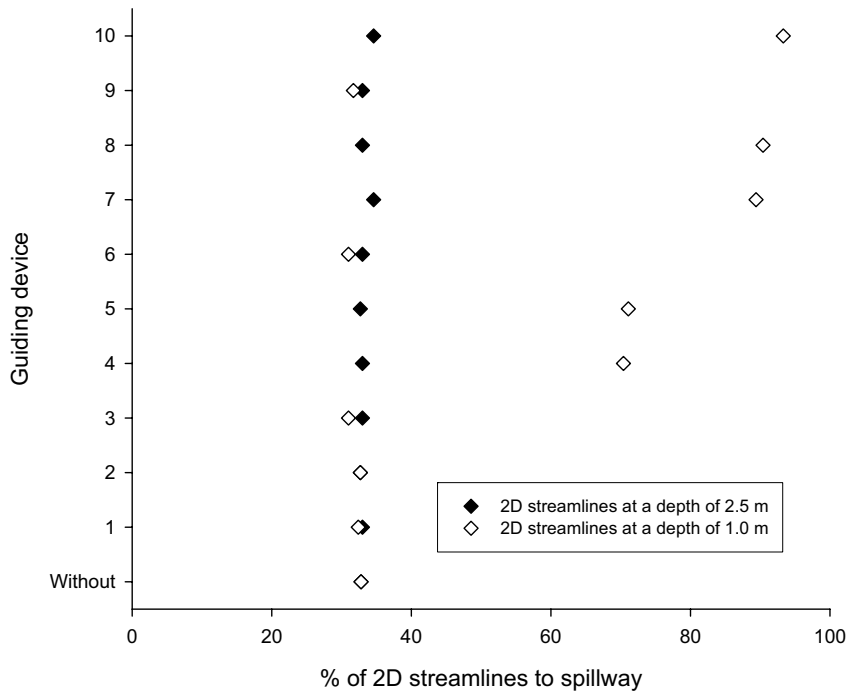


Figure 9. Plot of dimensionless dividing streamline at a depth of 1 m and 2.5 m at the entrance of the model as a function of guiding device. In essence the x-axis denote the fraction of these streamlines that goes through the spillways



Figure 10. Streamlines for device 10 and spill 1. The upper two figures shows 2D streamlines at a depth of 1 m at different magnifications and the lower figure to the left illustrate 3D-streamlines passing through spill-way B. The lower figure to the right shows 2D streamlines a depth of 2.5 m.

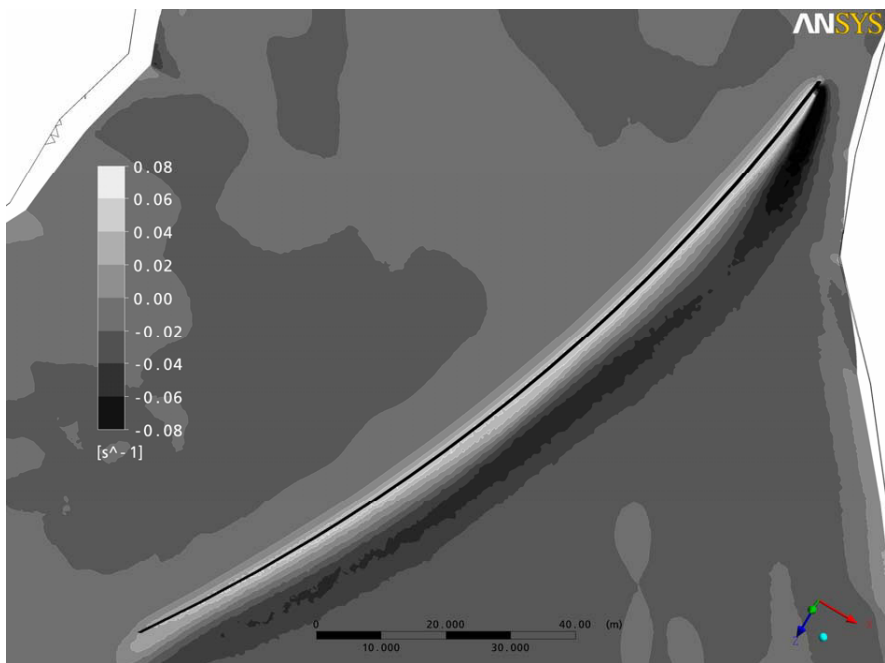


Figure 11. Gradient of velocity component v in the y -direction at a depth of 1 m for guiding device 10 and spilling 1.

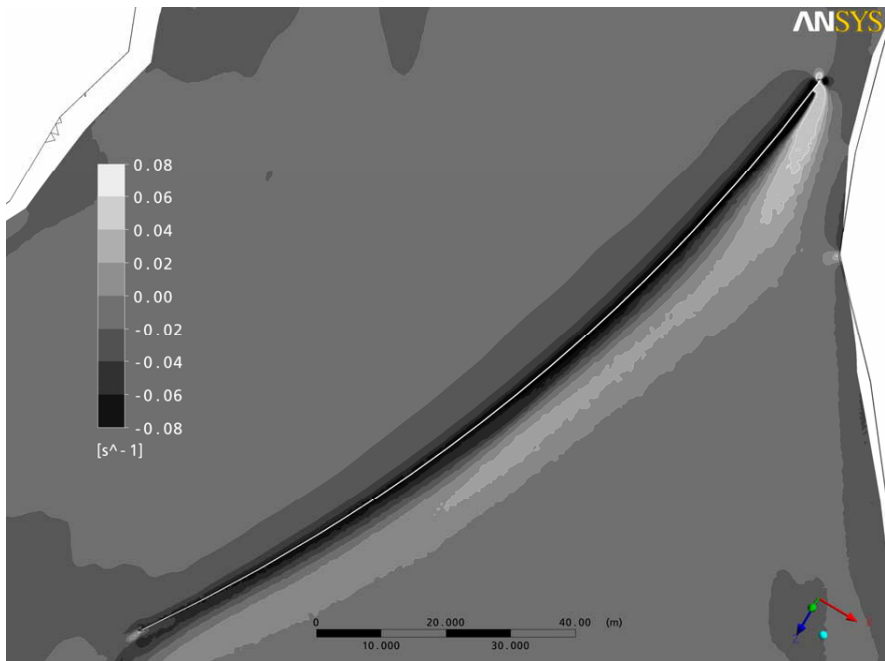


Figure 12. Gradient of velocity component u in the x -direction at a depth of 1 m for guiding device 10 and spilling 1.

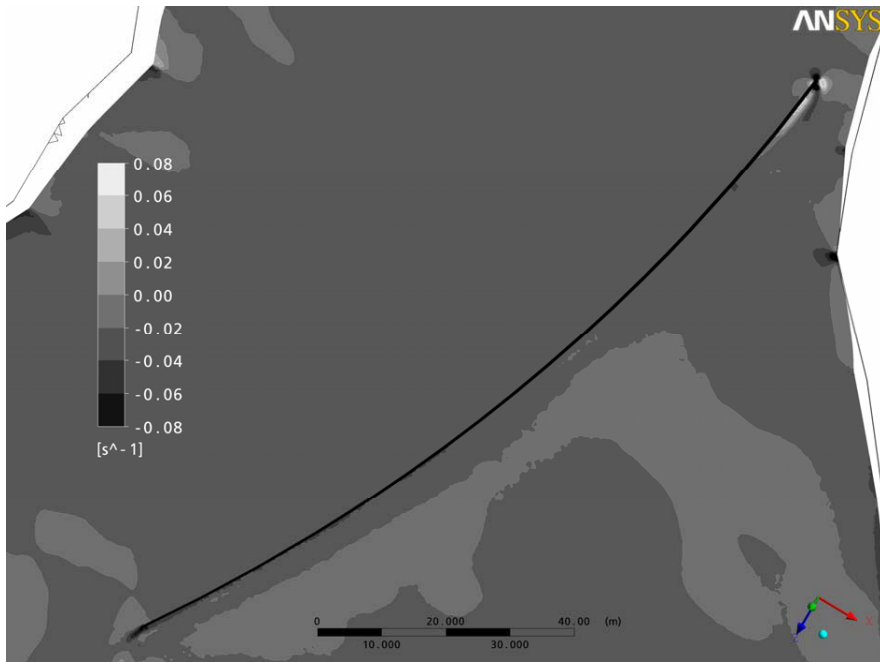


Figure 13. Gradient of velocity component w in the z -direction at a depth of 1 m for guiding device 10 and spilling 1.

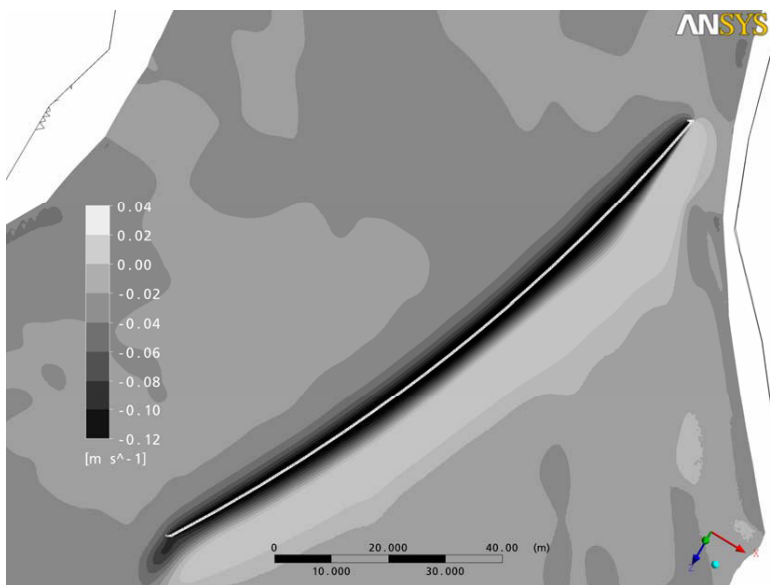
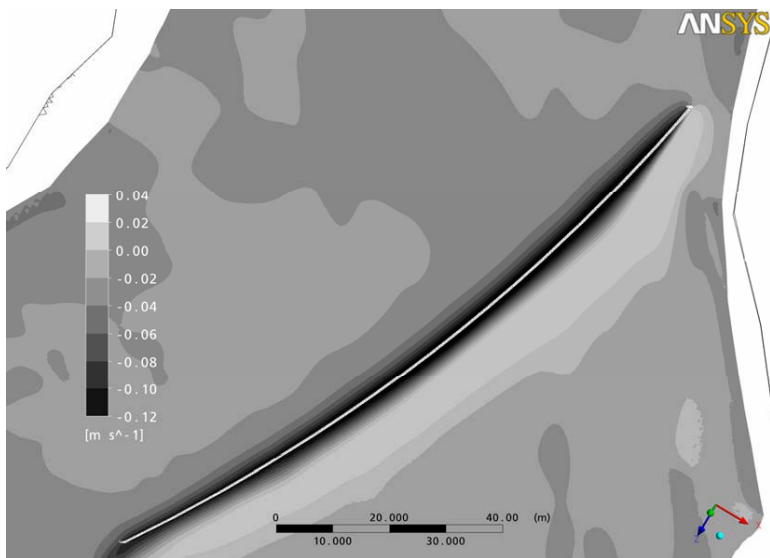


Figure 14. Velocity component v at a depth of 2.5 m for guiding devices 7 (upper figure) and 8 (lower figure) at spilling 1.

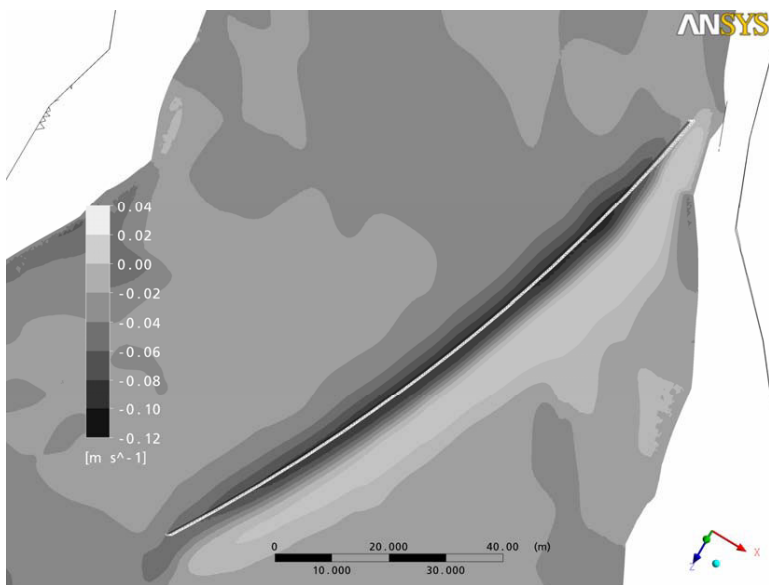
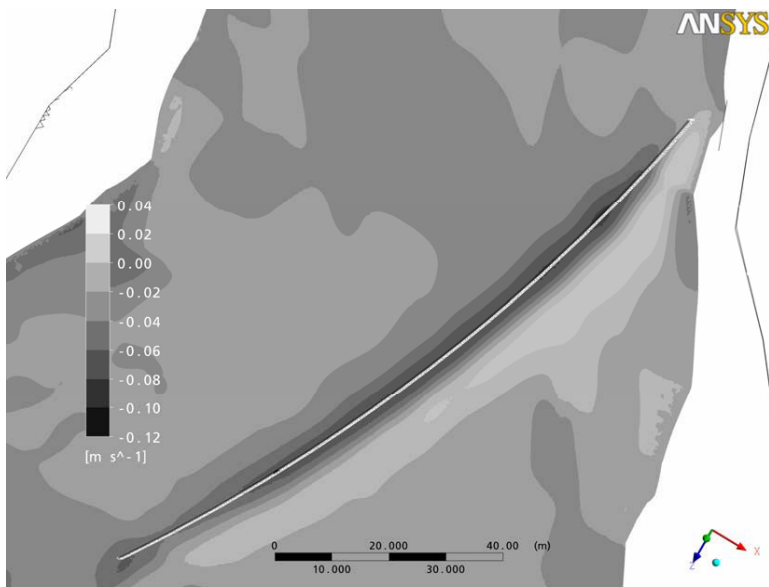


Figure 15. Velocity component v at a depth of 4.5 m for guiding devices 7 (upper figure) and 8 (lower figure) at spilling 1.

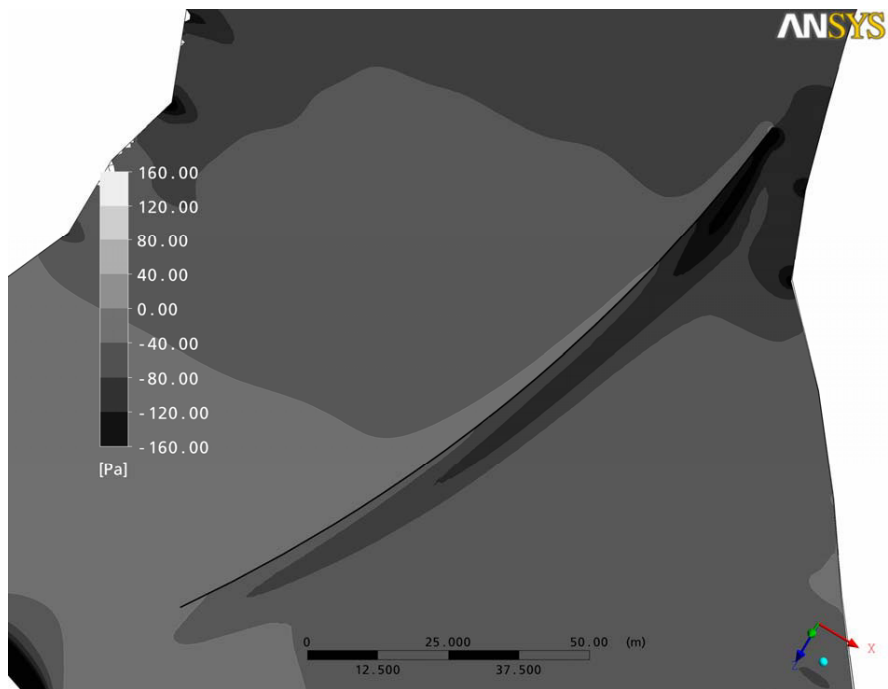


Figure 16. Pressure on the rigid surface for guiding devices 10 at spilling 1.

